Ministry of Higher Education
and Scientific research
University of Babylon
College of Engineering
Chemical Engineering Department

Investigation of Corrosion Protection for Zinc Metal using Green Inhibitors

A Thesis

Submitted to the College of Engineering-University of Babylon in a Partial Fulfillment of the Requirement for the Degree of Master Engineering / Chemical Engineering

By

Haneen Faleh Wali saad

Supervisor

Asst. Prof. Dr. Shaker Salih Bahar

2022

﴿ وَأَنزَلَ اللَّهُ عَلَيْكَ الْكِتَابَ وَالْحِكْمَةَ وَعَلَّمَكَ مَا لَمْ تَكُن تَعْلَمُ وَكَانَ فَضْلُ اللَّهِ عَلَيْكَ عَظِيماً ﴾

النساء / الآية
(113)

Acknowledgments

First of all, I thank Allah for my success in my studies in particular and my life in general.

I would like to express my love and appreciation to my family, who encouraged me and stood by me despite all circumstances, and no word can express my gratitude to them.

I would like to express my deep gratitude to my supervisor, **Asst. Prof. Dr. Shaker Salih Bahar**, for his strong encouragement and important suggestions that have improved this work.

A special thanks to the chemical engineering department for their scientific assistance and to all the people who helped me complete this thesis.

Haneen Faleh Wali

Abstract

In this thesis, four green inhibitors were studied, namely: rosemary, reed leaves, reed stems, and orange peels for zinc. A zinc specimen with a length of 2 cm and a width of 2 cm immersed in hydrochloric acid and sodium chloride salt solution was studied without inhibitor and with rosemary, reed leaves, reed stems, and orange peels at concentrations of 1, and 5 gm/l by using different electrochemical techniques such as weight loss, free corrosion potential, and Tafel polarization.

The experiment medium consisted of a 3.5% sodium chloride salt solution and a 0.1N hydrochloric acid solution. The performance of the corrosion process was tested at temperatures of 20°C, 30°C, 40°C, 50°C, and 60°C for an immersion time of two hours.

The results showed in the weight loss experiment that the corrosion rate decreased with increasing inhibitor concentration in acid or salt solutions due to the formation of a film on the surface of zinc but increased with increasing temperature. Temperature affects the corrosion rate by changing two main parameters: oxygen solubility and diffusivity. It has been shown that the best efficiency in the salt solution, reed stems at a concentration of 5 gm/l, is the most effective green inhibitor, with an efficiency of 75%, while rosemary was found to be the most effective green inhibitor in acid solution, with a 49% efficiency.

According to the findings of free corrosion potential experiments, when temperature increased, the corrosion potential got more negative, and with increasing inhibitor concentration, it became nobler (less negative). The best results were when adding 5 gm/l of the reed stems to the salt medium, where it recorded -639 mV at 20 °C.

In polarization experiments, the anodic and cathodic polarization curves shift to lower current densities and less negative corrosion potentials when the inhibiter

is added, which means the corrosion rate decreases with the inhibitors. The reed stems had the best performance. At a concentration of 5 gm/l, the lowest corrosion potential was recorded - 670 mV and the corrosion current density was 0.9 mA/cm^2 in a salt solution at 20^oC. It has been concluded that the type of inhibitor is a mixed inhibitor.

The limiting current density can be deduced from the polarization curves and, from them, the mass transfer coefficient and Sherwood number were concluded. From this, it can be seen that limiting current density decreased with increasing inhibitor concentration due to the reduction of surface area in contact with the electrolyte by the adsorbed inhibitor. Also, the limited current density increases with increasing temperature.

List of Contents

List of Symbols and Abbreviations

List of Symbols and Abbreviations

List of Figures

List of Figures

List of Figures

List of Figures

List of Tables

List of Tables

List of Symbols

Symbol	Definition	Units
A	Specimen Surface Area	cm^2
C	Inhibitor Concentration	g/L
C_B	Solubility	mol/cm^3
C_R	Corrosion Rate	$gm/m^2.day$
D	Diffusivity	cm^2/s
E	Potential	mV
E_{corr}	Corrosion Potential	mV
F	Faraday No. = 96487	Columb/mol
I	Current	mA
i	Current Density	mA/cm^2
i_c, i_a	Cathodic and Anodic Current Density	mA/cm^2
i_{corr}	Corrosion Current Density	mA/cm^2
i_d	Dissolution Current Density	mA/cm^2
i_L	Limiting Current Density	mA/cm^2
i_o	Exchange Current Density	mA/cm
K	Mass Transfer Coefficient	m/s
L	Lengths of Specimen	cm
M.wt	Molecular Weight	g/mol
z	Number of Electron	
Sc	Schmidt Number	dimensionless
Sh	Sherwood Number	dimensionless
t	Time	hr,s
T	Temperature	˚C
w	Weight Loss	g
Greek Symbols		
η_A	Activation Overpotential	mV
η_c	Concentration Overpotential	mV

List of Symbols and Abbreviations

η	**Polarization Overpotential**	**mV**
η_{total}	**Total Overpotential**	**mV**
η_R	**Resistance Overpotential**	**mV**
βa , βc	**Anodic and Cathodic Tafel Slope**	**mV/decade**
δ	**The thickness of the diffusion layer**	**m**
η	**Efficiency**	
μ	**Dynamic Viscosity**	**Kg/m.s**
ν	**Kinematic Viscosity**	**m^2/s**
ρ	**Density**	**Kg/m^3**

List of Abbreviations

Subscripts	
A	**Activation**
C	**Concentration**
c, a	**Cathodic and Anodic Property**
Corr.	**Corrosion**
d	**Dissolution**
F	**Film**
M	**Metal**
R	**Resistance**
sol	**Solution**
Upscripts	
-	**negative Electrode**
+	**Positive Electrode**

Chapter One

Introduction

1.1 Background

The philosophy of corrosion is a natural, spontaneous, and thermodynamically favorable process. It is the expression of the desire of the metal to go back to its original state of ore. Even though the rate of corrosion can be controlled, corrosion cannot be completely prevented [Rajendran and Singh, 2019]. Corrosion is an unavoidable fact of life, but it is always under control due to its technical, economic, and aesthetic significance [Goni, and Mazumder, 2019]. Corrosion is often thought of only in terms of rusting and tarnishing. However, corrosion damage occurs in other ways as well, resulting, for example, in failure by cracking or in loss of strength or ductility [Revie, 2008].

Cost of corrosion studies have been undertaken by several countries and show that corrosion has a major impact on the economies of industrial nations [Thompson, et al. 2007]. Over the past 50 years, the studies all arrived at corrosion costs equivalent to about 3% – 4% of each nation's gross domestic product (GDP). Using a 3.4% global GDP (2013), the global cost of corrosion is estimated to be 2.5 trillion US dollars [Koch, 2017].

Corrosion is related to metals, For a metal to undergo corrosion, air (more precisely oxygen) and water are necessary. In the absence of any one of these, corrosion will not take place. This is illustrated in Figure (1-1). Some sites act as anodes, and some sites act as cathodes. An anode tends to lose electrons, and a cathode tends to accept those electrons. For electron transfer, a medium is usually called an electrolyte [Rajendran and Singh, 2019].

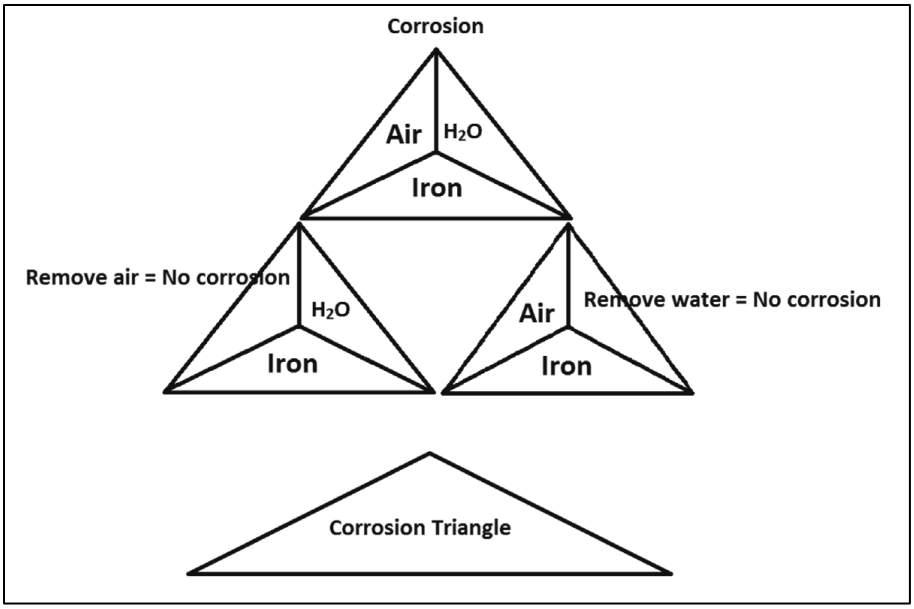

Figure 1-1:The corrosion triangle [Rajendran, and Singh, 2019].

1.2 Corrosion of Metals

Residents of industrialized nations live in metal-based societies where There are 85 metals in the Periodic Table [McCafferty, 2010]. In nature, most metals are found in chemical combination with other elements. These metallic ores are refined by man and formed into metals and alloys. Because the energy content of the metals and alloys is higher than that of their ores [Yadla, et al. 2012]. Only precious metals (gold, silver, platinum, etc.) are found in nature in their metallic state. It is necessary to remember that the choice of material depends on many factors, including corrosion resistance, cost, fabricability, strength, etc [Yadla, et al. 2012]. The corrosion resistance of the pure metal is usually better than that of one containing impurities or small amounts of other elements [Yadla, et al. 2012]. Metal corrosion, not just the metal, but also the energy, water, and human work that went into creating and fabricating the metal structures in the first place. The need to control corrosion almost always reduces to considerations of safety and economics. Machines,

equipment, and functional products may fail at a given time [Stansbury and Buchanan, 2000].

1.3 zinc metal

Zinc is 23rd among the elements in relative abundance in the earth's crust, amounting to 0.013%, compared with aluminum's 8.13% and iron's 5.0%. However, it ranks fourth among the metals in worldwide production and consumption, behind only iron, aluminum, and copper [Zhang, 1996]. The strength and hardness of unalloyed zinc are greater than those of tin or lead but appreciably less than those of aluminum or copper. Pure metal cannot be used in stressed applications because of its low creep resistance. Except when very pure, zinc is brittle at ordinary temperatures, but it is ductile at about 100 ^{o}C [Zhang, 1996]. The uses of zinc are manifold, ranging from galvanizing to die castings to electronics. It is a preferred anode material in high-energy-density batteries (e.g., Ni/Zn, Ag/Zn, Zn/air) [Thomas, et al. 2012]. Rolled zinc is produced as a sheet, strip, plate, rod, and wire in numerous compositions and alloys, depending on the ultimate uses of the rolled products. For the manufacture of cans that form the container and one of the electrodes of the dry cell (the “flashlight” battery), the battery manufacturers have special requirements for purity and for small alloying additions, both of which can improve the efficiency of the cell [Zhang, 1996]. The electrochemical properties of zinc metal were utilized to a large extent. Its utilization in alkaline batteries (primary alkaline zinc battery, secondary silver-zinc, and both primary and secondary zinc-air batteries) [Fouda, et al. 2014]. The use of zinc coatings for corrosion protection of steel structures is the most important application owing to the high corrosion resistance of zinc in atmospheric and other environments [Zhang, 1996].

1.4 Corrosion Inhibitors

Corrosion inhibition is a complex phenomenon and depends on the formation of protective layers on the metal surface [Sastri, 2012]. An inhibitor is a chemical added to a corrosive environment in a small amount to reduce the corrosion rate. Corrosion inhibitors are considered the first line of defense against oil and chemical industry corrosion. The corrosion inhibitors have a widespread application in various industries (oil and gas, steel industry, general cooling water systems, etc.) [Tansuğ, and Tüken, 2016]. Some inhibitors interface with the anode reaction, some with the cathode reaction, and some with both. Corrosion inhibitors act by (i) forming a film that is adsorbed on the metal surface, (ii) producing corrosion products, and (iii) yielding precipitates that can eliminate or inactivate an aggressive constituent [Goni and Mazumder, 2019]. Based on the chemical nature of the inhibitors, they can be divided into organic and inorganic. Organic and inorganic inhibitors, based on their compositions and mechanism of action, can be further classified into neutralizing, scavenging, barrier or film-forming, and other miscellaneous inhibitors [Goni and Mazumder, 2019].

1.5 Green Corrosion Inhibitor

Environmental concerns require corrosion inhibitors to be nontoxic and environment friendly and acceptable. Green chemistry serves as a source of environment-friendly green corrosion inhibitors. Corrosion inhibitors are extensively used in the corrosion protection of metals and equipment [Sastri, 2012]

Plant extracts are generally considered green corrosion inhibitors and the extract includes a part of phytochemicals, depending on the extraction procedure parameters (solvent type, pretreatments, temperature, etc.). The phytochemicals are of course with the type of plant, but generally, they are phenolic compounds, organic acids, esters, alkaloids, flavonoids, tannic acids, etc [Hart, 2017].

1.6 The Aim of The Study

This research aims to study the influence of temperature, and inhibitor concentration for four green inhibitors, namely; Rosemary, Reed Leaves, Reed stems, and Orange Peels, on Zinc corrosion that is immersed in an acid solution of 0.1N HCl and salt solution of 3.5% NaCl solution by using electrochemical techniques including weight-loss method, free corrosion, and electrochemical polarization.

Chapter Two

Theoretical Part and Literature Review

2.1 Definition of Corrosion

Corrosion is the destructive attack of a metal by a chemical or electrochemical reaction. Deterioration by physical causes is not called corrosion but is described as erosion, galling, or wear. In some instances, corrosion may accompany physical deterioration and is described by such terms as erosion-corrosion, corrosive wear, or fretting corrosion [Schweitzer, 2003]. By the word degradation in the definition, it is assumed that corrosion is an undesirable process. There are circumstances in which this is not true, in which case the process is not referred to as corrosion. The degradation involves not just a chemical but an electrochemical reaction. Electron transfer occurs between participants in the environment, which is a convenient name to describe all species adjacent to the corroding metal at the time of the reaction. Environments that cause corrosion are called corrosive. Metals are corrodible [Banerjee, 1985].

2.2 Forms of Corrosion

There are nine basic forms of corrosion, shown in figures (2-1), that metallic materials may be subject to:

2.2.1 Uniform Corrosion

The uniform attack is the most common form of corrosion. It is normally characterized by a chemical or electrochemical reaction that proceeds uniformly over the exposed surface or a large area. The metal becomes thinner and eventually fails. Uniform attack, or general overall corrosion, represents the greatest destruction of metal on a tonnage basis. However, this form of corrosion is not of too great

concern from a technical standpoint because the life of equipment can be accurately estimated based on comparatively simple tests [Al-Rawi, 2009].

2.2.2 Intergranular Corrosion

Intergranular corrosion is a form of localized attack in which a narrow path is corroded out preferentially along the grain boundaries of a metal. It often initiates on the surface and proceeds by local cell action near a grain boundary [Roberge, 2008].

2.2.3 Galvanic Corrosion

Galvanic corrosion occurs when two dissimilar metals or alloys come into electronic contact in a conductive solution the more anodic one corrodes [Sadek, 2012]. The metal with less or the most negative potential becomes the anode and starts corroding. The anode loses metal ions to balance electron flow [Hadi, 2019].

2.2.4 Crevice Corrosion

Crevice corrosion is a localized form of corrosion that occurs when an electrolyte (stagnant solution) is present beneath surface deposits, disbanded coating, lap joints, clamps, or in a small gap or crevice between two joining surfaces. The electrolyte may have been trapped upon application or penetrated through a hole or gap. These conditions can cause an aggressive attack in the area of the electrolyte [Abdul Jalell, 2019].

2.2.5 Pitting Corrosion

Pitting corrosion is a localized type of corrosion that attacks a small area of the metal, making the rate of corrosion in that area more than in other areas. This form is difficult to manage and its main reason is chloride agents [Hadi, 2019]. The pitting process occurs because of highly localized changes in the corrode in contact with the metal or one area of a metal surface becomes anodic with regards to the rest of the surface, as in crevices which give hurry localized attack [Hassan, 2020].

2.2.6 Erosion Corrosion

Erosion corrosion results from the movement of a corrodent over the surface of a metal. The movement is associated with mechanical wear. The increase in localized corrosion resulting from the erosion process is usually related to the removal or damage of the protective film. This type of corrosion is also referred to as impingement attack and is caused by contact with high-velocity liquids resulting in a pitting type of corrosion [Schweitzer, 2003].

2.2.7 Stress Corrosion Cracking

SCC is defined as the growth of cracks due to the simultaneous action of stress and a reactive environment [Marcus, 2012]. Stress corrosion cracking occurs at points of stress. Usually, the metal or alloy is virtually free of corrosion over most of its surface, yet fine cracks penetrate through the surface at the points of stress[Schweitzer, 2003].

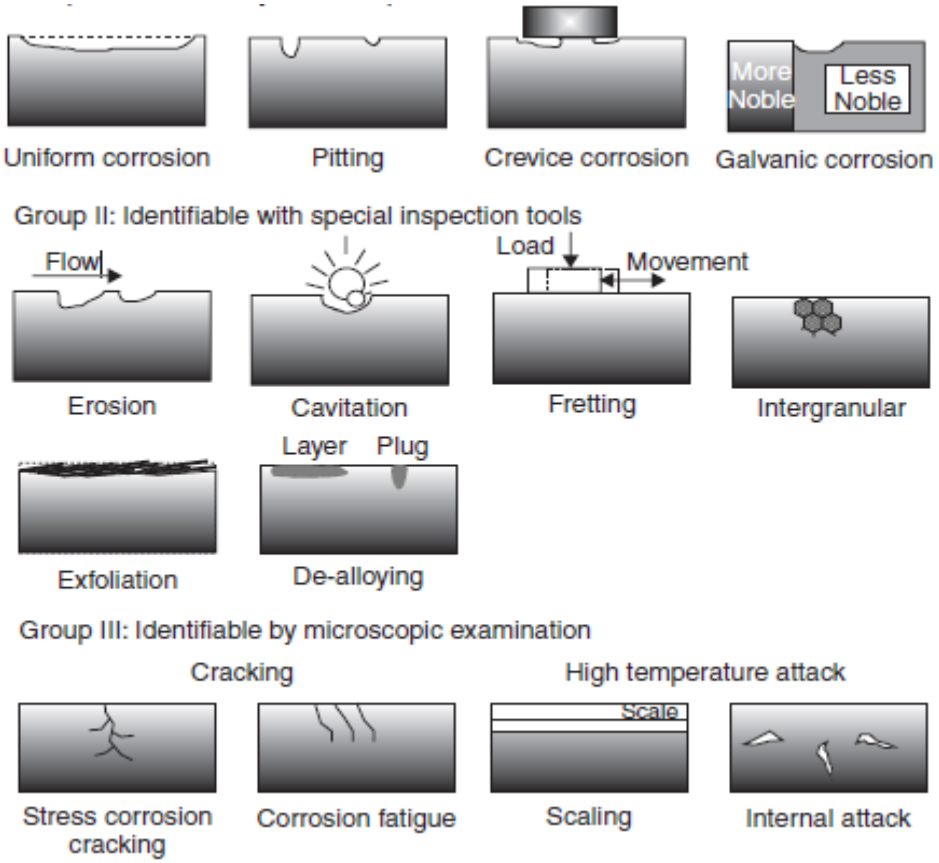

Figure 2-1: Main forms of corrosion [Roberge, 2008].

2.2.8 Biological Corrosion

Corrosive conditions can be developed by living microorganisms as a result of their influence on anodic and cathodic reactions. This metabolic activity can directly or indirectly cause the deterioration of a metal by the corrosion process [Schweitzer, 2003].

2.2.9 Selective Leaching (de–alloying)

This form of corrosion is observed in alloys in which one element is less noble than the other(s). The corrosion mechanism implies that the less noble element is removed from the material. A porous material with very low strength and ductility is the result [Bardal, 2004].

The most common example of selective corrosion is the dezincification of brass, in which zinc is removed from the alloy and copper remains. After cleaning the surface, dezincification is easy to demonstrate because the Zn–depleted regions have a characteristically red copper color in contrast to the original yellow brass[Bardal, 2004].

2.3 Corrosion of Zinc

Zinc is an industrially important metal and is corroded by many agents, of which aqueous acids are the most dangerous ones. Due to the increasing usage of zinc, the study of corrosion inhibition is the most important one. Every year, billions of dollars are spent on capital replacement and control methods for corrosion infrastructure [Petchiammal, et al. 2012]. Zinc metal is mainly used for the corrosion protection of steel, especially in building construction and automobile bodies and in solar energy technology [Taucher, et al. 1992]. Zinc, being an amphoteric metal, exhibits good corrosion resistance in water having a pH near neutral. Seawater contains salts of calcium, magnesium, iron, and manganese in addition to a high amount of sodium chloride. All these foreign substances in natural waters affect the

structure and composition of the films and corrosion products that form on the zinc surface and control corrosion rates. In addition to these substances, such other factors as pH, time of exposure, temperature, motion, and fluid agitation all influence the aqueous corrosion of zinc [Porter, 1994]. Depending upon the nature of the environment zinc can form a protective layer made up of basic carbonates, oxides, or hydrated sulfates [Schweitzer, 2003]. Below 200 ^{o}C, the film grows very slowly and is very adherent. Within the pH range of 6 to 12.5 the corrosion rate is low. The corrosive attack is most severe at pH values below 6 and above 12.5. Uniform corrosion rates of zinc are not appreciably affected by the purity of the zinc. However, the addition of some alloying elements can increase the corrosion resistance of zinc [Schweitzer, 2003]. The zinc-coated steel materials provide greater corrosion resistance, but they undergo rapid corrosion when exposed to a humid atmosphere, leading to the formation of a corrosion product known as white dust [Petchiammal, et al. 2012]. The corrosion forms that are commonly found to occur on zinc are general corrosion, galvanic corrosion, pitting corrosion, and intergranular corrosion. Other forms of corrosion, such as stress corrosion cracking and hydrogen embrittlement, are not common in zinc applications [Zhang, 1996].

2.3.1 Zinc Corrosion Mechanisms

In general, a mechanism of corrosion is the actual atomic, molecular, or ionic transport process that takes place at the interface of a material. These processes usually involve more than one definable step, and the major interest is directed toward the slowest step that essentially controls the rate of the overall reaction. potential and current[Stansbury and Buchanan, 2000]. when the specimen of zinc is exposed to the salty corrosive environment, the initial corrosion layer is basic zinc hydrochloride ($ZnCl_2.4Zn(OH)_2$) and finally changed to zincate ion. In The initial stage of zinc corrosion, the metal serves as an anode and it is dissolved to form

($ZnCl_2.4Zn(OH)_2$). The cathodic reaction is an oxygen reduction reaction. The overall reaction is expressed as follows [Hayashi and Miyoshi, 1994]:

$$5Zn + 5H_2O + 5/2O_2 + 2Cl^- \rightarrow ZnCl_2.4Zn(OH)_2 + 2OH^- \quad (2.1)$$

This reaction is based on the fact that the pH rises with the formation of basic zinc hydrochloride [Hayashi and Miyoshi,1994].

basic zinc hydrochloride cannot remain intact but dissolves, and changes to zincate ions ($Zn(OH)_2$ to ZnO). The reaction proceeds as follows:

$$ZnCl_2.4Zn(OH)_2 + 2OH^- \rightarrow 5Zn(OH)_2 + 2Cl^- \quad (2.2)$$

$$Zn(OH)_2 \rightarrow ZnO + H_2O \quad (2.3)$$

The corrosion behavior of zinc has been carried out in acid solutions. In these media the corrosion of zinc proceeds via two partial reactions [Stanojevic, et al. 2005]:

(i) The partial cathodic reaction involves the evolution of hydrogen gas:

$$2H^+(aq) + 2e^- \rightarrow H_2\,(g) \qquad E = 0\ V \quad (2.4)$$

(ii) The partial anodic reaction involves the oxidation of the metal and formation of soluble $Zn2^+$[Stanojevic,et al. 2005]:

$$Zn \rightarrow Zn^{2+} + 2e^- \qquad E = -0.763\ V \quad (2.5)$$

For example, when zinc is placed in dilute hydrochloric acid, a vigorous reaction occurs; hydrogen gas is evolved and zinc dissolves, forming a solution of zinc chloride [Yadla, et al. 2012]. The reaction is:

$$Zn + 2HCl \rightarrow ZnCl_2 + H_2 \quad (2.6)$$

2.4 Factors influence Corrosion Rate

2.4.1 Effect of oxidants

The effect of oxidizer additions or the presence of oxygen on corrosion rate depends on both the medium and the metals involved. The corrosion rate may be increased by the addition of oxidizers, oxidizers may not affect the corrosion rate, or a very complex behavior may be observed. By knowing the basic characteristics of a metal or alloy and the environment to which it is exposed, it is possible to predict in many

instances the effect of oxidizer additions [Al-Anbaky,2006]. For the diffusion-controlled process, an increase in the concentration of the diffusing species in the bulk of the environment increases the concentration gradient at the metal interface. The concentration gradient provides the driving force for the diffusion process. Thus, the maximum rate at which oxygen can be diffused to the surface (the limiting diffusion current) would be essentially directly proportional to the concentration in the solution [Al-Anbaky, 2006].

2.4.2 Effect of Temperature

As a general rule, increasing temperature increases corrosion rates. This is due to a combination of factors- first, the common effect of temperature on the reaction kinetics themselves and the higher diffusion rate of many corrosive by-products at increased temperatures. This latter action delivers these by-products to the surface more efficiently. Occasionally, the corrosion rates in a system will decrease with increasing temperature. This can occur because of certain solubility considerations [Al-Kelaby, 2007].

2.4.3 Effect of agitation and Velocity

The effects of velocity on corrosion rate are complex and depend on the characteristics of the metal and the environment to which it is exposed. Figures 2-2 show typical observations when agitation or solution velocity is increased. For corrosion processes that are controlled by activation polarization, agitation and velocity do not affect the corrosion rate as illustrated in curve B. If the corrosion process is under cathodic diffusion control, then agitation increases the corrosion rate as shown in curve A, section 1[Fontana, 1987]. Some metals owe their corrosion resistance in certain mediums to the formation of massive bulk protective films on their surfaces. These films differ from the usual passivating films in that they are readily visible and much less tenacious. It is believed that both lead and steel are

protected from attack in sulfuric acid by insoluble sulfate films. When materials such as these are exposed to extremely high corrosive velocities, mechanical damage or removal of these films can occur, resulting in accelerated attack as shown in curve C [Fontana, 1987].

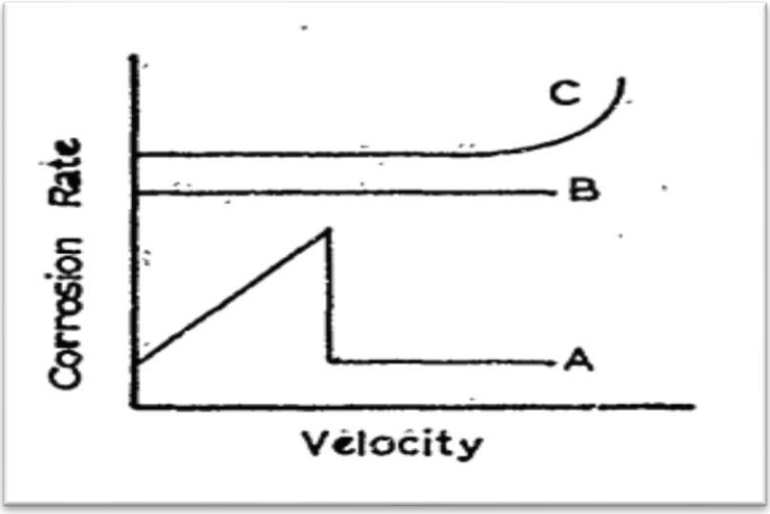

Figure 2-2: Effect of Velocity on Corrosion Rate [Fontana, 1987].

2.4.4 Effect of Impurities

Impurities in a corrodent can be good or bad. The presence of a small amount of chloride in a fluid can break down the passive oxide film on the metal. Some impurities may act as inhibitors to retard corrosion. For instance, inorganic oxidizers such as chromates are used as corrosion inhibitors in cooling water systems. However, if the impurity is removed, a marked increase in corrosion rates may result [Charng, and Lansing, 1982].

2.5 Methods of Preventing Corrosion

To prevent corrosion, five main principles can be used:

1. Appropriate materials selection
2. Application of coatings
3. Suitable design

4. Electrochemical, i.e., cathodic and anodic protection

5. Change of environment

The choice between these possibilities is usually based upon economic considerations, but in many cases, aspects such as appearance, environment, and safety must also be taken care of [Bardal, 2004].

2.5.1 Appropriate materials selection

The most common and important method of controlling corrosion is the selection of the right and proper materials for the particular corrosive environment. The corrosion behavior of each metal and alloy is unique and inherent, and corrosion of metal and alloy has a strong relation to the environment to which it is exposed. The rate of corrosion directly depends upon the corrosivity of the environment and is inversely proportional to the corrosion resistance of the metal. Hence, the knowledge of the nature of the environment to which the material is exposed is very important. Moreover, the corrosion resistance of each metal can be different in different exposure conditions. Therefore, the right choice of the materials in the given environment (metal corrosive environment combination) is very essential for the service life of equipment and structures made of these materials. The selection of correct material depends on various factors such as their cost, availability, physical, mechanical, and chemical properties [Dhawan, et al. 2020].

2.5.2 Application of Coatings

The application of Coatings to metallic objects for corrosion control has been known for a long time. The mechanism of protection by paint films was viewed as a source of insulation of the metal from the corrosive environment such as oxygen and water and inhibiting the cathodic reaction [Sastri, et al. 2007]. There are three general classes of coatings: organic, inorganic, and metallic The use of organic or metallic barrier coatings between a possibly aggressive environment and a material surely

has become the most widely used method of protecting most engineered materials. coatings. However, protective coatings often refer to integrated multifunctional systems that may combine more than one type of coatings [Piere, 2008].

2.5.3 Suitable Design

The prevention of corrosion must begin at the design stage, and full advantage should be taken of the range of protective coatings and corrosion-resistant materials available. Furthermore, at this stage, particular attention should be paid to the avoidance of geometrical details that may promote or interfere with the application of protective coatings and their subsequent maintenance. Consideration should also be given to the materials to be used, the methods of protection, fabrication, and assembly, and the conditions of service[Shreir, 1976].

2.5.4 Electrochemical

2.5.4.1 Cathodic Protection

Cathodic protection is unique amongst all the methods of corrosion control in that if required it can stop corrosion completely, but it remains within the choice of the operator to accept a lesser, but quantifiable, level of protection. Manifestly, it is an important and versatile technique. In principle, cathodic protection can be applied to all the so-called engineering metals. In practice, it is most commonly used to protect ferrous materials and predominantly carbon steel. It is possible to apply for cathodic protection in most aqueous corrosive environments, although its use is largely restricted to natural near-neutral environments (soils, lands, and waters, each with air access)[Shreir, et al. 1994]. Cathodic protection is achieved by applying electrochemical principles to metallic components buried in soil or immersed in water. It is accomplished by flowing a cathodic current through a metal–electrolyte interface favoring the reduction reaction over the anodic metal dissolution. This enables the entire structure to work as a cathode. The flux of electrons can be

provided by one of two methods. By use of a rectifier, a direct current may be impressed on an inert anode and the components. The alternative method is to couple the components with a more active metal, such as zinc or magnesium, to create a galvanic cell [Schweitze, 2006].

2.5.4.2 Anodic Protection

Anodic protection is a method of corrosion control that is developed more recently than cathodic protection, but it is used less frequently. As its name implies, anodic protection shields the anodic electrode in the system from corrosion rather than the cathodic electrode as in cathodic protection[Benjamin, et al. 2006]. Anodic protection possesses unique features. For example, the applied current is usually equal to the corrosion rate of the protected system. Thus, anodic protection not only protects but also offers a direct means for monitoring the corrosion rate of a system. The main advantages of anodic protection are (1) low current requirements; (2) large reductions in corrosion rate (typically 10,000-fold or more); and (3) applicability to certain strong, hot acids and other highly corrosive media. It is important to emphasize that anodic protection can only be applied to metals and alloys possessing active-passive characteristics such as titanium, stainless steel, steel, and nickel-base alloys. Anodic protection has been most extensively used to protect equipment for handling sulfuric acid. Sales of anodically protected heat exchangers used to cool sulfuric acid manufacturing plants have represented one of the more successful ventures for this technology [Piere, 2008].

2.5.5 Change of Environment

The environment may be changed in the following ways to reduce corrosion rates[Bardal, 2004]:

a) Decreasing (or increasing) the temperature

b) Decreasing (or increasing) the flow velocity

c) Decreasing (or increasing) the content of oxygen or aggressive species

d) Addition of Inhibitors.

2.6 Addition of Inhibitors

Corrosion of metallic surfaces can be reduced or controlled by the addition of chemical compounds to the corrodent. This form of corrosion control is called inhibition and the compounds added are known as corrosion inhibitors. These inhibitors will reduce the rate of either anodic oxidation or cathodic reduction or both. The inhibitors themselves form a protective film on the surface of the metal. It has been postulated that the inhibitors are adsorbed into the metal surface either by physical (electrostatic) adsorption or chemosorption[Schweitzer, 2010].

Usually, the corrosion inhibitor is rated in terms of inhibition efficiency η and is given by the relationship [Sastri, et al. 2007].

$$\eta = \frac{(\mathbf{CR})\mathbf{o} - (\mathbf{CR})\mathbf{I}}{(\mathbf{CR})\mathbf{o}} \times 100 \qquad (2.7)$$

Where CR refers to corrosion rate and the subscripts o and I refer to the absence and presence of the inhibitor[Sastri, et al. 2007]. Examples Of Application Of Inhibitors [Ahmad, 2006]:

- cooling water systems.
- the feedwater and boiler sections.
- Petroleum Industry.
- Sour Gas Systems.
- Potable Water Systems.
- Engine Coolants.
- Packaging Industry.
- Construction Industry.

The corrosion inhibitors can be chemicals either synthetic or natural and could be classified by:

• the chemical nature as organic or inorganic;

• the mechanism of action as anodic, cathodic, or an anodic-cathodic mix and by adsorption action, or;

• as oxidants or not oxidants. [Dariva, and Galio, 2014]

2.6.1 Organic or Inorganic Inhibitors

Organic inhibitors are abundantly used in the oil industry to control oil and gas well corrosion [Ahmad, 2006]. These materials build up a protective film of adsorbed molecules on the metal surface that provide a barrier to the dissolution of the metal in the electrolyte. Since the metal surface covered is proportional to the inhibitor concentrates, the concentration of the inhibitor in the medium is critical [Schweitzer, 2010]. The inorganic inhibitors are usually metal salts, which will passivate the surface of the metal that normally would not be passivated in the environment [Aliofkhazraei, 2014]. Although inorganic compounds like chromates, silicates, phosphates, molybdates, and nitrates as well as organic compounds containing heteroatoms (N, O, and S) and/or π-electrons in their molecules have enjoyed high patronage as metal corrosion inhibitors for decades, the adverse effect of inorganic compounds on the ecosystem and the exorbitant prices of the organic counterparts have come under severe criticism particularly in the 21st century [Umoren, and Solomon, 2017].

2.6.2 Anodic or Cathodic or Mixed Inhibitors

Anodic inhibitors (also called passivation inhibitors) act by a reducing anodic reaction, that is, block the anode reaction and support the natural reaction of passivation metal surface, also, due to the forming of a film adsorbed on the metal[Aliofkhazraei, 2014] .In the class of anodic inhibitors, calcium nitrate, sodium nitrite, sodium benzoate, and sodium chromate are commonly used[Ahmad, 2006] .

As for the cathodic corrosion inhibitors, they prevent the cathodic reaction of the metal. These inhibitors have metal ions able to produce a cathodic reaction due to alkalinity, thus producing insoluble compounds that precipitate selectively on cathodic sites [Aliofkhazraei, 2014]. Cathodic inhibitors mainly consist of amines, phosphates, zincates, aniline, and its chloroalkyl nitro substituted form and aminoethanol groups [Ahmad, 2006] .

Those substances, which affect both the cathodic and anodic reactions, are called mixed inhibitors. Such mixed inhibitors include commercially available polyphosphates. Potential change in such a case is smaller and its direction is determined by the relative size of the anodic and cathodic effects [Al-Anbaky, 2006] .Cathodic, anodic, or passivating inhibitors are commonly used to prevent corrosion of steel reinforcement. The anodic inhibitors provide a larger degree of protection than cathodic inhibitors because of their direct influence on the passivation of steel surfaces [Ahmad, 2006].

2.6.3 Oxidising or Non-oxidising Inhibitors

These are characterized by their ability to passivate the metal. In general, non-oxidizing inhibitors require the presence of dissolved oxygen in the liquid phase for the maintenance of the passive oxide film, whereas dissolved oxygen is not necessary with oxidizing inhibitors[Shreir,1976].

2.7 Green Inhibitor

In the last decade, green chemistry has been attracting great interest in many contexts by designing chemicals, chemical technologies, and commercial products to avoid toxins and reduce waste [Marzorati, et al. 2019]. Thus, Green corrosion inhibitors are becoming more popular among scientists and engineers that are inexpensive, readily available, environmentally friendly and ecologically acceptable, and renewable [Goni and Mazumder, 2019]. Green corrosion inhibitors are

biodegradable and do not contain heavy metals or other toxic compounds[Rani, and Basu, 2012]. The corrosion inhibiting of natural products can be ascribed to phytochemical substances containing alkaloids, carboxylic acids, ketones, alcohols, ascorbic acids, tannins, nitrogen bases, carbohydrates, proteins, flavonoids, organic pigments, phenolic compounds, amino acids, and their acid hydrolysis products. Extracts of natural inhibitors like extracts from leaves, barks, seeds, fruits, and roots include mixtures of organic compounds which have nitrogen, sulfur, and oxygen atoms in functional groups (O-H, C=C, C=O, N-H, C=O) as well as multiple bonds, and aromatic rings that act as impressive inhibitors in a corrosive environment [Nasab, et al. 2019]. The use of green inhibitors is one of the most practical methods by which to protect zinc from corrosion in various environments [Sun, et al. 2017] such as Aloe vera extract [Abiola, and James, 2010], Citrullus vulgaris peel [Petchiammal, et al. 2012], mansoa alliacea plant extract [Suedile, et la. 2014], fenugreek [Shimaa, and Hamedh, 2016], and natural onion juice [El-Etre, 2006].

In this sense, green inhibitors become an important alternative to sustainable technological development. Rosemary, reed leaves, reed stems, and orange peels have been studied in this thesis.

2.7.1 Rosmarinus

Rosmarinus Officinalis L. (rosemary), a member of the family Lamiaceae, is an attractive evergreen shrub with pine needle-like leaves that grow wild in most Mediterranean countries[Rezanejad, et al. 2019]. Rosemary essential oil also has the efficacy of sterilization, insecticidal and anti-inflammatory. It is widely used in perfume, bath liquid, cosmetics, shampoo, air freshener, ant repellent, and other daily chemicals. As for spices, rosemary has been widely used in the food industry. A lot of in-depth studies have been done on its extracts in food preservation, color protection, oil stabilization, and meat flavor stabilization [Zheng, et al. 2019]. The plant has been reported to possess antioxidative, anti-inflammatory, antibacterial,

antitumor effects, and antiandrogenic effects[Murata, et al. 2013]. Rosemary includes phenolic compounds with inhibitory properties, such as carnosol, carnosic acid, rosmanol, rosmadial, epirosmanol, rosmadiphenol, and rosmarinic acid [Bozin, et al 2007].

Figure 2-3: rosemary Plant

2.7.2 Reed leaves and reed stems

Reed, a scientifically named phragmites australis, belongs to the family Phragmites .generally found in the coastal region of China and found widely in the middle and south regions of Iraq. Reed is found to contain alkaloids, lignans, naturally occurring phenolic dimmers, flavonoids, and O-substituted aromatic amines [Cang, et al. 2012]. Few works have been performed using reed leaves extract as a corrosion inhibitor of mild steel [Hadi, et al. 2020].

Figure 2-4: Reed Plant

2.7.3 Orange Peels

The orange is a citrus fruit consumed in high quantities all over the world in natural and peeled forms and as a juice. It is associated with a low cost and contains many nutrients, including vitamin C, A, and B, minerals (calcium, phosphorus, potassium) [Rezzadori, et al. 2012]. The orange peel, which represents roughly half of the fruit mass, contains the highest concentrations of flavonoids of any citrus fruit [Rocha, et al. 2014]. Orange peels are rich sources of antioxidant compounds such as polyphenols and carotenoids. Phenolic compounds, particularly flavonoids, have been shown to possess important antioxidant activity, which is principally based on their structural characteristics [Da Rocha, et al. 2010]. Already used in the fields of functional food, cosmetics, and pharmaceuticals [M'hiri, et al. 2016]. Aqueous extracts of orange peel are used against corrosion of mild steel, aluminum, zinc, and copper in HCl and H_2SO_4 solutions [Da Rocha, et al. 2010].

Figure 2-5: Orange peels

2.8 Adsorption Mechanisms

Adsorption is the adhesion of atoms, ions, or molecules from a gas, liquid, or dissolved solid to a surface. The first step in the inhibition process is the adsorption of banners on the metal surface to prevent occurring corrosion. The various components may react with produced ions on a corroding metal surface and make organometallic complexes. The adsorption process of an inhibitor occurs with the replacement of one or more water molecules which are preadsorbed on the metal surface. Then adsorbed inhibitors may combine with ions on the metal surface [Nasab, et al. 2019].

Based on interaction forces between adsorbate and adsorbent, adsorption is of two types :

Physical adsorption is also known as physisorption. It is due to weak Van der Waals forces between adsorbate and adsorbent. Physical adsorption is not specific and takes place all over the adsorbant. Surface area, temperature, pressure, nature of adsorbate effects physisorption.

Chemical adsorption is also known as chemisorption. It is due to strong chemical forces of bonding type between adsorbate and adsorbent. This type of adsorption is almost a single-layered phenomenon. Chemisorption is highly specific and takes place at reaction centers on the adsorbent. Surface area, temperature, and nature of

adsorbate effects chemisorption. Inhibition performance depends on the rate of adsorption of its ingredients on a metal surface, but the stability of adsorbed molecules (inhibition period) changes with the kind of adsorption, chemical/physical/both, to a great extent. Therefore, it becomes urgent to study metal-inhibitor interaction through adsorption isotherm. Adsorption isotherms that are used to describe adsorption mechanisms include Langmuir, Temkin, Frumkin, Florry–Huggins, Freundlich, and Elawady [Nasab, et al. 2019].

2.9 Polarization

Polarization is defined as a type of perturbation, which results in disturbing the equilibrium and producing a dynamic situation [Sastri, et al. 2007]. Polarization measurements are an important research tool in investigations of a variety of electrochemical phenomena. Such measurements permit studies of the reaction mechanism and the kinetics of corrosion phenomena and metal deposition[Stern, 1957]. The three types of polarization are concentration polarization, activation polarization, and IR drop [Sastri, et al. 2007].

.

2.9.1 Types Of Polarization

2.9.1.1 Activation Polarization

In general, activation polarization is an electrochemical phenomenon related to a charge-transfer mechanism, in which a particular reaction step controls the rate of electron flow from a metal surface undergoing oxidation. This is the case in which the rate of electron flow is controlled by the slowest step in the half-cell reactions[Perez, 2004]. The activation polarization η_A of any kind increases with anodic and cathodic current density in accord with the Tafel equation[Fontana, 1987]:

For anodic reaction $$\eta_A = \frac{2{\cdot}303RT}{\alpha zF}\log\left(\frac{i_a}{i_0}\right) \qquad (2\text{-}7)$$

For cathodic reaction $\eta_A = \frac{2{\cdot}303RT}{\alpha zF}\log\left(\frac{i_c}{i_0}\right)$ (2-8)

Activation polarization refers to electrochemical reactions which are controlled by a slow step in the reaction sequence. The species must first be adsorbed or attached to the surface before the reaction can proceed according to (step1). Following this, electron transfer (step2) must occur, resulting in a reduction of the species. in (step3), two hydrogen molecules then combine to form a bubble of hydrogen gas (step4). The speed of reduction of the hydrogen ions will be controlled by the slowest of these steps[Al-Kelaby, 2007].

2.9.1.2 Concentration Polarization

Concentration polarization is the polarization component caused by concentration changes in the environment adjacent to the surface. A frequent case of concentration polarization occurs when the cathodic processes depend on the reduction of dissolved oxygen since it is usually in low concentration, that is, in parts per million (ppm)[Roberge, 2008].

At very high reduction rates, the region adjacent to the electrode surface will become depleted of ions. If the reduction rate is increased further, a limiting rate will be reached which is determined by the diffusion rate of ions to the electrode surface. This limiting rate is the limiting diffusion current density i_l. It represents the maximum rate of reduction possible for a given system; the expression of this parameter is [Al-Kelaby, 2007]:

$$i_l = \frac{DnFC_B}{\delta} \quad (2\text{-}9)$$

where i_l is the limiting diffusion current density, D is the diffusion coefficient of the reacting ions, C_B is the concentration of the reacting ions in the bulk solution, and δ is the thickness of the diffusion layer. By combining the laws governing diffusion with the Nernst equation [Fontana,1987]:

$$E_i - E = \eta_c = \frac{2{\cdot}303RT}{nF}\log\left(1 - \frac{i}{i_l}\right) \quad (2\text{-}10)$$

2.9.1.3 Combined Polarization

Both activation and concentration polarization usually occurs at an electrode. At low reaction rates, activation polarization usually controls, while at higher reaction rates concentration polarization becomes controlling. The total polarization of an electrode is the sum of the contribution of activation polarization and concentration polarization [Al-Kelaby, 2007]:

$$\eta_T = \eta_A + \eta_C \quad (2\text{-}11)$$

where (η_T) is total overvoltage.

2.9.1.4 Resistance Polarization.

Since in corrosion the resistance of the metallic path for charge transfer is negligible, resistance overpotential η^R is determined by factors associated with the solution or with the metal surface. Thus, resistance overpotential may be defined as [Farhan, 2016]:

$$\eta^R = I\,(R_{sol.} + R_F) \quad (2\text{-}12)$$

Where $R_{sol.}$ is the electrical resistance of the solution, which depends on the electrical resistivity (Ω cm) of the solution and the geometry of the corroding system, and R_F is the resistance produced by films or coatings formed on or applied to the surface of the sites [Farhan, 2016]. Thus, in addition to the resistivity of the solution, any insulating film deposited either at the cathodic or anodic sites that restricts or completely blocks contact between the metal and the solution will increase the resistance overpotential, although the resistivity of the solution is unaffected [Farhan, 2016].

2.9.2 Polarization Methods

The polarization resistance (R_P)of a metal/electrolyte system and the pitting can be determined using at least two-electrode systems. Subsequently, the rate of metal

dissolution or corrosion rate is calculated using a function of the form ($i_{Corr} = f(\beta, R_p) > i_0$) The methods are [Perez, 2004] :

- Linear Polarization (LP) schematically covers both anodic and cathodic portions of the potential (E)versus current density (*i*) curve for determining (R_P).

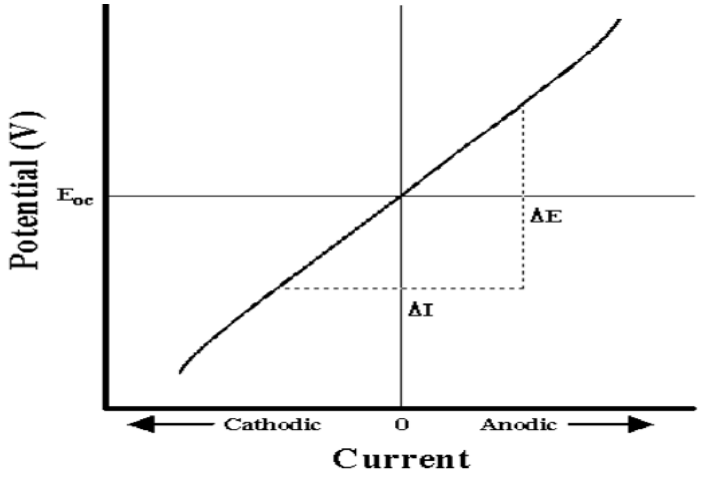

Figure 2-6: Linear polarization resistance (Enos, and Scribner, 1997).

- Tafel Extrapolation technique (TE) takes into account the linear parts of the anodic and cathodic curves for determining (R_P).

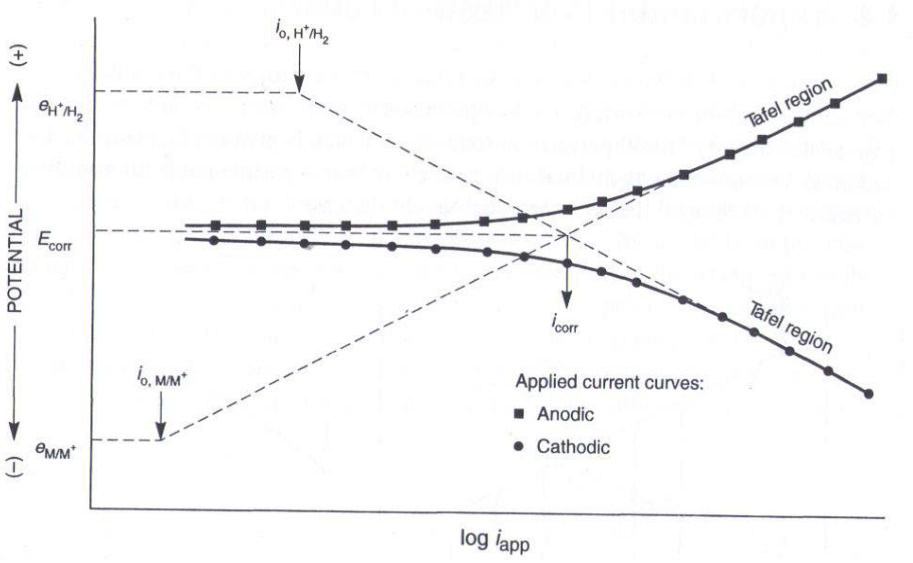

Figure 2-7: Tafel polarization curve (Sanchez, 2011).

- Electrochemical Impedance Spectroscopy (EIS) schematically requires an alternating current (AC) and the output is a Nyquist plot for charge-transfer or diffusion control process, which can be used to determine(R_P) which in turn, is inversely proportional to the corrosion current density (i_{Corr}).

2.10 Limiting Current Density

The limiting current is defined as the maximum current that can be generated by a given electrochemical reaction, at a given reactant concentration, under well-established hydrodynamic conditions, in the steady-state. This definition implies that the limiting rate is determined by the composition and transport properties of the electrolytic solution and by the hydrodynamic conditions at the electrode surface[Al-Anbaky, 2006]. The limiting current is an important parameter for the characterization of mass transport rates in electrochemical systems. When an electrochemical system operates under limiting current conditions, the reaction proceeds at the maximum rate, and hydrodynamic properties can be characterized, facilitating comparison with other electrochemical systems[Sadek, 2012].

2.11 Literature Review

In addition to the studies stated previously, some studies in the literature considered the effect of various factors on the corrosion and inhibition of zinc in different solutions.

2.11.1 Green Inhibitors on zinc

- El-Etre,(2006), The inhibitive effect of the natural juice of the onion bulb on the corrosion of zinc surface area of 16 cm2 in 0.1 M HCl solution was determined using hydrogen evolution and weight loss measurements as well as the potentiodynamic polarization technique. Potentiodynamic anodic polarization

was used to determine the effect of the juice on the pitting corrosion of zinc in a 3.5% NaCl solution. The immersion time was extended to four days, at 298±1K. It is found that the presence of onion juice reduced markedly the corrosion rate of zinc in the acid solution. The inhibition efficiency increases as the juice concentration are increased. Moreover, the presence of the juice in the 3.5% NaCl solution shifts the pitting potential toward a more positive direction.

- Abiola and James, (2010) The effect of the extract of Aloe vera leaves on the corrosion of Zinc sheets (98.53%) of 0.038 cm in thickness in 2 M HCl solution at 30 ^{O}C ,40 ^{O}C was studied using weight loss technique. Aloe vera extract inhibited(1,1.5, 2, 2.5, 4, and 10% v/v concentrations) the corrosion of zinc in 2 M HCl solution and the inhibition efficiency increased with increasing concentration of the extract but decreased with increasing temperature.
- Petchiammal, et al. (2012), The effect of Citrullus Vulgaris peel on the corrosion of zinc each of dimension exactly 5x2x2cm in natural seawater has been studied by mass loss measurements at different times and temperatures. The Zinc specimens were withdrawn from the test solutions after an hour at the temperature range of 303K to 333K and after 24 to 480hrs at room temperature. The present investigation revealed that the percentage of inhibition efficiency is increased with the increase of inhibitor concentration and decreased with rising in the period of contact. The temperature studies reflect that the percentage of inhibition efficiency is decreased with the increase in temperature and it indicates the mechanism of physical adsorption. The observed results concluded that the Citrullus Vulgaris peel could serve as an effective inhibitor of zinc in the natural seawater environment.
- Ali, et al. (2014), studied the effect of Achillea fragrantissima on the corrosion of Zinc sheets with the dimension of (1.0 – 1.0 – 0.1 cm) in 0.5 M HCl for 24 hrs, using weight loss, hydrogen evolution, and polarization measurements. the concentration of the extract was (50,100,200,400,800) expressed as part per

million (ppm) .The inhibition efficiency was found to increase with increasing concentration and decrease with increasing temperature. The inhibition effect was explained based on the adsorption of Achillea fragrantissima components on the metal surface through the active centers contained in their structures.

- Fouda, et al. (2014), In this work, moringa extract was examined as a green corrosion inhibitor for zinc (20 x 20 x 2 mm)in 3.5 % NaCl and 16 ppm Na2S solution in the absence and presence of different concentrations of moringa extract (50 - 500 ppm), were determined at different times of immersion (30 to 180 min.) at 30℃ by using weight loss, potentiodynamic polarization, electrochemical impedance spectroscopy (EIS), and electrochemical frequency modulation (EFM) techniques. Results obtained showed that this extract of moringa offered good protection against corrosion of zinc metal and exhibited high inhibition efficiencies. The inhibition efficiency was found to increase with an increase in the extract concentration. The adsorption of the inhibitor molecules on the zinc metal surface follows the Temkin adsorption isotherm and behaves as a mixed-type inhibitor.
- Suedile, et al. (2014), tested ethanol extract of Mansoa alliacea as a corrosion inhibitor for zinc in NaCl 3% media using polarization and electrochemical impedance spectroscopy (EIS). All the tests were performed at ambient temperature (25 °C). The concentration range of extract from Mansoa alliacea plant employed was 10 – 200 mg L^{-1}. Potentiodynamic polarization curves indicated that the plant extract behaves as a mixed-type inhibitor. Impedance measurements showed that there are two phenomena in the process of inhibition. The results obtained show that this plant extract could serve as an effective inhibitor for the corrosion of zinc in NaCl 3% media. The extract obtained gives inhibition of around 90%.
- ALI, & Al Lehaibi, (2016), Fenugreek seeds extract was examined as a green corrosion inhibitor for Zn in 2.0 mol/L HCl solutions by mass loss and

electrochemical measurements. Scanning electron microscope (SEM) images show that the surface damage is decreased in the presence of the inhibitor. The maximum inhibition efficiency value is 66.6% after 0.5 h by 200 mL/L of fenugreek extract in HCl solution. Potentiodynamic polarization and EIS measurements prove the inhibition ability of fenugreek for Zn corrosion in HCl as indicated by the decreased corrosion current density and increased charge transfer resistance values in the presence of fenugreek.

- Lebrini, et al. (2020), in this study is the evaluation of Bagassa guianensis extract on the corrosion behavior of zinc in chloride medium (3%) with and without different concentrations(10, 25, 50,100 mg/L) of EEBGP at 25 °C was realized using electrochemical techniques (polarization and AC impedance). This study demonstrated that the plant extract of Bagassa guianensis is a real sustainable and green inhibitor for zinc corrosion in 3% NaCl with an inhibition efficiency of about 97% at 100 ppm.
- Al-Areqi and Al-Maleeh, (2021), The inhibitive effects of chlotrimazole (CTM) and potassium iodate (PI), two environmentally friendly compounds, on the corrosion of zinc metal in an aqueous solution of HCl with concentrations of (0.50.5, 1.01.0, 1.51.5, 2.0 M). solution. The inhibitors were added to the HCl solution in concentrations of 0.0050.005, 0.015, and 0.025 g/ 100 ml. The tested aqueous solution has been investigated using chemical (weight loss) and electrochemical (open-circuit potential) techniques. It was found that the inhibition efficiencies of CTM and PI remarkably increase as the inhibitor concentration increases, and drop with increasing temperature.

2.11.2 Rosemary Extract Inhibitors

- Kliškić, et al. (2000), The first neutral phenol subfraction of the aqueous extract of rosemary leaves was studied as a corrosion inhibitor for the Al±2.5Mg alloy in a 3% NaCl solution at 25 ^{o}C for 30 min. Experiments were carried out over a

wide range of concentrations. The results show that the additive adsorbs on the alloy according to the Freundlich isotherm. The polarization curves show that the first neutral subfraction acts as a cathodic-type inhibitor.

- Pourriahi, et al. (2014), The inhibitive action of rosemary extract, on the corrosion of 304L stainless steel (0.025% C, 1.86% Mn, 0.037% P, 0.024% S, 0.71% Si, 18.56% Cr,9.36% Ni and Fe balance) in 3.5% NaCl solution has been investigated through electrochemical techniques and surface analysis. Experiments were performed at 25°C with different concentrations of rosemary extracts (0,0.1,0.5,1 g/l). The immersion time for the weight loss test is 360 h. Polarization measurements indicate that the investigated compounds are mixed-type inhibitors, and the higher the inhibitor concentration, the higher the inhibition efficiency. Maximum inhibition efficiencies of 90.2% of rosemary extracts are obtained at 1.0 g/L. The polarization curves show that rosemary extracts act as an anodic type inhibitor.
- Velázquez-González, et al. (2014), The use of Rosmarinus officinalis as a corrosion inhibitor for 1018 carbon steel in 0.5 M H2SO4 has been evaluated by using weight loss, potentiodynamic polarization curves, and electrochemical impedance spectroscopy techniques at 25˚C. Inhibitor concentrations were included within the range between 0 and 1000 ppm using three extract solvents, namely acetone, hexane, and methanol. Results have shown that Rosmarinus officinalis is a good corrosion inhibitor with its efficiency increasing with concentration.
- Ćatić, et al. (2016), The research of plant extracts has become a great area of interest in the study of corrosion inhibitors. Testing the ability to protect steel in 3% NaCl with different concentrations of inhibitor Rosmarinus (0, 0.005, 0.01, 0.1 mg/ml). To determine the basic parameters that show the effectiveness of green inhibitors, electrochemical measurements of corrosion rate were carried out. Results obtained by DC techniques (method of Tafel extrapolation) showed

that the corrosion rate decreases in the presence of the tested corrosion inhibitor. Studies have shown that, in a certain concentration, rosemary (Rosmarinus officinalis L.) has the effect of protecting steel in 3% NaCl, and as such, it is considered an acceptable corrosion inhibitor.

- Deyab, (2016), Rosemary extract was used to control aluminum corrosion of different concentrations of the extract were obtained by dissolving 0.1,0.2,0.3,0.4and0.5 g of the extract powder in 10 mL ethanol(95%) and biodiesel at 298K. Weight loss and polarization methods were used to test corrosion inhibitor efficiency. The inhibition efficiency increased with an increase in extract concentration and decreased with temperature, suggesting the occurrence of physical adsorption. Adsorption of the extract on the aluminum surface is spontaneous and obeys Langmuir's isotherm. Polarization measurements revealed that Rosemary extract acts as a mixed-type inhibitor with predominant Anodic effectiveness.
- Ur Rahman, et al. (2016), The rosemary (Rosmarinus Officinalis L) leaves extract was evaluated for inhibitive action towards the corrosion of mild steel in 0.1 N HCl at ambient temperature by gravimetric and potential monitoring techniques. Four concentrations of extract (25, 50, 75 and 100 %)were made. The corrosion inhibition efficiency of extract varied with the concentration of extract and duration of immersion of mild steel in the corrosive medium. The 100% leave extract of Rosmarinus officinalis L gave 98.33% corrosion inhibition efficiency as compared to control.
- Loto, (2018), Electrochemical analysis of the corrosion inhibition and surface protection properties of the combined admixture of Rosmarinus officinalis and zinc oxide on low carbon steel in 1 M HCl and H_2SO_4 solution was studied by potentiodynamic polarization, open circuit potential measurement, optical microscopy, and ATR-FTIR spectroscopy. The combined admixture of the compounds (ROZ) was prepared in molar concentrations of 6.47x 10^3, 1.29 x

10^2, 1.94 x 10^2, 2.59 x 10^2, 3.24 x 10^2, 3.88 x 10^2 in 200 mL for 2400s . Results obtained confirmed the compound to be more effective in HCl solution, with optimal inhibition efficiencies of 93.26% in HCl and 87.7% in H_2SO_4 acid solutions with mixed type inhibition behavior in both acids.

2.11.3 Reed Extract Inhibitors

- Cang et al. (2012), investigated the impact of reed leaves extract inhibitor on mild steel specimens of size (1 cm × 2.5 cm × 0.05 cm) in 1.0 M HCl and 0.5 M H_2SO_4 by potentiodynamic polarization methods and weight loss approaches. The measurements were performed at 298 K (except for temperature effect) for 6 h (except for immersion time effect) without and with various concentrations of inhibitors (100-800 mg/L). According to the results, inhibition efficiency was increased with increasing concentration of RLE. It was found that RLE is a mixed type inhibitor in HCl but a cathodic type inhibitor in H_2SO_4 solution. The best efficiency was achieved in a 0.5 M H_2SO_4 solution.
- Hadi, (2015), The main objective of the present work involved the study of the inhibitive properties of the natural product as reed leaves as safety and an environmentally friendly corrosion inhibitor for low carbon steel in (3.5% NaCl) solution. Results showed when the immersion model in (3.5% NaCl) solution and using (2, 4, 6, 8, and 10%) reed leaves the amount of loss weight decrease with increasing concentration of inhibitor and this shows the damper on his ability to form a protective layer.
- Hadi,et la. (2020), The effect of reed leaves extract (RLE) as an eco-friendly corrosion inhibitor at concentrations of 2 ,4 ,6 ,8, and 10% for reinforcing steel in concrete immersed in 3.5% NaCl solution was investigated. The work was carried out using Linear polarization resistance, Potentiodynamic polarization, cyclic polarization, photographic examination, impressed voltage, and compressive strength tests. Results obtained from Tafel polarization curves after

180 days of immersion showed that corrosion rate was decreased and efficiency was increased with increasing concentration of RLE inhibitor. The minimum corrosion rate was 2.259 mpy with maximum efficiency of 76.98% at 0.5% RLE concentration (by cement weight). The results of this study revealed that RLE acts as a good eco-friendly corrosion inhibitor.

2.11.4 Orange Peels Extract Inhibitors

- Saleh, et al. (1982), The inhibitive effects of aqueous extracts of Orange on the corrosion of mild steel, aluminum, zinc, and copper in HCl and H_2S0_4 solutions have been investigated using weight loss and polarization measurements. The extracts retard the dissolution reactions to an extent dependent on the metal used, the concentration of the additive, and the type, concentration, and temperature of the attacking acid. The additives provide adequate protection to steel in 5% HCl at 25°C and in 10% HCl at 25°C and 40°C. In the presence of a sufficient concentration of the extracts in 5% HCl at 25°c, the inhibitive efficiency towards steel decreases in Orange by 80%.
- Da Rocha, et al. (2010), The inhibitive action of the aqueous extracts of orange peels extract used was varied from 100 to 400 mg/L against corrosion of carbon steel in a 1 M HCl solution was investigated using electrochemical impedance spectroscopy, potentiodynamic polarization curves, weight loss measurements, and surface analysis. We analyzed aqueous extracts of orange in different concentrations and found that the extracts act as good corrosion inhibitors for the tested system. The inhibition efficiency increases with increasing extract concentration and decreases with temperature.
- Rezzadori, et al. (2012), In this study, information was collected on the technological potential of the solid and liquid residues generated in the processing of orange juice. Possible applications include human consumption, fertilizer, animal feed, charcoal, adsorption of chemical compounds, bio-oil

production, and extraction of essential oils and pectin. In this preliminary study, alternatives are proposed for the minimization and recovery of solid and liquid residues generated in the production of orange juice with a view to the implantation of industrial plants which can reuse this material, to add value to this solid and liquid waste and provide environmental benefits.

- Rocha, et al. (2014), In this paper, aqueous extracts of orange peels were shown to be good corrosion inhibitors for carbon steel in a 1 mol L^{-1} HCl solution. The inhibition efficiency increased as the extract concentration increased over a concentration range of 200-600 mg L^{-1}, varying from 84 to 91% (orange) using Tafel plots and from 76 to 90% (orange) using electrochemical impedance. In the presence of 400 mg L^{-1} of mango and orange peel extracts, the weight loss measurements showed an increase in the inhibition efficiency with immersion time, where the best results after 24 h of immersion were 97% and 95%, respectively.

Chapter Three

Experimental Work

3.1 Introduction

Experimental work was carried out to determine the corrosion rate of Zinc specimens under conditions temperatures (20,30, 40, 50, and 60) ^{o}C, with 0.1N HCl and 3.5% NaCl solutions. The experimental work was divided into three parts:

1- Weight loss measurements to determine the average corrosion rates under different green inhibitors concentrations and different values of temperature.

2- Free corrosion potential experiments to determine the corrosion potential E_{corr} by using a voltmeter at different green inhibitors concentrations and temperatures.

3- Electrochemical polarization measurements were performed to determine corrosion current i_{corr}, corrosion potential E_{corr}, and limiting current density i_L by using the Tafel extrapolation method of anodic and cathodic polarization curves under different inhibitor concentrations, and temperatures.

3.2 Preparing the Inhibitor

Before using the green inhibitor, it must be dried under the sun and then ground with an electric grinder until it becomes a powder.

Rosemary was immersed in one liter of water for 24 hours, and reed leaves, reed stems, and orange peels were immersed in boiling water for half an hour and then filtered. The green inhibitor compounds were identified by the Fourier Transform Infrared Technique.

3.3 Fourier Transform Infrared (FTIR)

Fourier transform infrared (FTIR) is one of the important analytical techniques for researchers. This type of analysis can be used for characterizing samples in the forms

of liquids, solutions, pastes, powders, films, fibers, and gases. This analysis is also possible for analyzing the material on the surfaces of the substrate (Fan et al., 2012). The FTIR spectrometer essentially uses an interferometer to measure the energy that is being transmitted to the sample. The infrared radiation emitted from the black body reaches the interferometer where the spectral encoding of signals happens. The resultant interferogram signal is transmitted through or bounces from the sample surface, where specific energy wavelengths are absorbed. The beam eventually passes through the detector and is further passed on to the processing computer for Fourier transformation of energy signals [Khandelwal, 2021].

The FTIR spectra have been conducted at Al-Muthanna university/college of Science., as shown in figures (3-2),(3-3),(3-4),(3-5), the FT-IR spectrum demonstrates the presence of many chemical functionality groups in inhibitors.

Figure 3-1: Fourier transforms infrared spectroscopy (FTIR).

3.3.1 FTIR test for Natural Rosmarinus Inhibitor

FTIR spectra in the diversity of 4000–500 on behalf of the rare Rosmarinus remain exposed. FTIR spectral teaching documented the harmfully charged functional

groups (hydroxyl, carboxyl, and amine) on the Rosmarinus surface. The whole band at 3383.26 cm^{-1} in unadulterated bark powder remains credited because of hydroxyl (-OH) stretching bands of alcohols and/or carboxylic acids vibrations or amine (-NH_2) stretching of polymeric complexes, followed by peaks of 2924.18 cm^{-1} and 2852.81 cm^{-1} assigned to vibration of the(-CH_3) asymmetric stretching and symmetric stretching absorption band of the methylene group vibration, respectively. Additionally, both peaks of 1741.78 cm^{-1} and 1651.12 cm^{-1} refer to the carbonyl group (–C=O). Instead, the aromatic rings remain signified through the 1516.10 cm-1 whereas 1452.45 and 1375.29 cm^{-1} are associated with the (–CH_3) and (C-O) in phenols, respectively. 1269.20 cm^{-1} means the aromatic rings, though 1026.16 remains related through the (C-O) in phenols and (-CH3) and the bands current underneath 825.56 remain fingerprint area of sulphur and phosphate functional groups. It is careful enough to leave an imprint on the Rosmarinus adsorbent around the presence of functional groups.

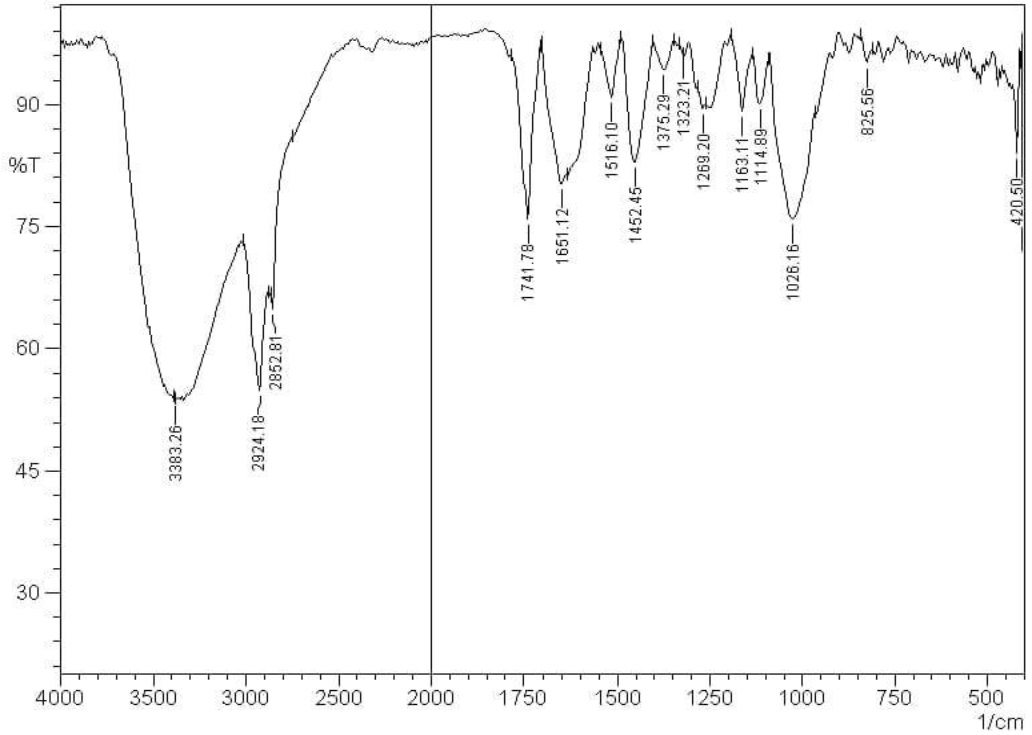

Figure 3-2: FTIR test for Natural Rosmarinus Inhibitor.

3.3.2 FTIR Test for Reed Leaves Inhibitor

Original absorption at 3369.75 cm^{-1} (associated hydroxyl) was overlapped by the strong stretching mode of (N-H) or (O-H), and that at 2920.32, and 2850.68 cm^{-1} is related to (C-H) stretching vibration. The strong band at 1653 cm^{-1} is assigned to (C=C) and (C=O) stretching vibration. Owing to the conjugation effect of flavonoids of Reed Leaves, the (C=O) peak shifts from about 1700 cm^{-1} to lower wavenumber (approximately 1653 cm^{-1}), (C=C) and (C=O) stretching vibration bands is superposition. The (C-H)bending bands in ($–CH_2$) and ($–CH_3$) are found to be at 1448.59 cm^{-1}. The absorption bands at 1247.99 cm^{-1} could be assigned to the framework vibration of the aromatic ring. Besides these, there are absorption bands at 1165.04 cm^{-1}, and 1055.10 cm^{-1}, which can be ascribed to the (C-N) or (C-O) stretching vibration. The absorption bands below 1000 cm^{-1} correspond to the aliphatic and aromatic (C-H) groups. These results indicate that Reed Leaves contain O and N atoms in the functional groups (O-H, N-H, C=C, C=O, C=N, C-N, C-O) and aromatic rings.

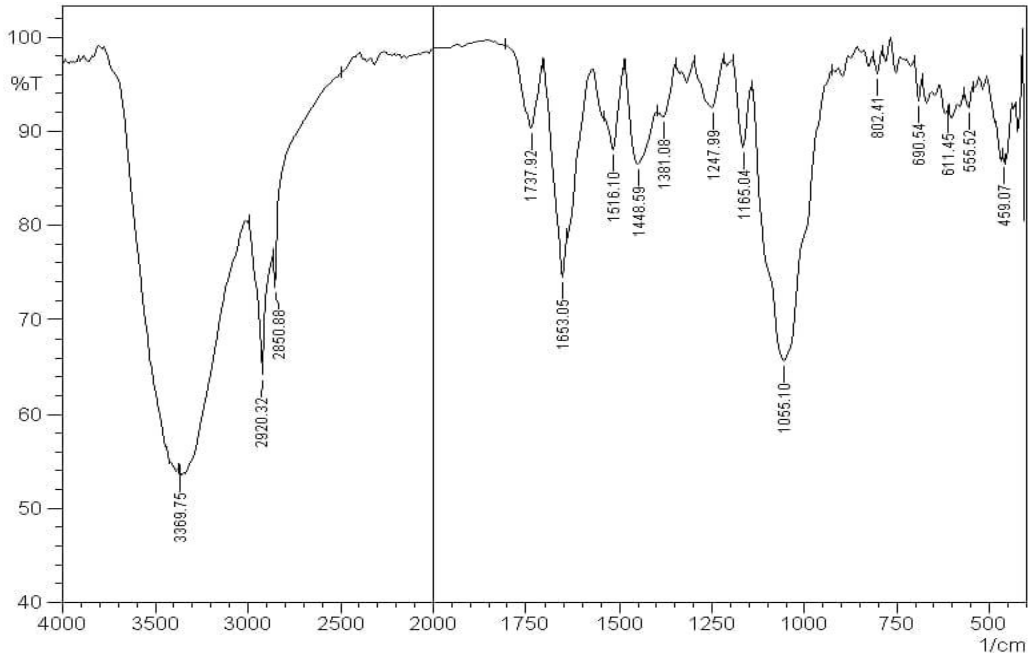

Figure 3-3: FTIR Test for Reed Leaves Inhibitor.

3.3.3 FTIR Test for Reed Stems Inhibitor

Original absorption at 3392.90 cm^{-1} (associated hydroxyl) was overlapped by the strong stretching mode of (N-H) or (O-H), and that at 2920.32 cm^{-1} is related to (C-H) stretching vibration. The strong band at 1633.76 cm^{-1} is assigned to (C=C) and (C=O) stretching vibration. Owing to the conjugation effect of flavonoids of Reed Leaves, the (C=O) peak shifts from about 1700 cm^{-1} to lower wavenumber (approximately 1633.76 cm^{-1}), (C=C) and (C=O) stretching vibration bands is superposition. The (C-H)bending bands in ($–CH_2$) and ($–CH_3$) are found to be at 1425.44 cm^{-1}. The absorption bands at 1246.06 cm^{-1} could be assigned to the framework vibration of the aromatic ring. Besides these, there are absorption bands at 1163.11 cm^{-1}, 1107.18 cm^{-1}, and 1053.17 cm^{-1}, which can be ascribed to the (C-N) or (C-O) stretching vibration. The absorption bands below 1000 cm^{-1} correspond to the aliphatic and aromatic (C-H) groups. These results indicate that Reed Leaves contain O and N atoms in the functional groups (O-H, N-H, C=C, C=O, C=N, C-N, C-O) and aromatic rings.

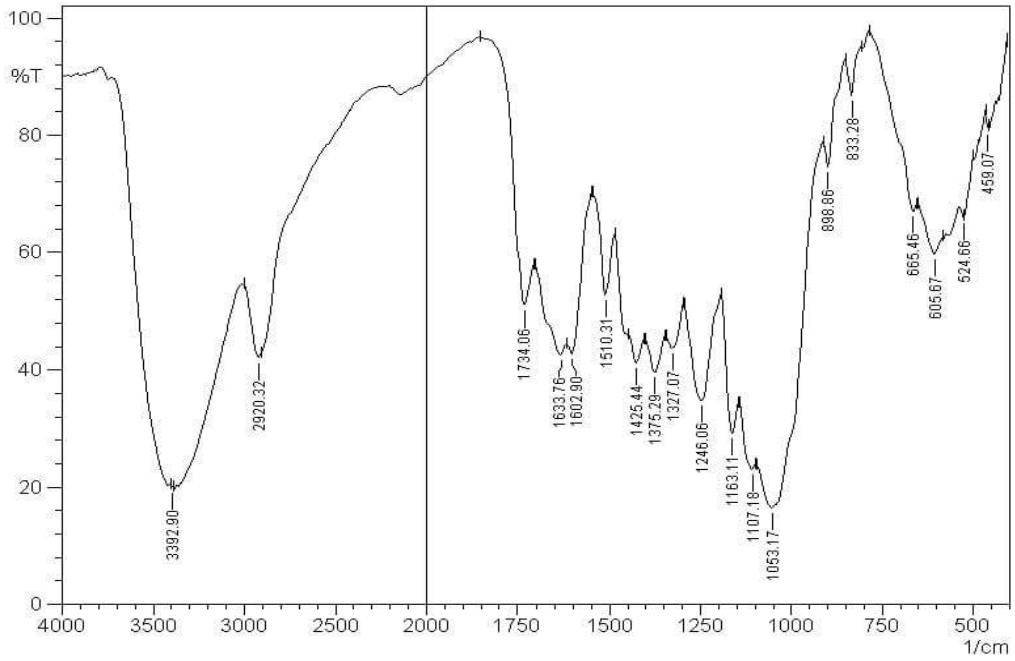

Figure 3-4: FTIR Test for Reed Stems Inhibitor.

3.3.4 FTIR Test for Orange Peels Inhibitor

Original absorption at 3410.26 cm^{-1} (associated hydroxyl) was overlapped by the strong stretching mode of (N-H) or (O-H), and that at 2928.04 is related to (C-H) stretching vibration. The strong band at 1631.83 cm^{-1} is assigned to (C=C) and (C=O) stretching vibration. Owing to the conjugation effect of flavonoids of Reed Leaves, the (C=O) peak shifts from about 1700 cm^{-1} to lower wavenumber (approximately 1631.83 cm^{-1}), (C=C) and (C=O) stretching vibration bands is superposition. The (C-H)bending bands in ($–CH_2$) and ($–CH_3$) are found to be at 1440.87 cm^{-1}. The absorption bands at 1269.20 cm^{-1} could be assigned to the framework vibration of the aromatic ring. Besides these, there are absorption bands at 1099.46 cm^{-1}, 1070.53 cm^{-1}, 1053.17 cm^{-1}, and 1030.02 cm^{-1}which can be ascribed to the (C-N) or (C-O) stretching vibration. The absorption bands below 1000 cm^{-1} correspond to the aliphatic and aromatic (C-H) groups. These results indicate that Reed Leaves contain O and N atoms in the functional groups (O-H, N-H, C=C, C=O, C=N, C-N, C-O) and aromatic rings.

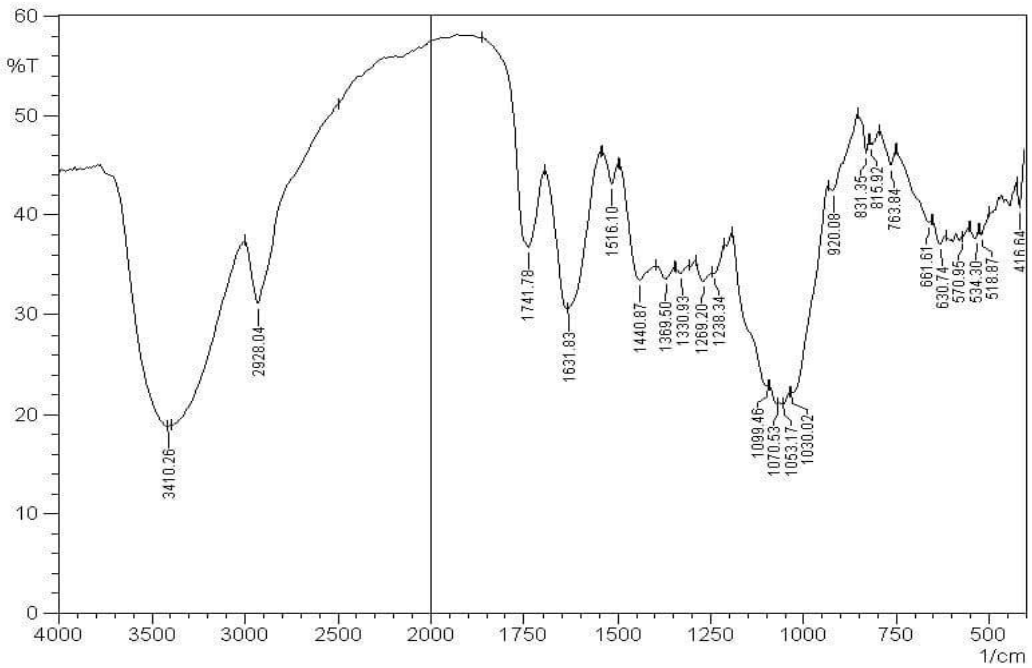

Figure 3-5: FTIR Test for Orange Peels Inhibitor.

3.4 The Corrosion Medium

Different solutions were used in the experiments:

1-The first type of solution consisting of acid is 0.1N HCl. The concentration of HCl was dissolved in distilled water to obtain the required concentration. Hydrochloric acid was produced by "Thomas Baker Company" having an assay of (35-38)% and a molecular weight of 36.46 g/mole and a specific gravity of 1.18.

2-The second type consisting of salt is 35 g/l NaCl. The concentration of NaCl was dissolved in distilled water to obtain the required concentration.

A sodium chloride (NaCl) used a salt Laboratory Sodium chloride from type HI Media Laboratories Pvt. Ltd. (India) and a molecular weight of 58.44 g/mole.

3.5 Preparing the cleaning solution

As a cleaning electrolyte for the metal specimen (before and after each test), 3% HCl is needed, which has been prepared according to the dilution law:

$$C_1 V_1 = C_2 V_2 \quad (3.1)$$

C_1: the first concentration,

C_2: the second concentration.

V_1: the first volume,

V_2: the second volume.

3.6 Experimental Apparatus

1. The working electrode (cathode): is a sheet of 99.9% pure zinc specimen with dimensions of (5 – 2 – 0.1)cm. The table (3-1) shows the physical properties of zinc metal.

Table 3-1: Physical Properties of Zinc [Zhang, 1996].

Atomic number	30
Atomic weight	65.38

Density	
Solid , 20 ° C Solid , 419.5 ° C Liquid , 419.5 ° C	7.14 g / cm³ 6.83 g / cm³ 6.62 g / cm³
Melting point	419.5 ° C
Boiling point, 1 atm	907 ° C
The heat of fusion, 419.5 ° C	7.28 kJ / mol
The heat of vaporization, 907 °C	114.7 kJ / mol
Heat capacity	
Solid , 25 ° C Liquid	25.4 J / mol 31.4 J / mol
Resistivity	
Solid , 20 ° C Liquid , 419.7 ° C	5.96 μΩ.cm 37.4 μΩ.cm
Thermal conductivity	
Solid , 18 °C Solid , 419.5 ° C Liquid , 419.5 ° C	113 W / (m.K) 96 W / (m.K) 61 W / (m.K)
viscosity,liquid,419.5 ° C	3.85 mN/m

2. Reference Electrode: A saturated calomel electrode (SCE) was used to measure the potentials. The lugging capillary of the reference electrode was placed 1mm downstream of the working electrode.

3. Auxiliary Electrode (counter): In polarization experiments, the auxiliary electrode was a rod made of high conductivity graphite, 1 cm in diameter, and located vertically opposite to the cathode at the same level.

4. Power Supply: A power supply was used to provide a constant applied voltage of 10 V between the electrodes.

5. Multimeter: Two multimeters were used. One worked as an ammeter and measured the current in mA; the other was used as a voltmeter to measure the potential in V.

6. Variable Resistance: also known as rheostat type PE 06 RN, is a type of rheostat manufactured by POPULAR that ranges from 0 to 10^6 Ohm and is used to control current flow.

7. Thermometer: the range (0 to 100) ^{O}C was used to measure the solution temperature.

8. Thermostat Water Bath: The thermostat water bath was manufactured by "The Memmert company" and has a maximum temperature range of 110 ^{o}C. It is used for high-precision temperature control of the cell.

9. The balance: was electronic with high accuracy of 4 decimal points of gram digital balance type BEL with a maximum weight of 120 g, which has an accuracy of 0.1 mg. This was used to weigh the specimen before and after the experiment in weight loss experiments.

10. An electrical oven: model DHG-9075A, with a temperature range of RT 300 ^{o}C and temperature stability ± 1.0˚C was used to dry zinc specimens.

3.7 Experimental Procedure

Before each experiment, the zinc specimen (working electrode) was polished with grit silicon carbide paper, washed with water, cleaned in 3% HCl for 5 minutes, washed in water, dried with a clean tissue, and then dried by using an electrical oven at a temperature of about 110 °C for 10 minutes.

3.7.1 Weight loss Experiments

Weight loss analysis is known to be the simplest, most reliable, and longest-established. method of assessing corrosion losses in plants and equipment.

After cooling the specimen, it is placed in the digital balance to measure the first weight, W1. After that, the specimen is exposed to a corrosion environment for 2 hours in the solution. The specimen is taken and cleaned and dried by the previous steps again, and then weighted with W_2 Where:

$$\Delta W = W_1 - W_2 \qquad (3.2)$$

By measuring the difference between two weights, the corrosion rate can be calculated using:

$$CR = \frac{\Delta W}{A \times t} \qquad (3.3)$$

The corrosion rate was also measured at different temperatures (20, 30, 40, 50, and 60)˚C, and at different green inhibitors concentrations.

3.7.2 Free corrosion potential Experiments

Free corrosion potential is the absence of a net electrical current that flows to and from a metal's surface. The corroding metal has a potential that is expressed as E_{corr}. The free corrosion potential is measured through the voltage difference between the immersed metal and the appropriate reference electrode in a given environment.

Measurements were obtained by using two electrodes: a zinc specimen as the working electrode and a saturated calomel electrode (SCE) as the reference electrode. After preparing the specimen with the previous steps, it was immersed in a salt solution of 3.5% NaCl and an acid solution of 0.1N HCl. A reading was taken every 10 minutes for 2 hours using a voltmeter, and the corrosion potential was determined at different temperatures and concentrations of inhibitor.

Figure 3-6: Picture of free corrosion potential Experiment.

3.7.3 Polarization Experiments

In electrochemical cells, an external source of power is used to drive current through the system, and hence there is a shift of electrode potential from its equilibrium value which is called polarization. Measurements were obtained by using a zinc electrode with a graphite electrode as a counter electrode and a saturated calomel electrode (SCE) as a reference with a Lugging capillary bridge. The tests were performed at (20,30,40,50,60 °C), with readings taken every 3 minutes.

The Electrochemical Polarization Experiments determine the E_{corr} corrosion current and corrosion potential using the Tafel method. The solution was prepared and heated to the required temperature by using a thermostat water bath. Then the electrical circuit was connected and after completing all electrical connections, the electrical circuit was switched on, the DC power supply constant at 10 V. Maximum current passes through the cell because the resistance is very low. After waiting some

time to reach the steady-state value, they recorded the readings of potential and cathodic current from the voltmeter and ammeter respectively. The specimen was cathodically polarized and could be drawn with the cathodic curve. By replacing the anodic and cathodic connections to the DC power supply changing the resistances from higher to lower values and recording the potential and anodic current, we can draw the polarization anodic curve by using a semi-log scale where the x-axis represents the current density (log scale) and the y-axis represents the potential in Fig. (3-7) and Fig. (3-8). The above procedure was repeated exactly for the other conditions of inhibitor concentrations, and different temperatures.

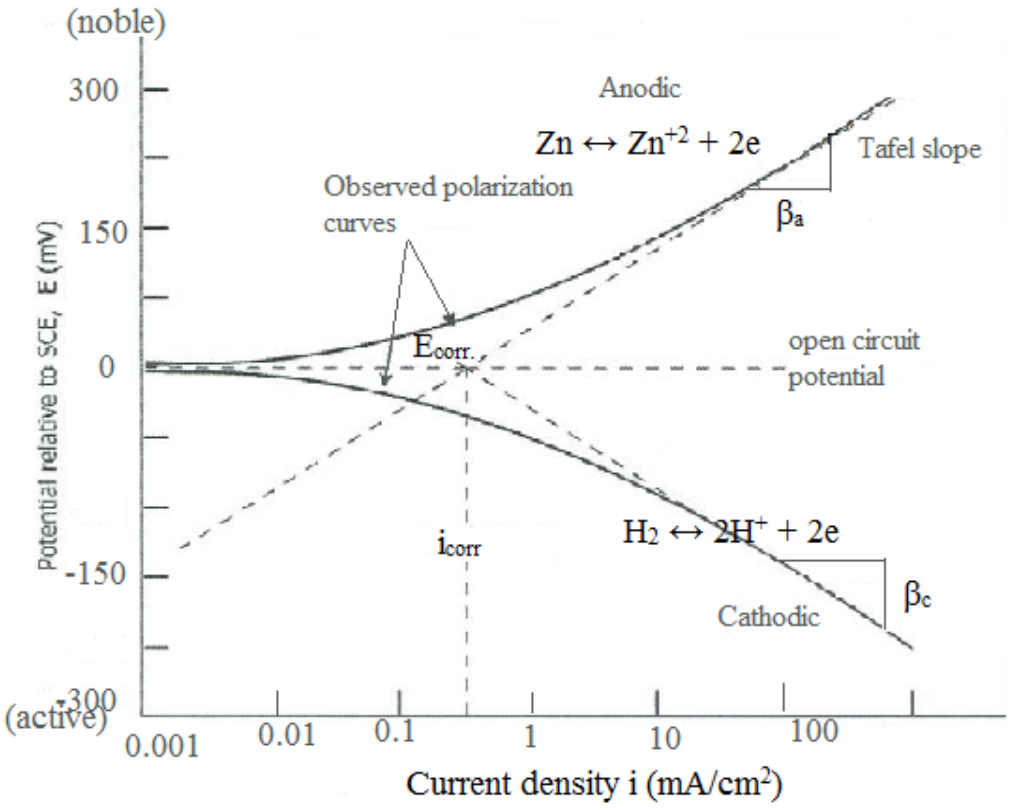

Figure 3-7: Polarization Plot for Acidic Solution.

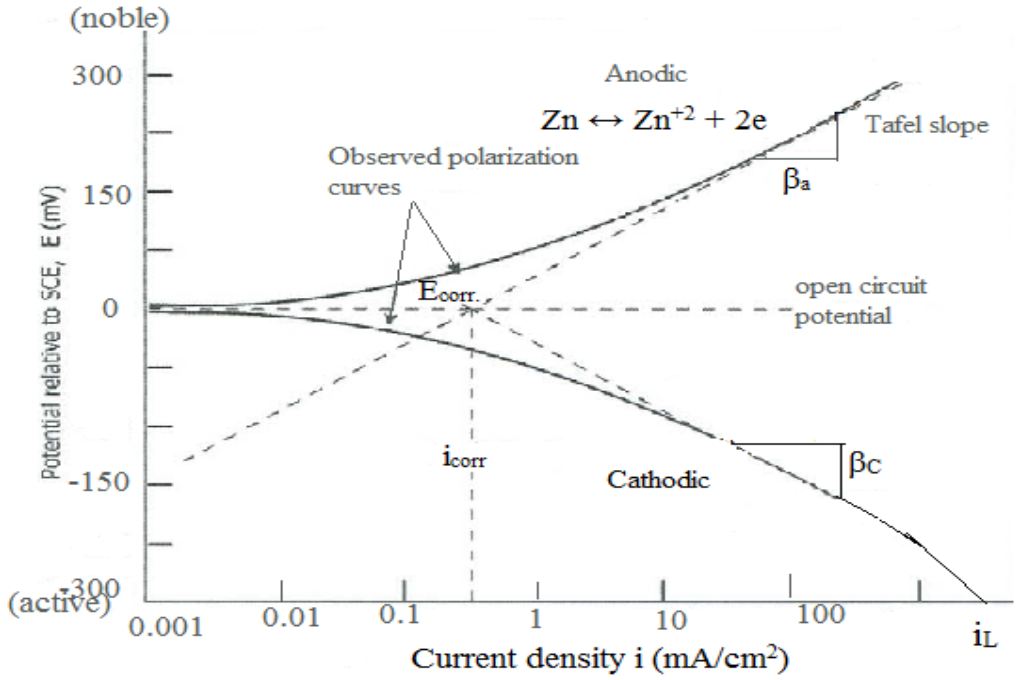

Figure 3-8: Polarization Plot for Salt Solution.

Figure 3-9: Picture of Polarization Experiment.

Chapter Four

Result And Discussion

This chapter presents the experimental results and discussions for the whole investigated ranges of inhibitor concentrations and temperatures because the influence of these variables on the experimental data in acid and salt solutions needs to be interpreted and understood. (4.1) explains the weight loss experiment results. (4.2)explains the free corrosion potential experiment. The results of the polarization experiments are explained in the (4.3) section. Also, limiting current density and Mass Transfer Results are explained in (4.4).

4.1 Weight loss experiment Results and Discussion

The weight loss of zinc in the absence and presence of different inhibitor concentrations and temperatures in acid and salt solutions. The rate of corrosion (gmd, mm/y), the values of dissolution current density (i_d), and the inhibition efficiency were calculated and given in five Tables (4-1 to 4-5). The properties of zinc and the equations are presented in appendix A.

Table 4-1:The Effect of rosemary Inhibitor (by weight loss)on Zinc Specimen in 0.1N HCl solution of at 2 hrs immersion period.

T °C	C (g/L)	ΔW (g)	C_R (gmd)	C_R (mm/y)	i_d (mA/cm^2)	η%
20	0	0.0161	96.64	35.27	0.3299	
	1	0.01	60.02	21.91	0.2049	37.89
	5	0.0082	49.22	17.96	0.1680	49.07
30	0	0.033	198.08	72.29	0.6761	

	1	0.0203	121.85	44.47	0.4159	38.48
	5	0.0172	103.24	37.68	0.3524	47.88
40	0	0.0646	387.76	141.52	1.3235	
	1	0.0419	251.50	91.79	0.8584	35.14
	5	0.035	210.08	76.67	0.7171	45.82
50	0	0.0967	580.43	211.84	1.9812	
	1	0.0685	411.16	150.06	1.4034	29.16
	5	0.0587	352.34	128.59	1.2026	39.30
60	0	0.1056	633.85	231.33	2.1635	
	1	0.0761	456.78	166.71	1.5591	27.94
	5	0.0673	403.96	147.43	1.3788	36.27

Table 4-2:The Effect of rosemary Inhibitor (by weight loss)on Zinc Specimen in 3.5%NaCl solution of at 2 hrs immersion period.

T °C	**C (g/L)**	**ΔW (g)**	**C_R (gmd)**	**C_R (mm/y)**	**i_d (mA/cm^2)**	**η%**
20	0	0.0004	2.401	0.876	0.008	
	1	0.0002	1.200	0.438	0.004	50.00
	5	0.0001	0.660	0.241	0.002	72.50
30	0	0.0010	6.002	2.191	0.020	
	1	0.0005	3.241	1.183	0.011	46.00
	5	0.0004	2.101	0.767	0.007	65.00
40	0	0.0052	31.212	11.391	0.107	
	1	0.0029	17.407	6.353	0.059	44.23
	5	0.0021	12.605	4.600	0.043	59.62

50	0	0.0070	42.017	15.335	0.143	
	1	0.0043	25.810	9.420	0.088	38.57
	5	0.0029	17.407	6.353	0.059	58.57
60	0	0.0109	65.426	23.878	0.223	
	1	0.0072	43.217	15.773	0.148	33.94
	5	0.0053	31.813	11.610	0.109	51.38

Table 4-3:The Effect of reed leaves Inhibitor (by weight loss) on Zinc Specimen in 3.5%NaCl solution of at 2 hrs immersion period.

T °C	**C (g/L)**	**ΔW (g)**	**C_R (gmd)**	**C_R (mm/y)**	**i_d (mA/cm^2)**	**η%**
20	0	0.0004	2.401	0.876	0.0082	
	1	0.0002	1.140	0.416	0.0039	52.50
	5	0.0001	0.660	0.241	0.0023	72.50
30	0	0.0010	6.002	2.191	0.0205	
	1	0.0005	3.001	1.095	0.0102	50.00
	5	0.0003	1.921	0.701	0.0066	68.00
40	0	0.0052	31.212	11.391	0.1065	
	1	0.0029	17.407	6.353	0.0594	44.23
	5	0.0020	12.005	4.381	0.0410	61.54
50	0	0.0070	42.017	15.335	0.1434	
	1	0.0043	25.810	9.420	0.0881	38.57
	5	0.0033	19.808	7.229	0.0676	52.86
60	0	0.0109	65.426	23.878	0.2233	
	1	0.0065	39.016	14.239	0.1332	40.37
	5	0.0053	31.813	11.610	0.1086	51.38

Table 4-4: The Effect of reed stems Inhibitor (by weight loss)on Zinc Specimen in 3.5%NaCl solution of at 2 hrs immersion period.

T °C	C (g/L)	ΔW (g)	C_R (gmd)	C_R (mm/y)	i_d (mA/cm^2)	η%
20	0	0.0004	2.401	0.876	0.0082	
	1	0.0002	1.020	0.372	0.0035	57.50
	5	0.0001	0.600	0.219	0.0020	75.00
30	0	0.0010	6.002	2.191	0.0205	
	1	0.0004	2.641	0.964	0.0090	56.00
	5	0.0003	1.741	0.635	0.0059	71.00
40	0	0.0052	31.212	11.391	0.1065	
	1	0.0021	12.605	4.600	0.0430	59.62
	5	0.0017	10.204	3.724	0.0348	67.31
50	0	0.0070	42.017	15.335	0.1434	
	1	0.0034	20.408	7.448	0.0697	51.43
	5	0.0026	15.606	5.696	0.0533	62.86
60	0	0.0109	65.426	23.878	0.2233	
	1	0.0055	33.013	12.049	0.1127	49.54
	5	0.0045	27.011	9.858	0.0922	58.72

Table 4-5: The Effect of orange peels Inhibitor (by weight loss)on Zinc Specimen in 3.5%NaCl solution of at 2 hrs immersion period.

T °C	C (g/L)	ΔW (g)	C_R (gmd)	C_R (mm/y)	i_d (mA/cm^2)	η%
20	0	0.0004	2.401	0.876	0.0082	
	1	0.0002	1.405	0.513	0.0048	41.50

	5	0.0002	1.261	0.460	0.0043	47.50
30	0	0.0010	6.002	2.191	0.0205	
	1	0.0007	3.902	1.424	0.0133	35.00
	5	0.0006	3.361	1.227	0.0115	44.00
40	0	0.0052	31.212	11.391	0.1065	
	1	0.0034	20.408	7.448	0.0697	34.62
	5	0.0030	18.007	6.572	0.0615	42.31
50	0	0.0070	42.017	15.335	0.1434	
	1	0.0050	30.012	10.953	0.1024	28.57
	5	0.0044	26.411	9.639	0.0901	37.14
60	0	0.0109	65.426	23.878	0.2233	
	1	0.0087	52.221	19.059	0.1782	20.18
	5	0.0075	45.018	16.430	0.1537	31.19

4.1.1 Effect of Temperature on Corrosion Rate

The temperature has a great effect on the rate of metal dissolution. Figures 4-1, 4-5, and Tables 4-1 to 4-5. Results shown in the table revealed that corrosion rates increase with the increase in temperature for all the systems studied. The highest corrosion rate (231.33 mm/y) and 23.878 mm/y was obtained at 60 ◦C in acidic solution and salt solution. In the presence of rosemary, reed leaves, reed stems, and orange peels, the corrosion rate was observed to reduce significantly indicating that green inhibitors inhibited the corrosion of zinc metal in the acidic and slat solution. environment. Further reduction in corrosion rate was observed with the addition of 5g/l. The protective films on the metal surface become more soluble with increasing temperatures. The presence of a high concentration of oxygen caused the metal to corrode faster. Also, for solids, solubility generally increases with increasing

temperature. This may explain why the protective film became more soluble as the temperature increased. It follows from the figure that the current density (and hence the rate of corrosion) increased, and therefore the corrosion inhibition decreased, with an increase in temperature. This shows that the inhibitor has experienced a significant decrease in its protective properties of the inhibitor with an increase in temperature. One possible mechanism of inhibition action of inhibitors as reported by Umoren and Ebenso [Umoren, & Ebenso, 2007] is the adsorption of the inhibitor onto the metal surface, which blocks the metal surface and does not permit the corrosion process to take place, but after immersion time in solutions, the Increasing temperature leads to change two variables that act in a conflicting way. Firstly, increasing temperature accelerates the reaction rate as dictated by the Arrhenius equation. Moreover, the diffusion rate of dissolved oxygen by increasing the molecular diffusion coefficient. Secondly, as the temperature increases the oxygen solubility decreases [Kader, 2013].

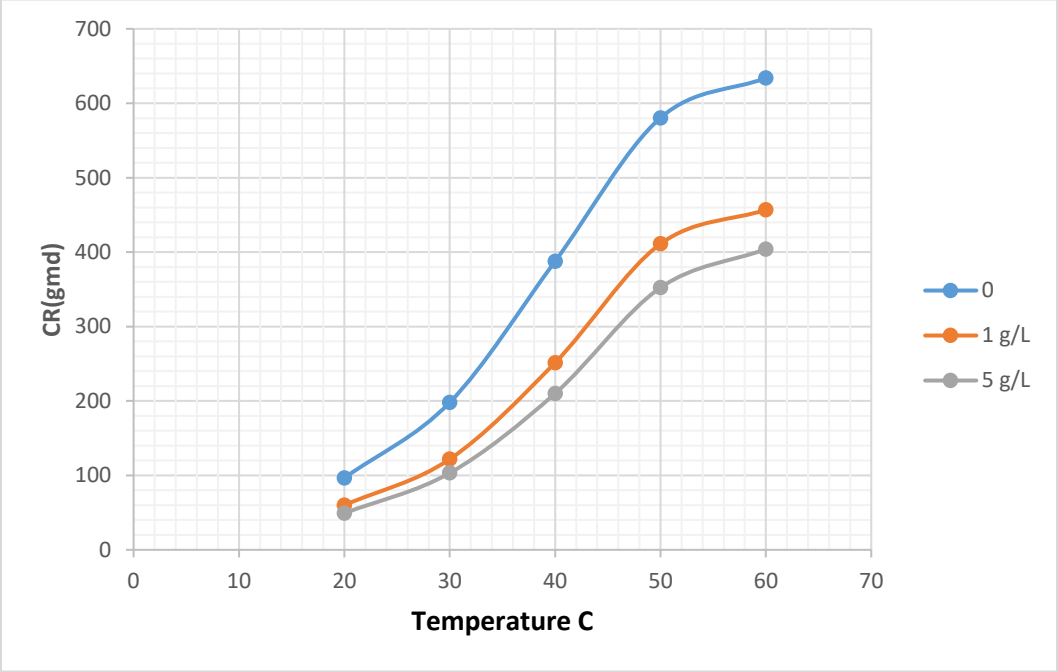

Figure 4-1: Effect of Temperature on Corrosion Rate of Zinc Specimen in 0.1N HCl solution with different concentrations of rosemary.

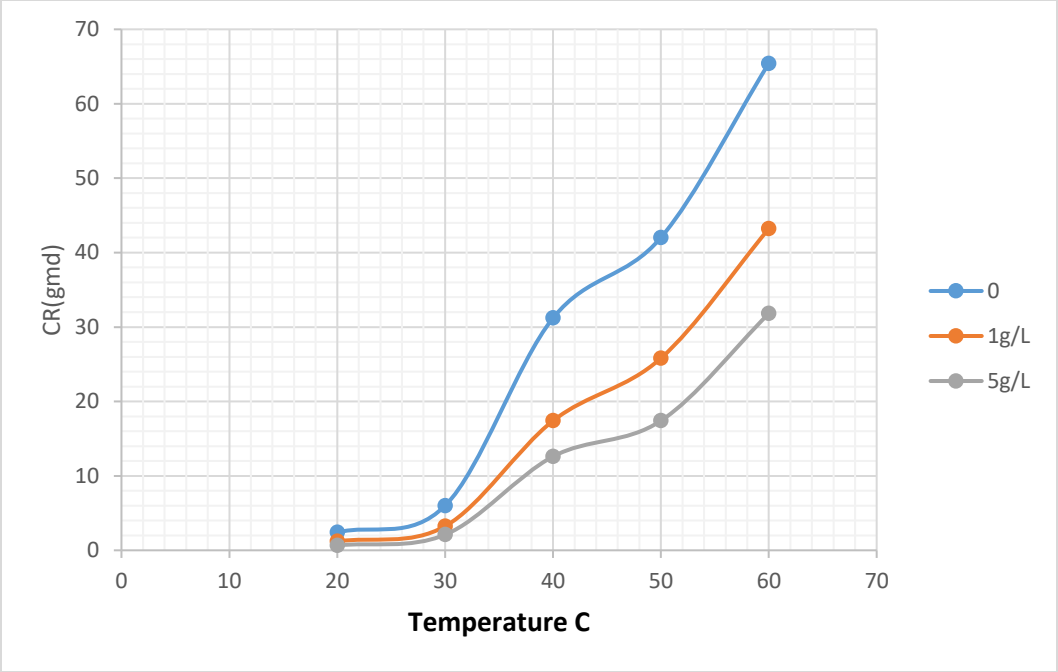

Figure 4-2: Effect of Temperature on Corrosion Rate of Zinc Specimen in 3.5%NaCl solution with different concentrations of rosemary.

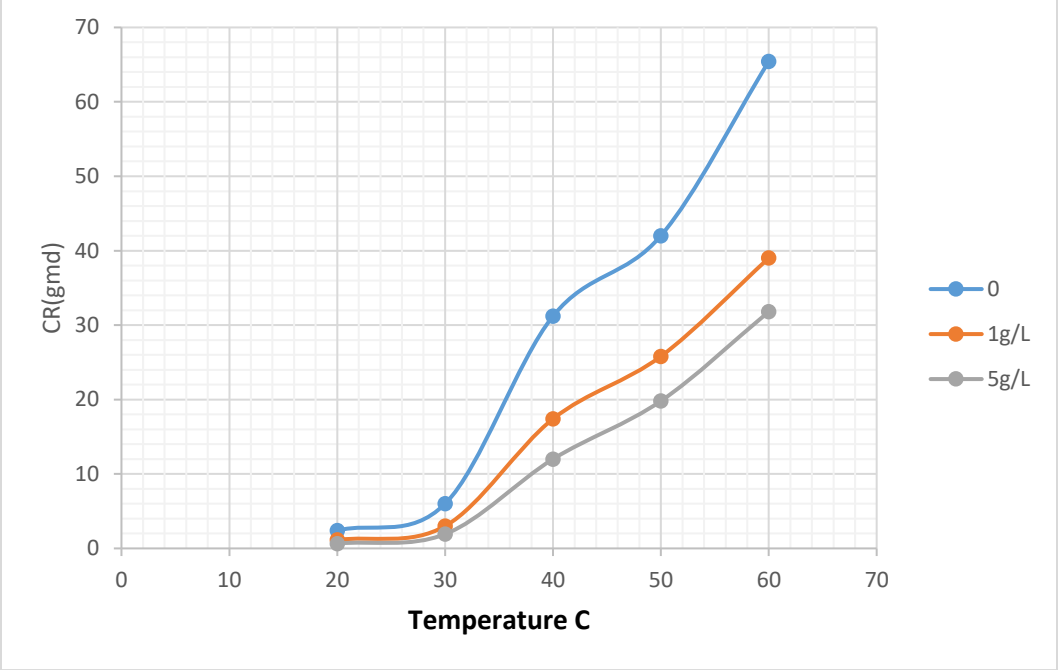

Figure 4-3: Effect of Temperature on Corrosion Rate of Zinc Specimen in 3.5%NaCl solution with different concentrations of reed leaves.

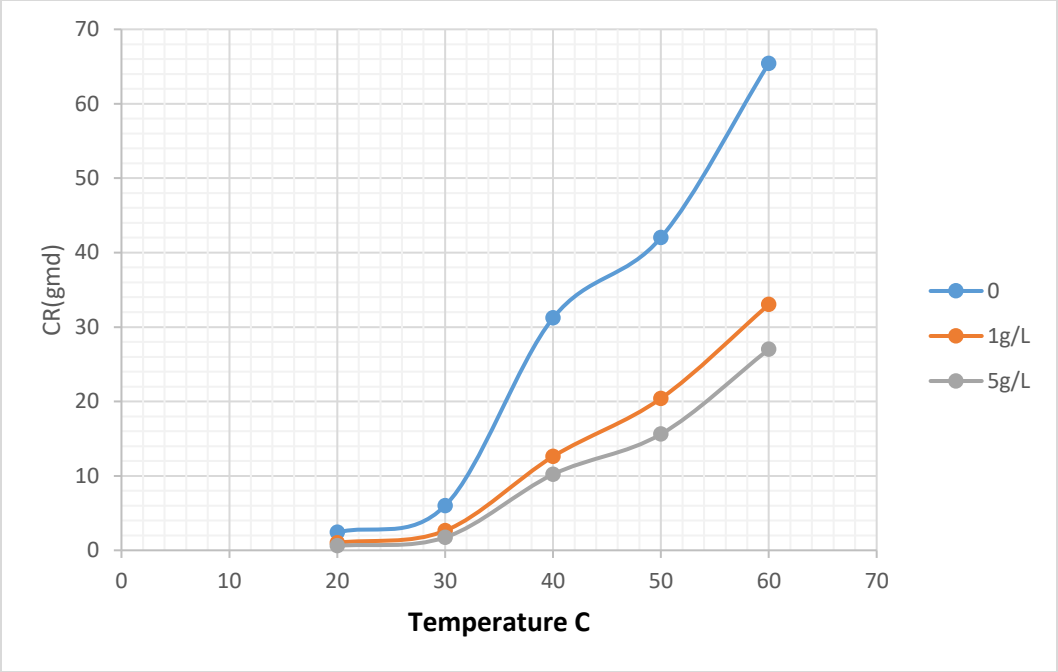

Figure 4-4: Effect of Temperature on Corrosion Rate of Zinc Specimen in 3.5%NaCl solution with different concentrations of reed stems.

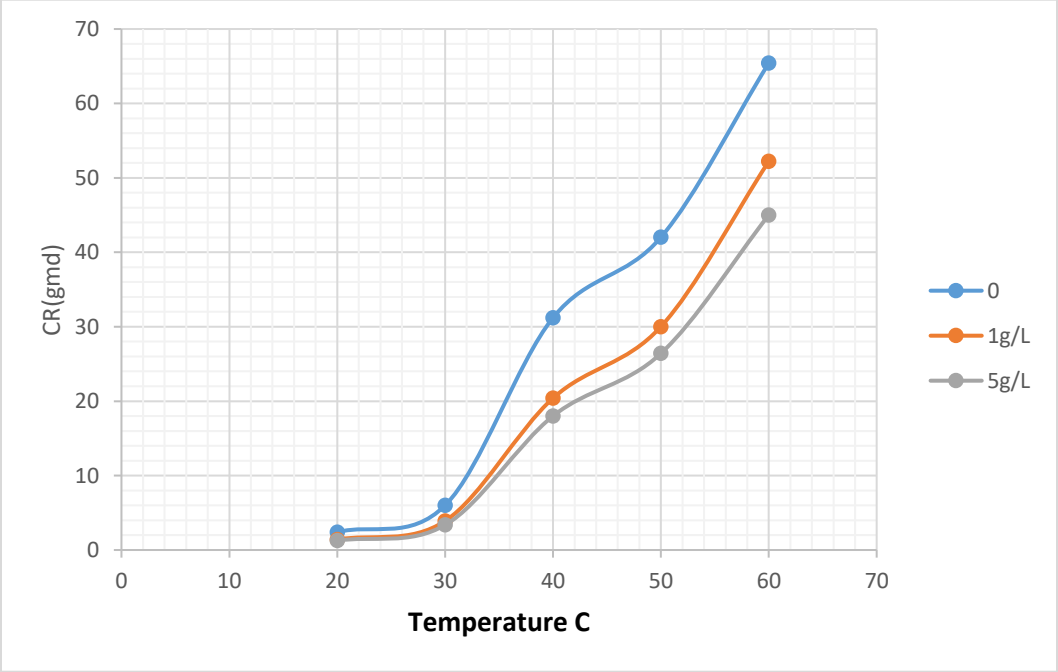

Figure 4-5: Effect of Temperature on Corrosion Rate of Zinc Specimen in 3.5%NaCl solution with different concentrations of orange peels.

4.1.2 Effect of Inhibitor Concentration on Corrosion Rate

From Figures 4-6 to 4-10 and Tables 4-1 to 4-5, it is clear that the inhibition efficiency increases gradually at all studied temperatures. Examination of the figures revealed that the inhibition efficiency increases with the increasing concentration of the inhibitor and decreases with increasing temperature. Where the highest inhibition efficiency was obtained 49.0% and 75% at 20 °C for the acid and saline solution, respectively. The decrease in the inhibition efficiency with increasing temperature may be attributed to the increase in the solubility of the protective films and any of them are the reaction products deposited on the surface of the metal that may inhibit the reaction rate in another way .

Inhibitors form films in several ways: by adsorption, the formation of bulky precipitates, and/or the formation of a passive layer on the metal surface. Some inhibitors retard corrosion by adsorption to form a thin, invisible film only a few molecules thick. Others form bulky precipitates that coat the metal and protect it from attack. A third mechanism consisted of causing the metal to corrode in such a way that a combination of adsorption and corrosion product forms a passive layer [Ibrahim, and Zour, 2011] .

Adsorption of inhibitors results in the formation of bulky precipitates as shown in fig (4-6). The efficiency of inhibition improves as the inhibitor concentration increases. His results show that increasing the extract concentration increases the number of inhibitor molecules adsorbed onto the zinc surface and decreases the surface area available for a direct acid attack. It is well known that many organic compounds can reduce the corrosion rate of metals significantly. Inhibitors reduced the rate of either or both of the partial reactions of the corrosion process: the anodic metal dissolution and the cathodic oxygen reduction [Marcus, 2002].

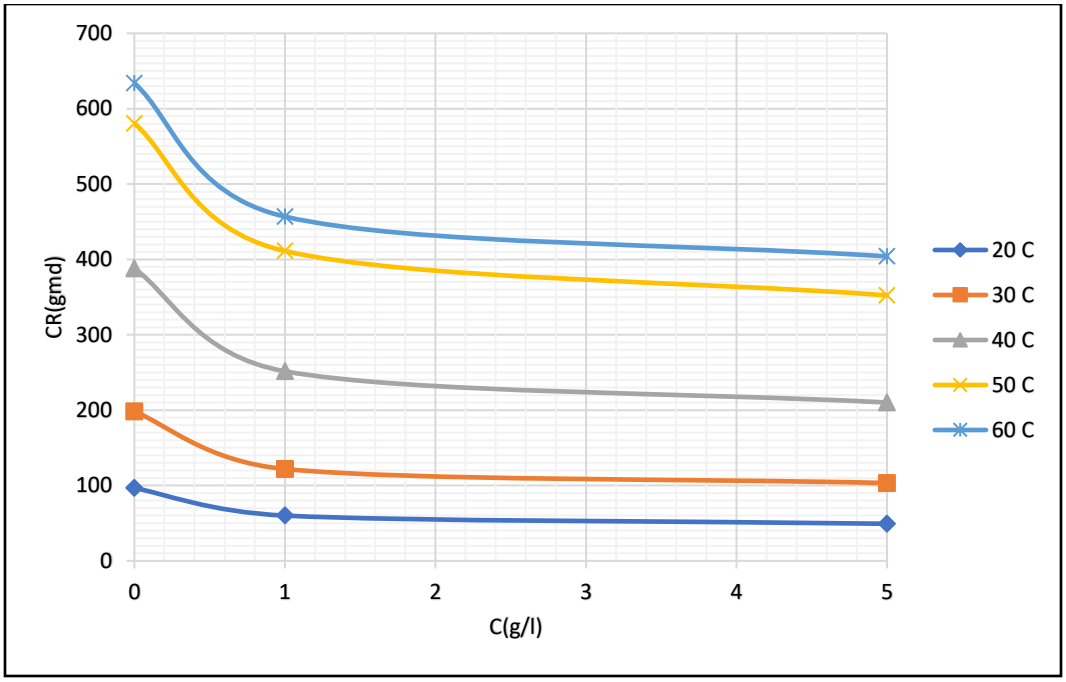

Figure 4-6: Effect of rosemary Inhibitor Concentration on Corrosion Rate of Zinc Specimen in 0.1N HCl solution.

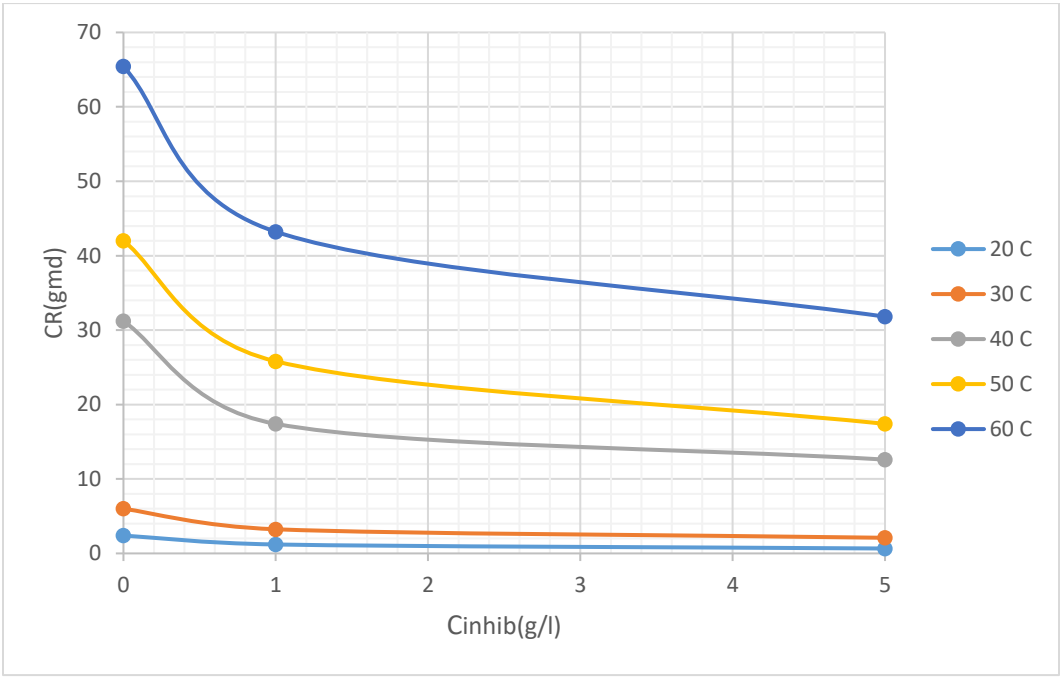

Figure 4-7 : Effect of Inhibitor rosemary Concentration on Corrosion Rate of Zinc Specimen in 3.5% NaCl solution.

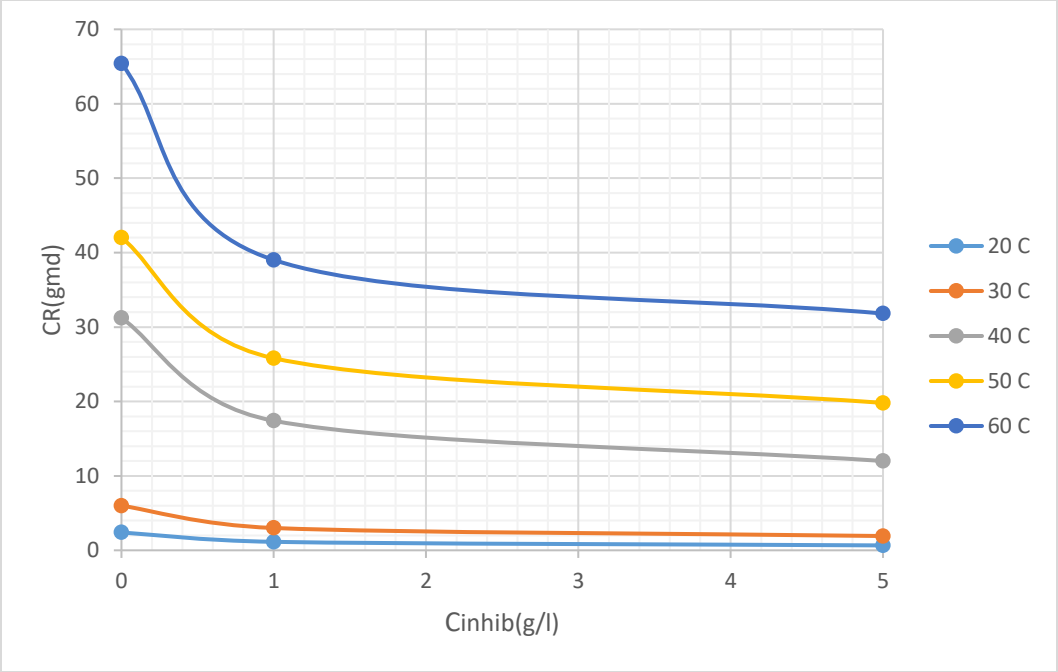

Figure 4-8 : Effect of Inhibitor reed leaves Concentration on Corrosion Rate of Zinc Specimen in 3.5%NaCl solution.

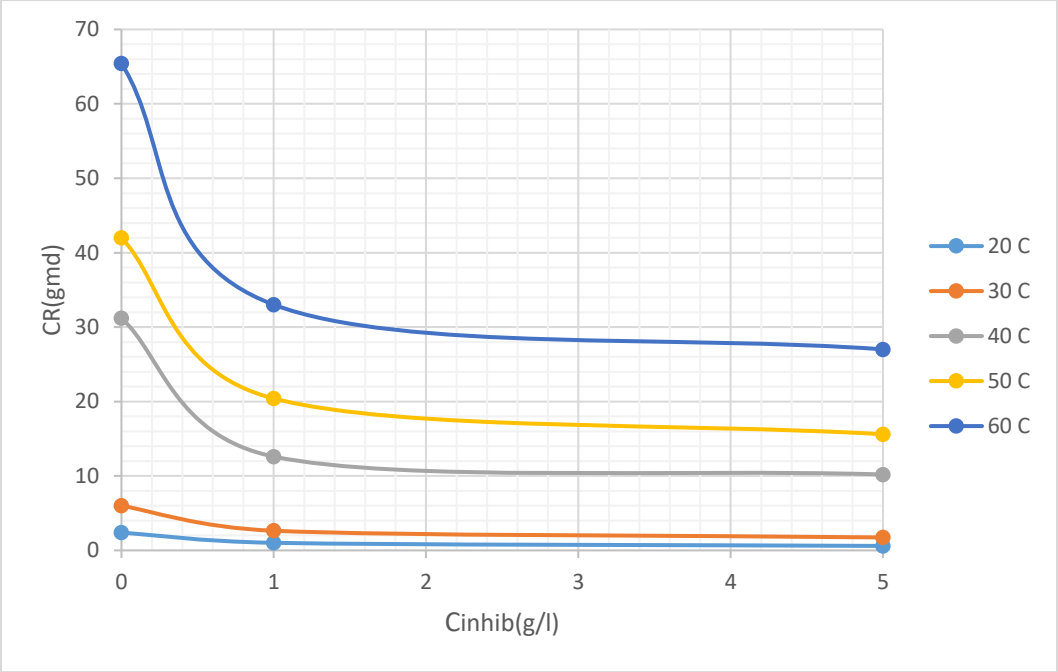

Figure 4-9: Effect of Inhibitor reed stems Concentration on Corrosion Rate of Zinc Specimen in 3.5%NaCl solution.

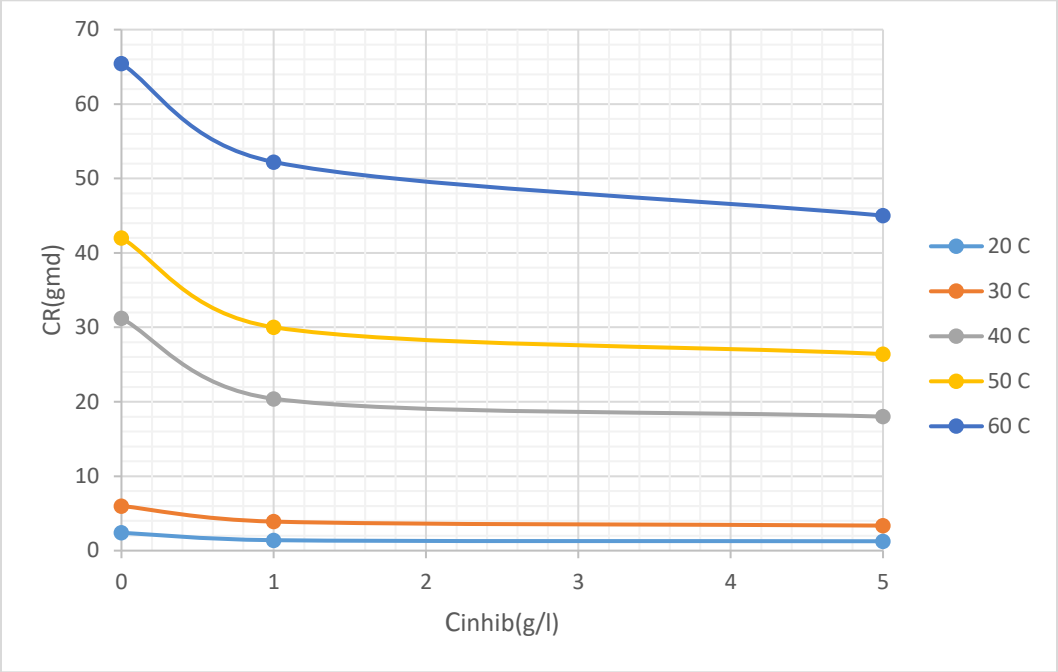

Figure 4-10: Effect of Inhibitor orange peels Concentration on Corrosion Rate of Zinc Specimen in 3.5%NaCl solution.

4.2 Free corrosion potential experiment Results and Discussion

Figures from (4-11) to (4-23) show the behavior of zinc corrosion potential with time in acid solution and salt solution at different temperatures. From these figures and appendix B, it can be noticed that the potential becomes more negative with time. This behavior was due to the depletion of O_2 because of its high reduction on the metal surface. It is known that a simple way to study the film formation and passivation of materials in a solution is to monitor the E_{corr} as a function of time.

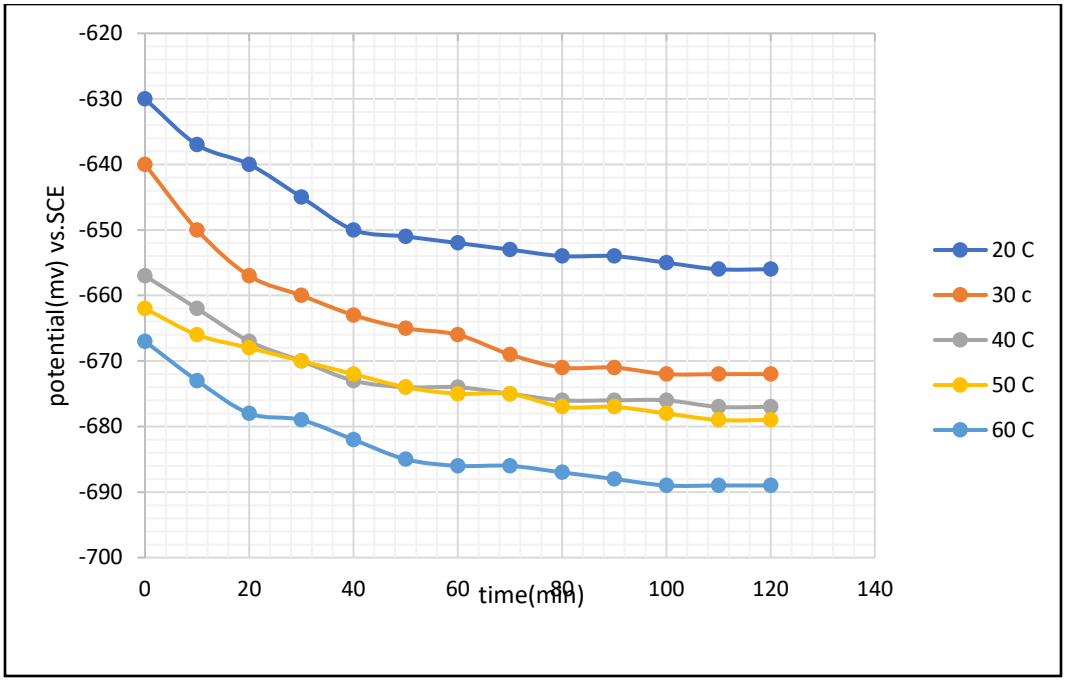

Figure 4-11: Behavior of Zinc Corrosion Potential vs. SCE with Time in 0.1N HCl solution without Inhibitor.

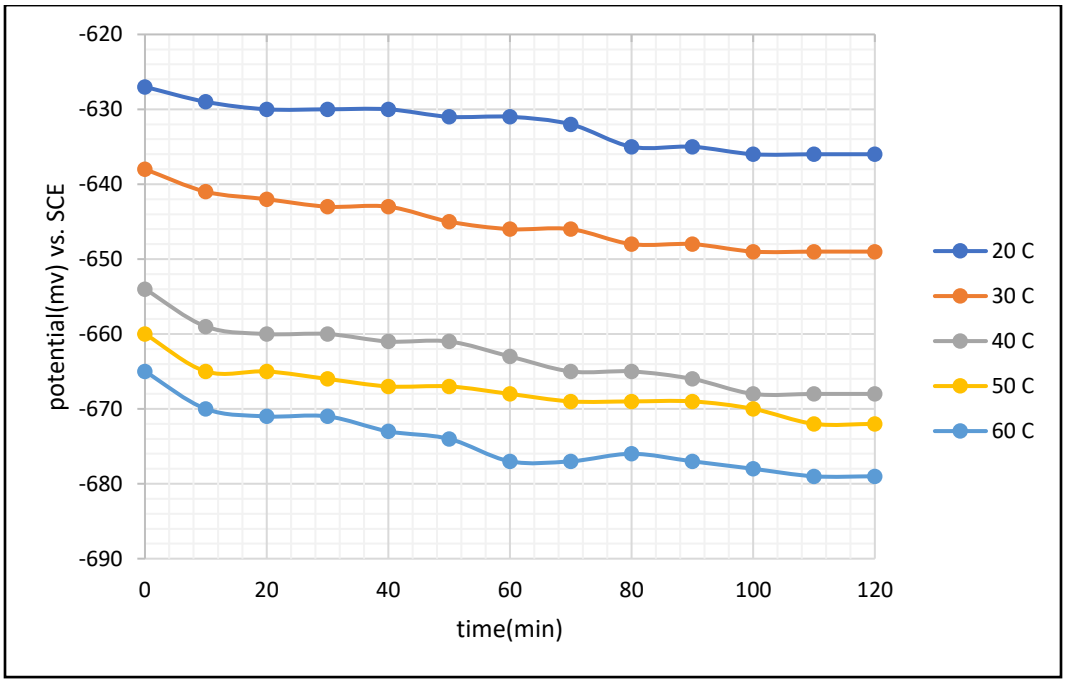

Figure 4-12: Behavior of Zinc Corrosion Potential vs. SCE with Time in 0.1N HCl solution with 1gm/l rosemary Inhibitor.

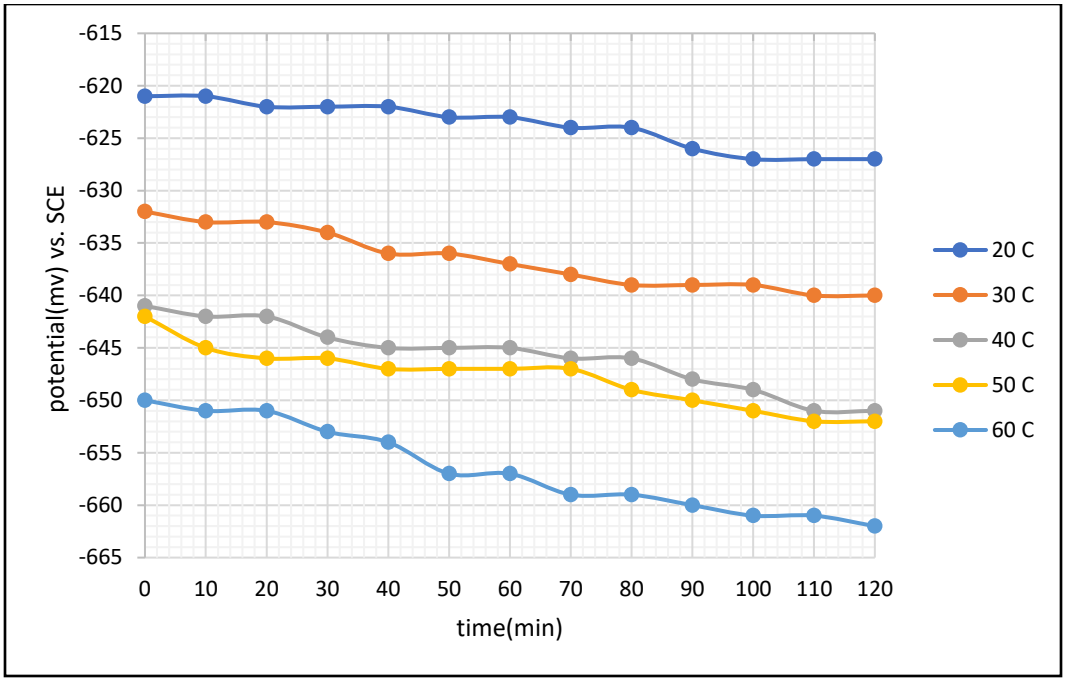

Figure 4-13: Behavior of Zinc Corrosion Potential vs. SCE with Time in 0.1N HCl solution with 5gm/l rosemary Inhibitor.

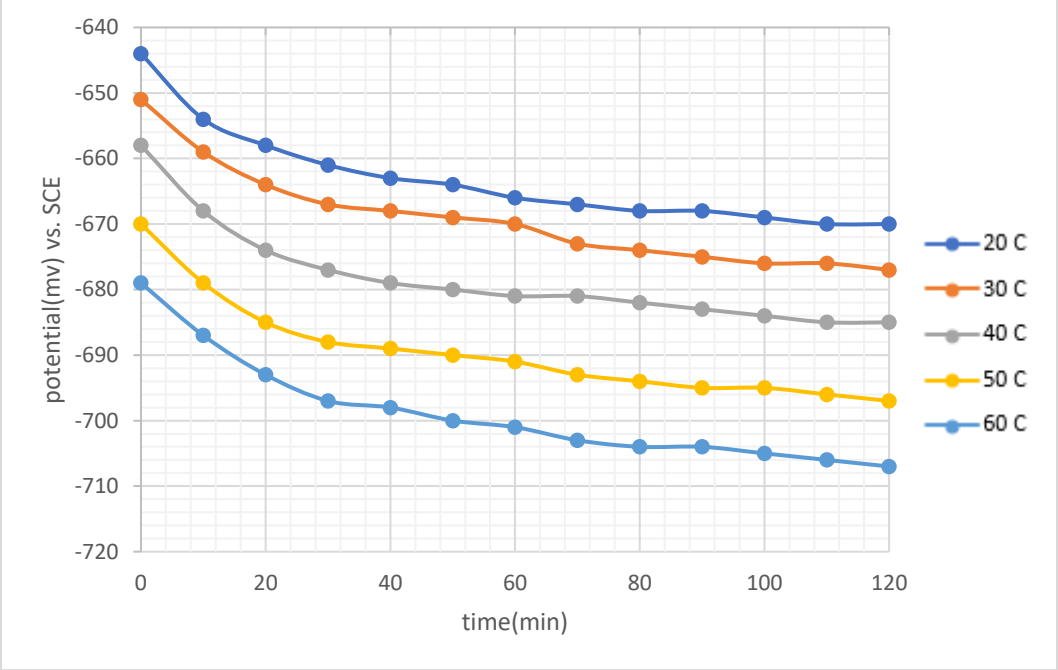

Figure 4-14: Behavior of Zinc Corrosion Potential vs. SCE with Time in 3.5%NaCl solution without Inhibitor.

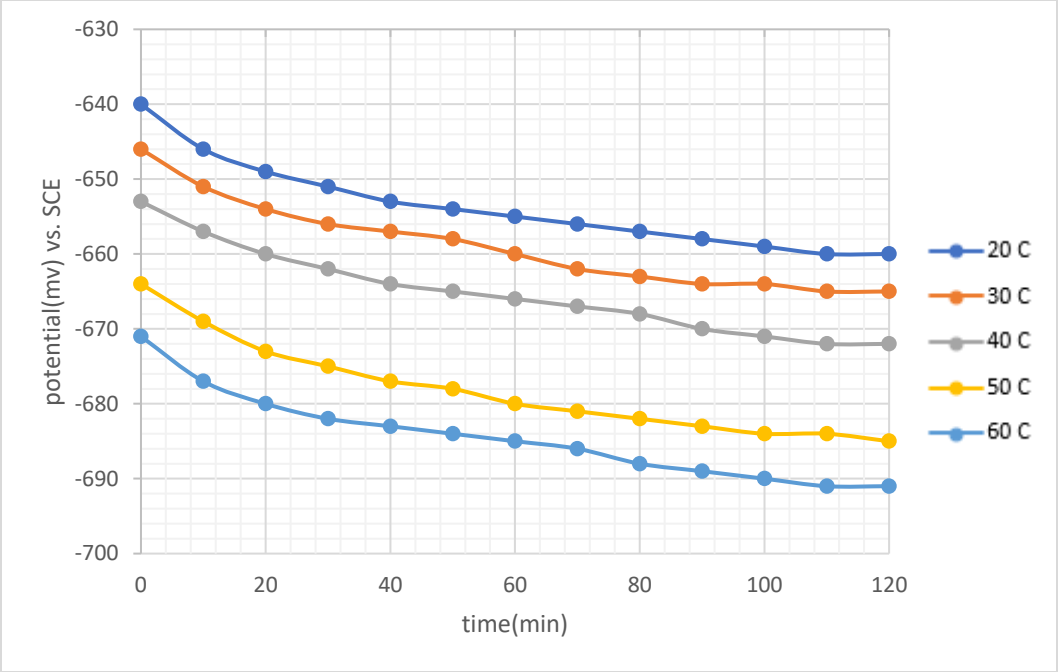

Figure 4-15: Behavior of Zinc Corrosion Potential vs. SCE with Time in 3.5%NaCl solution with 1gm/l rosemary Inhibitor.

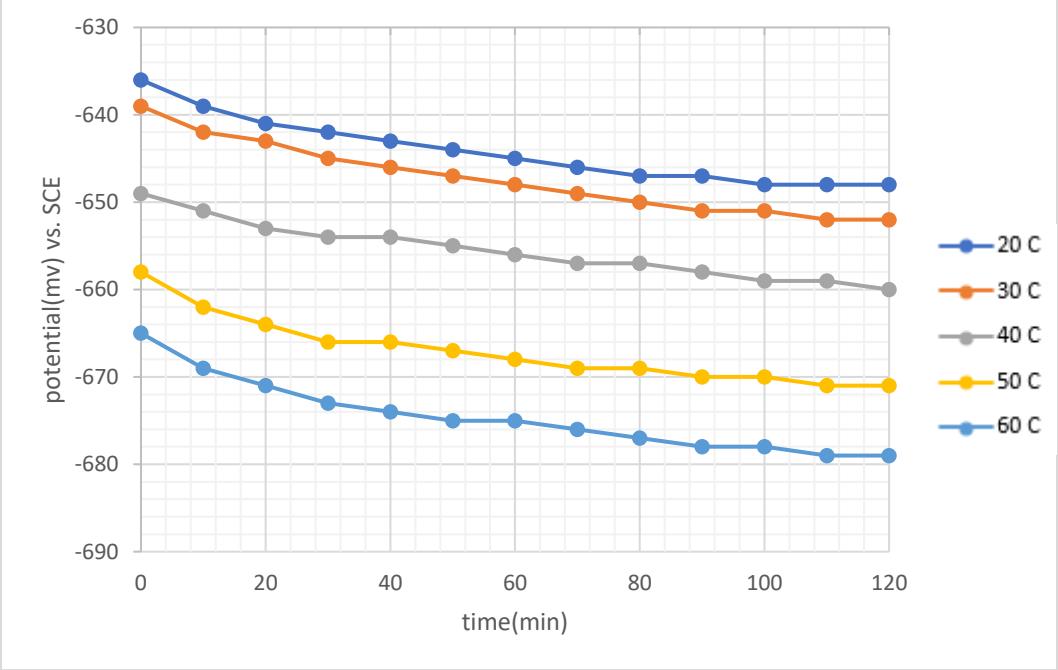

Figure 4-16: Behavior of Zinc Corrosion Potential vs. SCE with Time in 3.5%NaCl solution with 5gm/l rosemary Inhibitor.

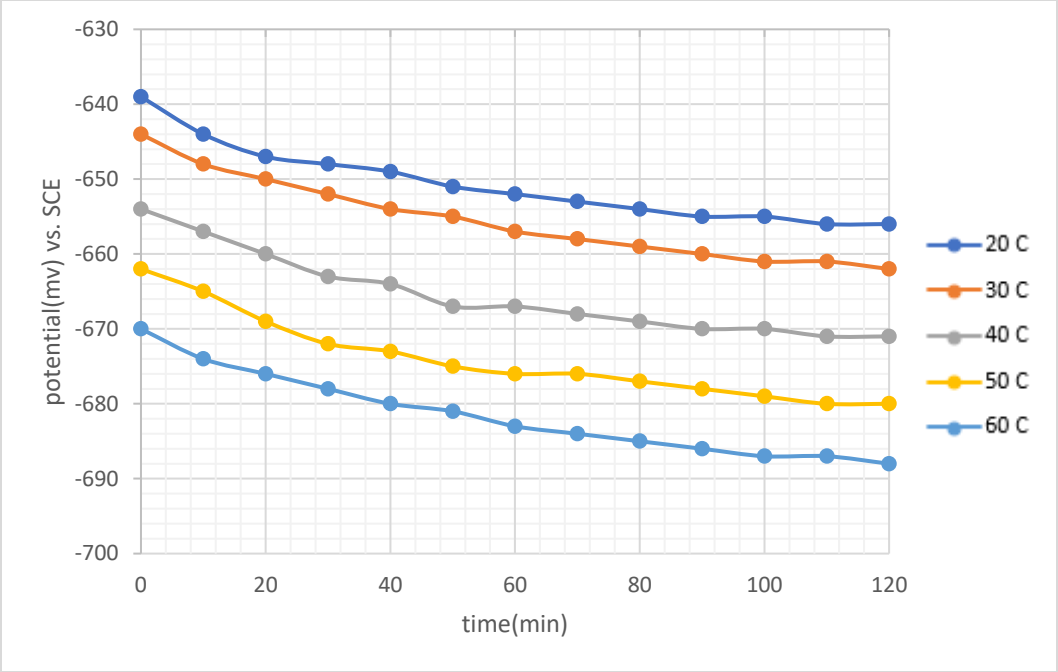

Figure 4-17: Behavior of Zinc Corrosion Potential vs. SCE with Time in 3.5%NaCl solution with 1gm/l reed leaves Inhibitor.

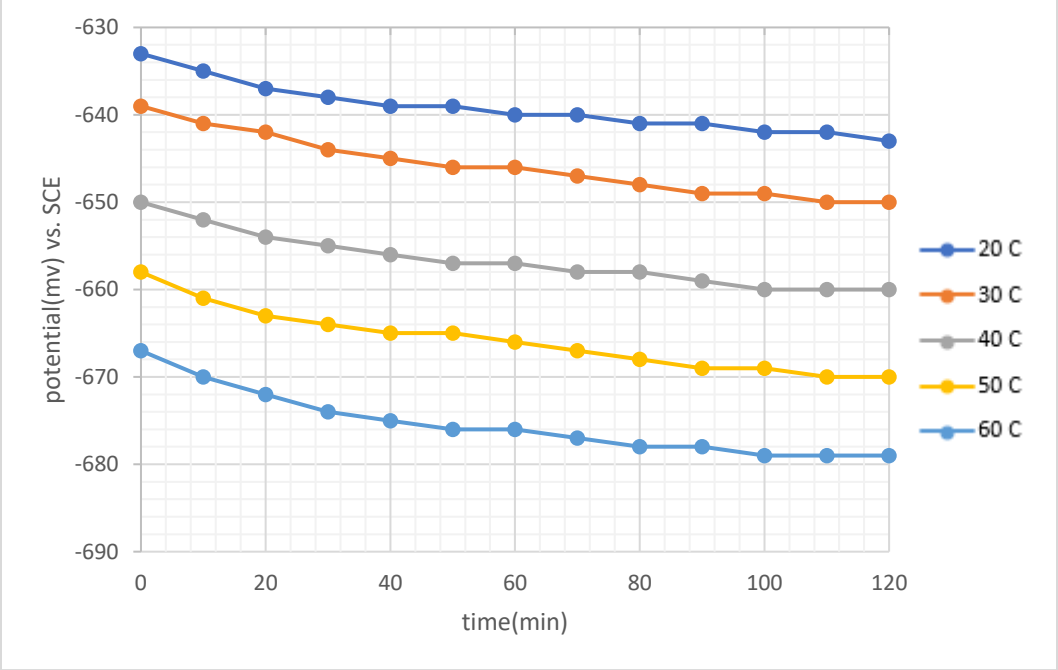

Figure 4-18: Behavior of Zinc Corrosion Potential vs. SCE with Time in 3.5%NaCl solution with 5gm/l reed leaves Inhibitor.

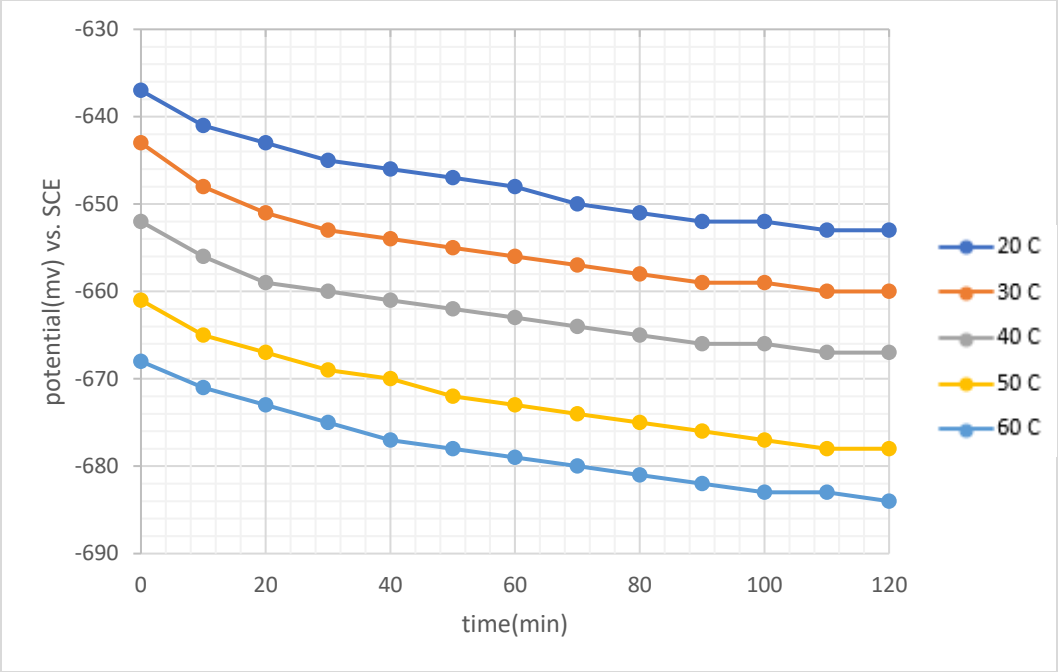

Figure 4-19: Behavior of Zinc Corrosion Potential vs. SCE with Time in 3.5%NaCl solution with 1gm/l reed stems Inhibitor.

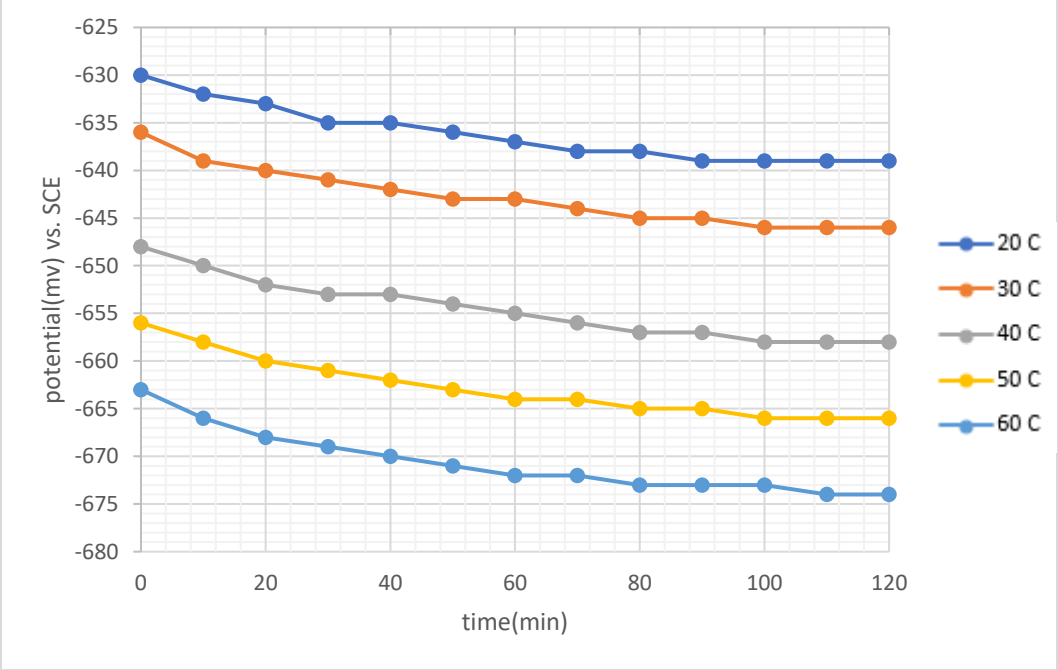

Figure 4-20: Behavior of Zinc Corrosion Potential vs. SCE with Time in 3.5%NaCl solution with 5gm/l reed stems Inhibitor.

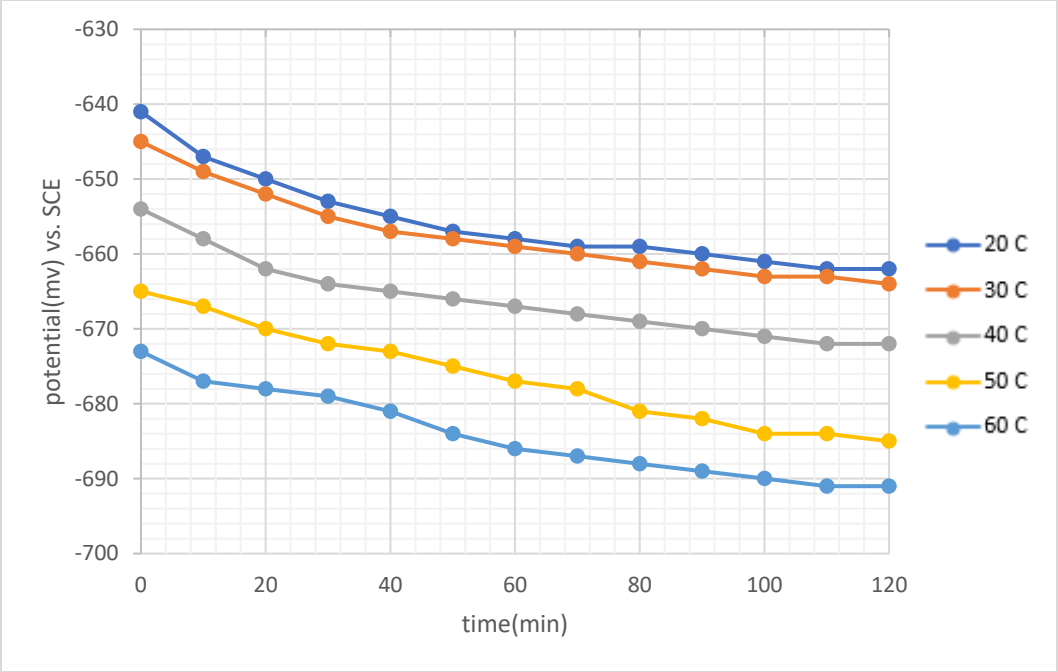

Figure 4-21: Behavior of Zinc Corrosion Potential vs. SCE with Time in 3.5%NaCl solution with 1gm/l orange peels Inhibitor.

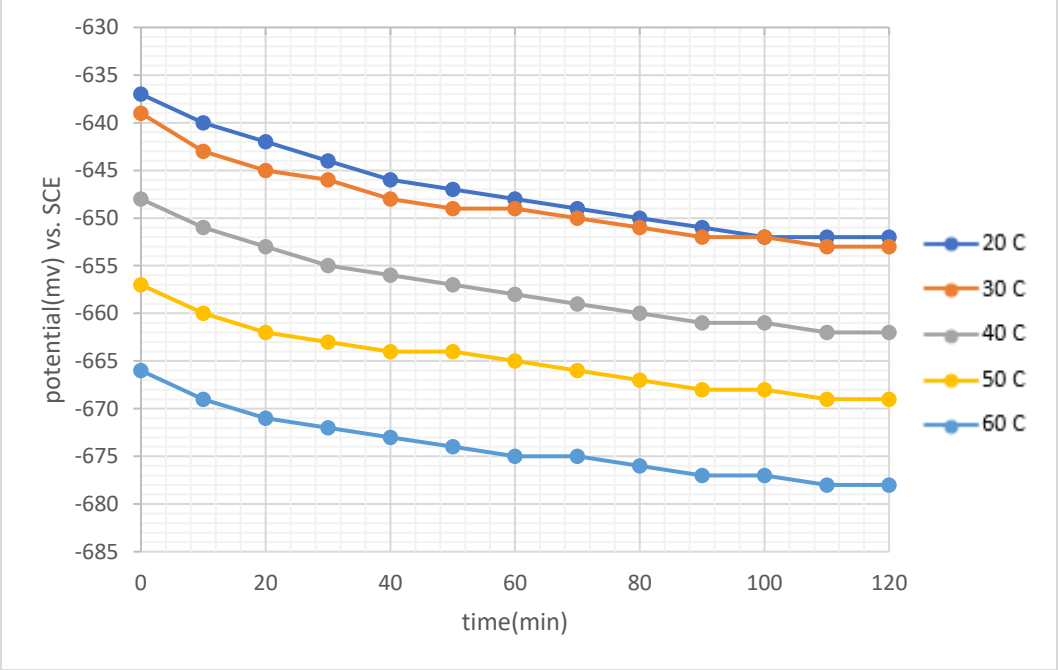

Figure 4-22: Behavior of Zinc Corrosion Potential vs. SCE with Time in 3.5%NaCl solution with 5gm/l orange peels Inhibitor.

4.2.1 Effect of Temperature on Corrosion Potential

From Figures 4-11 to 4-23, and appendix B , In the acidic medium, the voltmeter recorded -656 mv at a temperature of 20 °C, and when the temperature was increased to 30 °C, it became more negative, about -672 mv, until it reached -689 mv at 60 ° C. In the saline medium, the voltages were more negative, and at 20 °C, it recorded -670 mv to It reached -707mv at 60 °C. The corrosion potential shifted to more negative with increasing temperature. This occurred due to the decrease in oxygen solubility fractions. Oxygen has a lower solubility in open systems at higher temperatures and it causes corrosion potential to be more negative and the corrosion rate to increase.

4.2.2 Effect of Inhibitor Concentration on Corrosion Potential

From Figures (4-11) to (4-23), and appendix B, it can be noticed that corrosion potential became less negative as the inhibitor concentration increased .

In the acidic medium, the voltmeter recorded -656 mv at a temperature of 20 °C and when adding 1 gm/l of rosemary, the potentials became less negative and recorded -636 mv at 1 gm/l and -648 mv at 5 gm/l. The best results are when adding the reed stems in the salt medium, where it recorded -653 mv at 20 ^{o}C at a concentration of 1 gm/l, and when the concentration increased by 5 gm/l recorded -639 mv.

Displacement of the corrosion potential in the positive direction means the inhibitor was an anodic inhibitor. But the displacement of the potential in the negative direction indicated the process was cathodic control. A little change in the corrosion potential suggests that both anodic and cathodic processes occurred [Shreir, 1976]. The addition of oxidizing agents may act as inhibitors by shifting the corrosion potential into the passive region. However, the presence of chloride oxidizers can cause pitting as a consequence of the intersection of the anodic and cathodic

polarization curves in the pitting region. Since the presence of an oxidizing agent tends to raise the corrosion potential to more noble values, the possibility also existed that a limited amount of oxidizing agent might increase corrosion rates in the active region before reaching a concentration that would cause passivity [Forest, 1983]. In the presence of corrosion inhibitors, the steady-state potential is shifted more towards a noble direction by increasing the concentration of the inhibiting blend and temperature. Shifting the corrosion potential to a more positive direction indicates the mechanism of passivation to protect zinc in the salt solution [Slaiman, and Al-Khasab, 2015].

4.3Polarization Results and Discussion

The cathodic and anodic polarization curves of zinc in 3.5% NaCl solution are shown in figures (4-23 to 4-31) at different temperatures and concentrations of inhibitors. Tables (4-6 to 4-9) show the corrosion potential ,and corrosion current .A sample of data for polarization experiments is tabled in Appendix C.

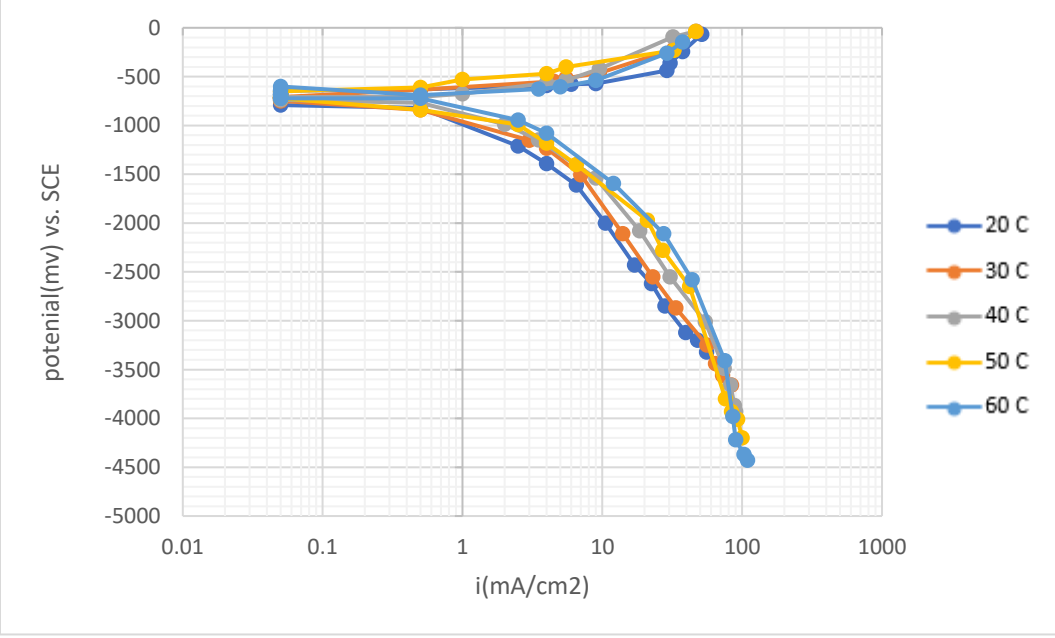

Figure 4-23: Anodic and cathodic polarization curves of Zinc in 3.5%NaCl without Inhibitor at different temperatures.

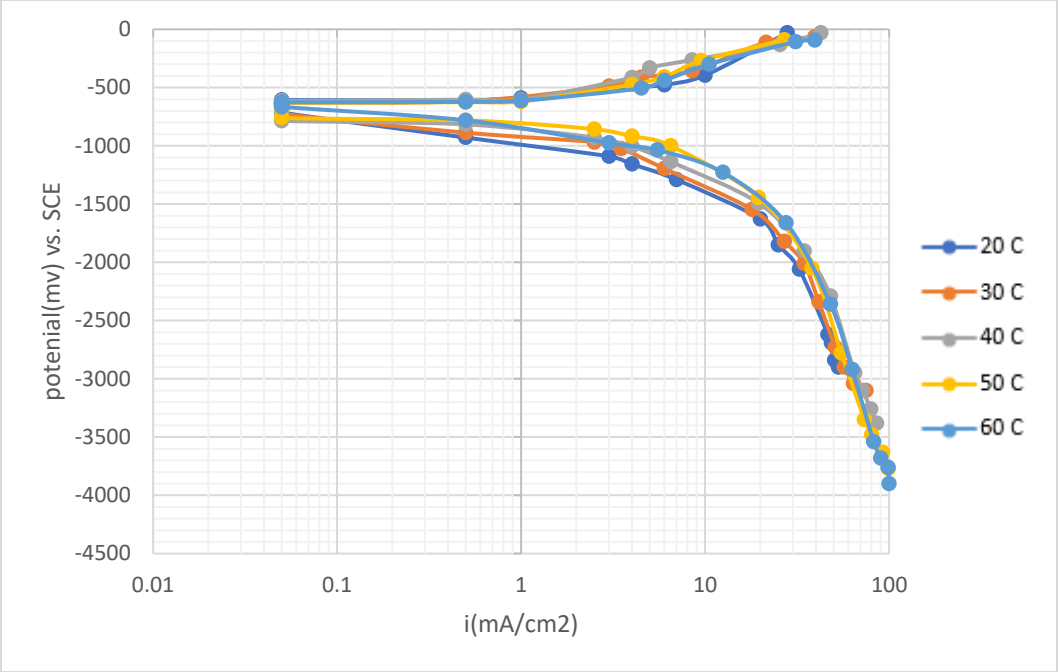

Figure 4-24: Anodic and cathodic polarization curves of Zinc in 3.5%NaCl with 1gm/l rosemary Inhibitor at different temperatures.

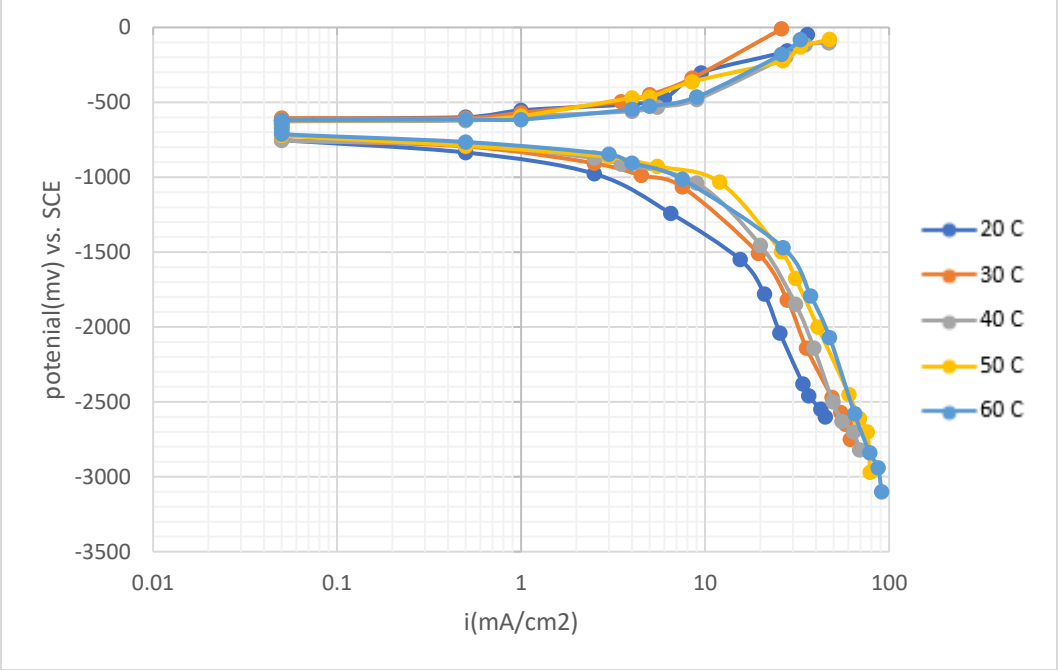

Figure 4-25: Anodic and cathodic polarization curves of Zinc in 3.5%NaCl with 5gm/l rosemary Inhibitor at different temperatures.

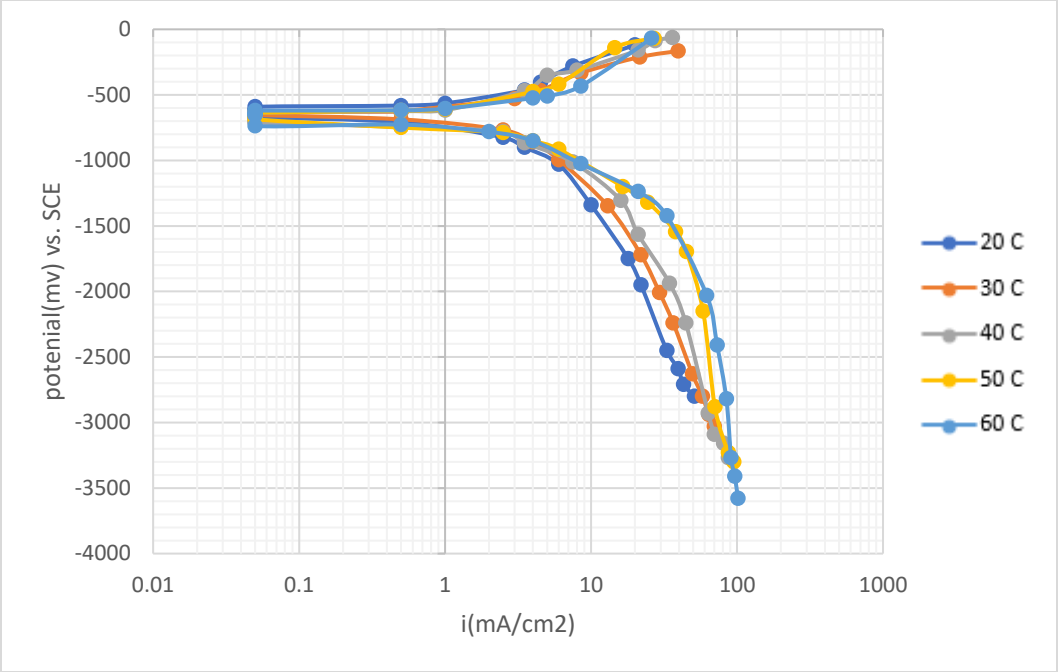

Figure 4-26: Anodic and cathodic polarization curves of Zinc in 3.5%NaCl with 1gm/l reed leaves Inhibitor at different temperatures.

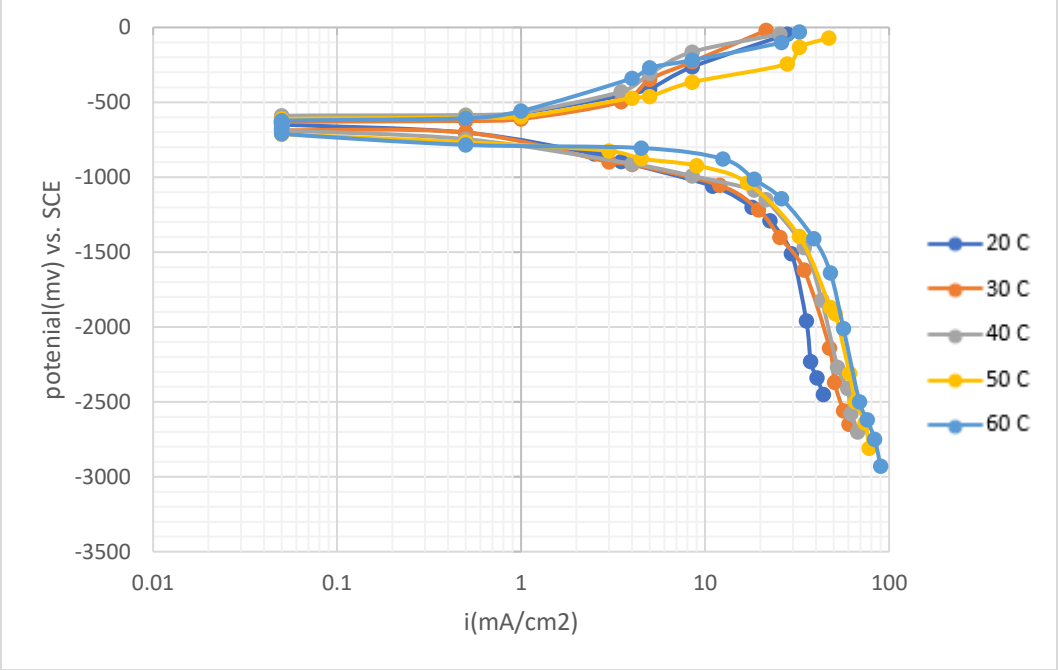

Figure 4-27: Anodic and cathodic polarization curves of Zinc in 3.5%NaCl with 5gm/l reed leave Inhibitor at different temperatures.

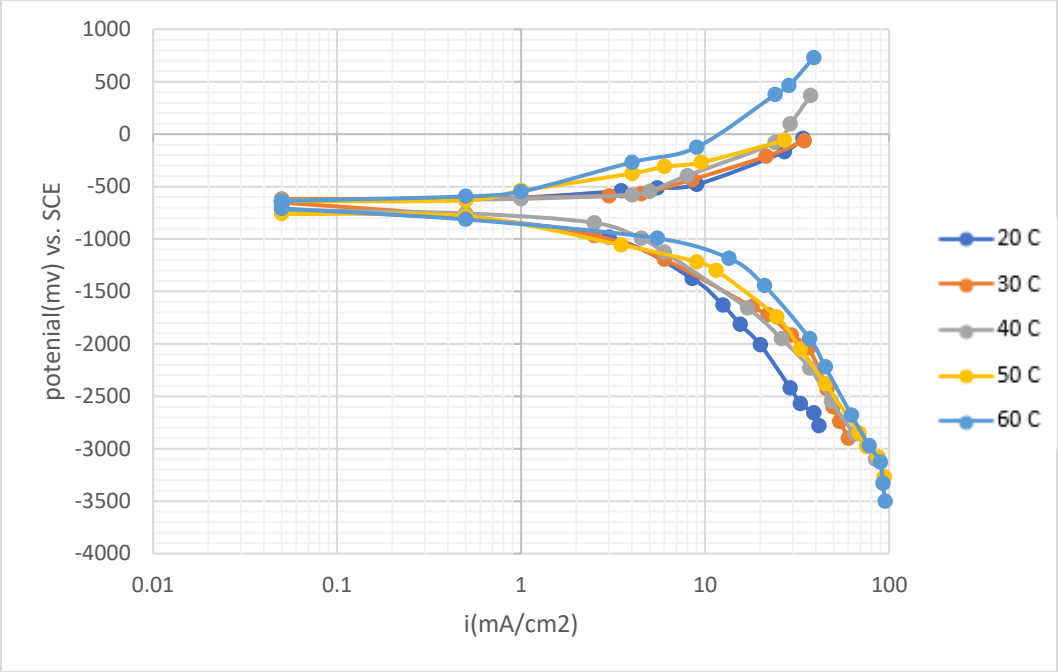

Figure 4-28:Anodic and cathodic polarization curves of Zinc in 3.5%NaCl with 1gm/l reed stems Inhibitor at different temperatures.

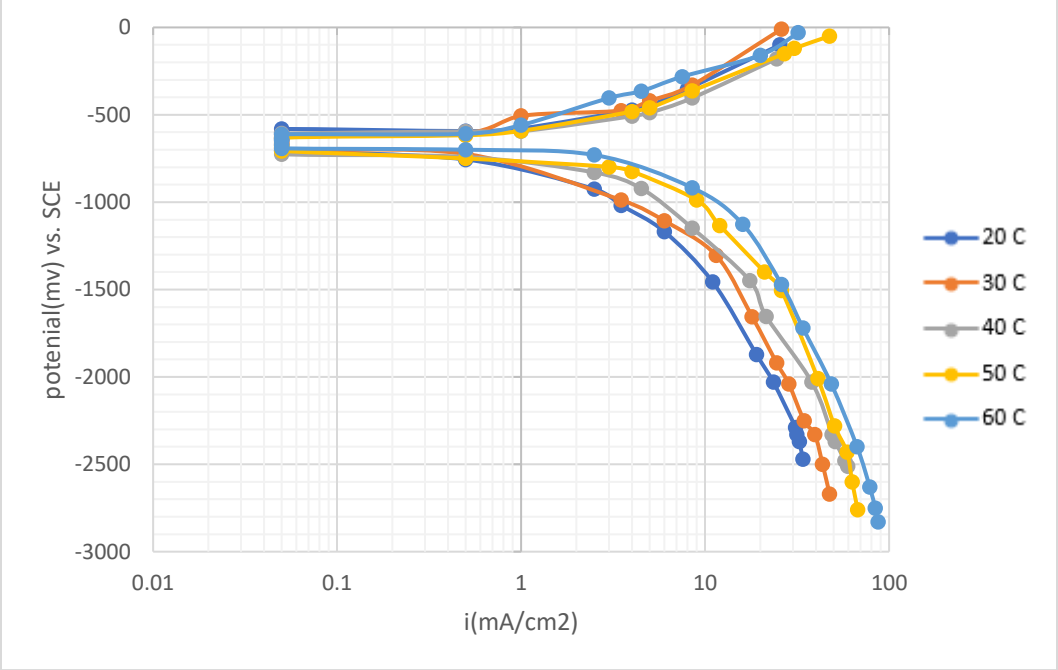

Figure 4-29: Anodic and cathodic polarization curves of Zinc in 3.5%NaCl with 5gm/l reed stem Inhibitor at different temperatures.

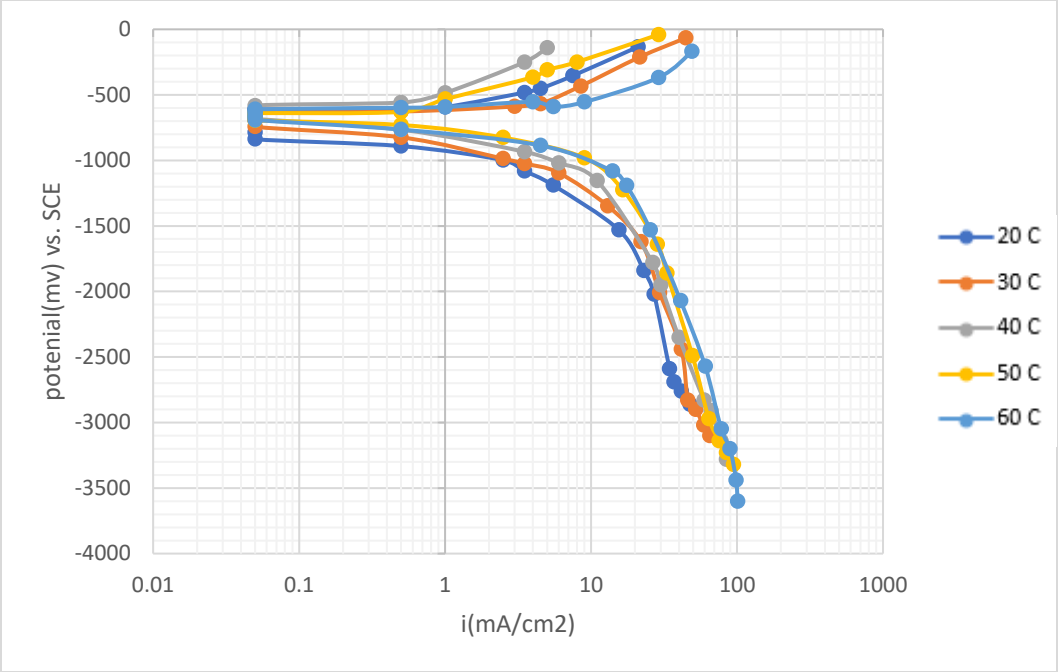

Figure 4-30: Anodic and cathodic polarization curves of Zinc in 3.5%NaCl with 1gm/l orange peel Inhibitor at different temperatures.

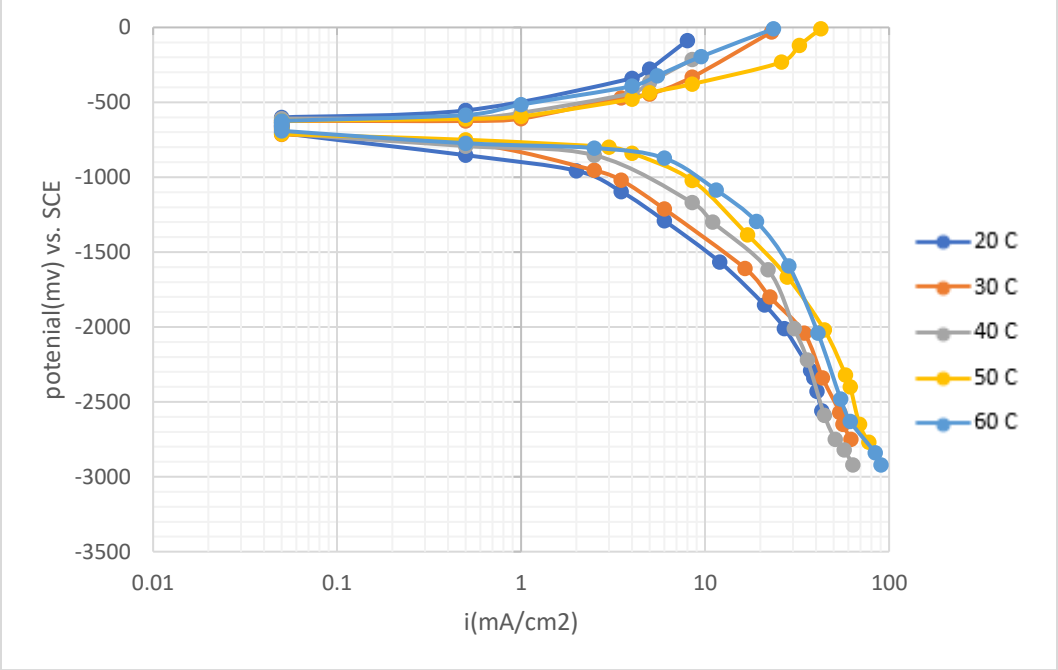

Figure 4-31: Anodic and cathodic polarization curves of Zinc in 3.5%NaCl with 5gm/l orange peel Inhibitor at different temperatures.

Table 4-6: Effect of corrosion parameter from polarization for zinc in 3.5% NaCl with rosemary inhibitor at different temperatures.

T (^{O}C)	C $_{Inhibitor}$ (g/l)	I_{corr} (mA/cm^2)	E_{corr} (mV)
20	0	2.2	-750
	1	1.8	-710
	5	1.3	-670
30	0	2.6	-760
	1	2.3	-720
	5	1.8	-700
40	0	3.2	-790
	1	2.5	-750
	5	2.3	-730
50	0	3.7	-820
	1	3.2	-750
	5	2.8	-720
60	0	4	-850
	1	3.5	-790
	5	3.1	-760

Table 4-7: Effect of corrosion parameter from polarization for zinc in 3.5% NaCl with reed leaves inhibitor at different temperatures.

T (^{O}C)	C $_{Inhibitor}$ (g/l)	I_{corr} (mA/cm^2)	E_{corr} (mV)
20	0	2.2	-750

	1	1.5	-720
	5	1.2	-680
30	0	2.6	-760
	1	2	-700
	5	1.6	-660
40	0	3.2	-790
	1	2.5	-750
	5	2	-710
50	0	3.7	-820
	1	3	-720
	5	2.6	-690
60	0	4	-850
	1	3.2	-750
	5	2.8	-720

Table 4-8: Effect of corrosion parameter from polarization for zinc in 3.5% NaCl with reed stems inhibitor at different temperatures.

T (^{O}C)	**C $_{Inhibitor}$ (g/l)**	**I_{corr} (mA/cm^2)**	**E_{corr} (mV)**
20	0	2.2	-750
	1	1.3	-700
	5	0.9	-670
30	0	2.6	-760
	1	2	-700
	5	1.5	-680
40	0	3.2	-790

	1	2.5	-730
	5	2.1	-700
50	0	3.7	-820
	1	2.8	-760
	5	2.3	-680
60	0	4	-850
	1	3	-750
	5	2.5	-700

Table 4-9: Effect of corrosion parameter from polarization for zinc in 3.5% NaCl with orange peels inhibitor at different temperatures.

T (^{O}C)	**C $_{Inhibitor}$ (g/l)**	**I_{corr} (mA/cm^2)**	**E_{corr} (mV)**
20	0	2.2	-750
	1	2	-740
	5	1.5	-700
30	0	2.6	-760
	1	2.2	-730
	5	1.6	-720
40	0	3.2	-790
	1	2.8	-770
	5	2.5	-750
50	0	3.7	-820
	1	3.3	-790
	5	2.5	-740
60	0	4	-850

	1	3.7	-800
	5	3.3	-780

4.3.1 Effect temperature on polarization curves

The corrosion potential and the corrosion current were concluded from the polarization curves, according to the table (4-12 to 4-15) in the salt medium, the corrosion potential is -750 mv and the corrosion current is 2.2 mA/cm^2 at a temperature of 20 °C and it gradually increases until it reaches at 60 °C about -850 mv and 4 mA/cm^2 It is concluded from that when the temperature increases, it increases Corrosion current and the Corrosion potential becomes more negative.

The result reveals that increasing temperatures have a great effect on corrosion rates, especially in acid solutions, The corrosion potential (E_{corr}) shifts towards more negative values and both anodic and cathodic current densities of corrosion were enhanced upon increasing temperature. This has the consequence that the amount of oxygen that can be held by the water depends on the water temperature, salinity, and pressure. Oxygen solubility decreases with increasing temperature, increasing salinity, or decreasing pressure. the general shape of the polarization curves is unaffected by temperature changes

4.3.2 Effect of Inhibitor Concentration on polarization curves

The polarization curves shown in the figure, show the change of corrosion rate with the corrosion rates can obtain by extrapolation of the anodic and cathodic Tafel lines .

According to the tables in the salt medium, when adding a rosemary inhibitor at a concentration of 1 gm/l, the corrosion potential became -710 mv and the corrosion

current was 1.8 mA/cm^2 at a temperature of 20 °C and gradually decreased until it reached a concentration of 5 gm/l about -670 mv and 1.3 mA/cm^2. It is concluded from this that when the concentration of the inhibitor increases, the current decreases corrosion, and corrosion potential becomes more positive. The anodic and cathodic polarization curves shift to lower current densities when the inhibiter is added which means The corrosion rate decreases with the inhibitors; i.e., retards the corrosion of zinc in solution .The data shows that adding a green inhibitor reduces the corrosion current density and that the corrosion potential shifts slightly to fewer negative values as the concentration of the added inhibitor are increased, and a large number of corrosion pits form on the surface of the zinc. This could be attributed to the adsorption of the inhibitor molecules on the metal's surface .

This result indicates that the four green inhibitors act as a mixed inhibitor and the reed stems had the best performance Where the lowest corrosion potential was recorded - 670 mv and the corrosion current was 0.9 mA/cm^2. However, it should be noted that this behavior corresponds to the beginning of the corrosion process, and this trend may change in long-term exposures.

4.4 Limiting Current Density and Mass Transfer Coefficient

The limiting current density can be obtained from the curves as per the method given by Gabe and Makangula for determining the limiting current as shown below [Sadek, 2012]:

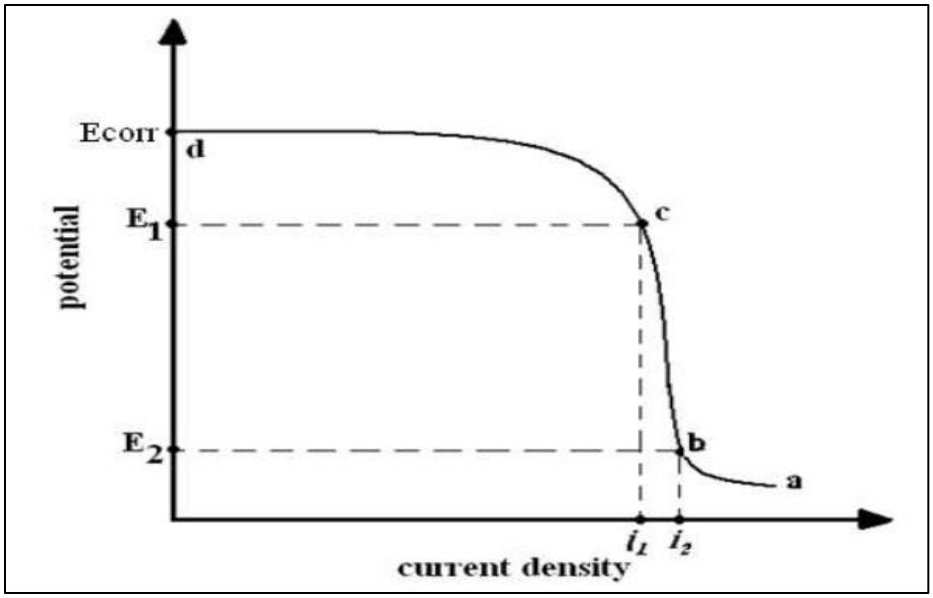

Figure 4-32:Typical polarization curve [Sadek, 2012]

$$i_L = \frac{i_1 + i_2}{2} \qquad (4\text{-}1)$$

The mass transfer dimensionless groups, Sh , then can be calculated from K or i_L:

$$Sh = k\,L/D \qquad (4\text{-}2)$$

The properties required for performing the above calculations, i.e., (C_b, D, μ, and ρ) are presented in appendix A. The data in the tables(4-16 to 4-19) are selected from the polarization charts(4-24 to 4-35).

Table 4-10: The Values of Limiting Current Density, Mass Transfer Coefficient, and Sherwood number in 3.5%NaCl with rosemary.

T (^oC)	C Inhibitor (g/l)	i_L (mA/cm^2)	k (cm/s)	sh	sc
20	0	29	3.76E+02	1.35E+08	756.896
	1	28.25	3.66E+02	1.32E+08	756.896

	5	25.75	3.34E+02	1.20E+08	756.896
30	0	43.5	6.65E+02	1.28E+08	323.443
	1	38.75	5.93E+02	1.14E+08	323.443
	5	32	4.89E+02	9.39E+07	323.443
40	0	46	8.10E+02	9.59E+07	164.554
	1	44	7.74E+02	9.17E+07	164.554
	5	35.75	6.29E+02	7.45E+07	164.554
50	0	51.25	1.04E+03	8.26E+07	93.179
	1	50.5	1.02E+03	8.13E+07	93.179
	5	41	8.31E+02	6.60E+07	93.179
60	0	55.75	1.81E+03	9.38E+07	49.243
	1	51.5	1.67E+03	8.66E+07	49.243
	5	47	1.52E+03	7.91E+07	49.243

Table 4-11: The Values of Limiting Current Density, Mass Transfer Coefficient, and Sherwood number in 3.5%NaCl with reed leaves Inhibitor.

T (^{O}C)	C $_{Inhibitor}$ (g/l)	i_L (mA/cm^2)	k (cm/s)	sh	sc
20	0	29	3.76E+02	1.35E+08	756.896
	1	26.75	3.47E+02	1.25E+08	756.896
	5	23.75	3.08E+02	1.11E+08	756.896
30	0	43.5	6.65E+02	1.28E+08	323.443

	1	36.25	5.54E+02	1.06E+08	323.443
	5	31.75	4.85E+02	9.32E+07	323.443
40	0	46	8.10E+02	9.59E+07	164.554
	1	44.75	7.88E+02	9.32E+07	164.554
	5	35.75	6.29E+02	7.45E+07	164.554
50	0	51.25	1.04E+03	8.26E+07	93.179
	1	48.75	9.88E+02	7.85E+07	93.179
	5	40.5	8.21E+02	6.52E+07	93.179
60	0	55.75	1.81E+03	9.38E+07	49.243
	1	51.75	1.68E+03	8.71E+07	49.243
	5	47.25	1.53E+03	7.95E+07	49.243

Table 4-12: The Values of Limiting Current Density, Mass Transfer Coefficient, and Sherwood number in 3.5%NaCl with reed stems Inhibitor.

T (^{O}C)	**C $_{Inhibitor}$ (g/l)**	**i_L (mA/cm^2)**	**k (cm/s)**	**sh**	**sc**
20	0	29	3.76E+02	1.35E+08	756.896
	1	22.25	2.88E+02	1.04E+08	756.896
	5	18.25	2.36E+02	8.52E+07	756.896
30	0	43.5	6.65E+02	1.28E+08	323.443
	1	31.5	4.82E+02	9.25E+07	323.443
	5	25.5	3.90E+02	7.48E+07	323.443

40	0	46	8.10E+02	9.59E+07	164.554
	1	43.5	7.66E+02	9.06E+07	164.554
	5	31	5.46E+02	6.46E+07	164.554
50	0	51.25	1.04E+03	8.26E+07	93.179
	1	48.75	9.88E+02	7.85E+07	93.179
	5	35.75	7.25E+02	5.76E+07	93.179
60	0	55.75	1.81E+03	9.38E+07	49.243
	1	50.25	1.63E+03	8.45E+07	49.243
	5	44.75	1.45E+03	7.53E+07	49.243

Table 4-13: The Values of Limiting Current Density, Mass Transfer Coefficient, and Sherwood number in 3.5%NaCl with orange peels Inhibitor.

T (^{O}C)	**C $_{Inhibitor}$ (g/l)**	**i_L (mA/cm^2)**	**k (cm/s)**	**sh**	**sc**
20	0	29	3.76E+02	1.35E+08	756.896
	1	25	3.24E+02	1.17E+08	756.896
	5	22.5	2.91E+02	1.05E+08	756.896
30	0	43.5	6.65E+02	1.28E+08	323.443
	1	33.75	5.16E+02	9.91E+07	323.443
	5	32.25	4.93E+02	9.47E+07	323.443
40	0	46	8.10E+02	9.59E+07	164.554

	1	44	7.74E+02	9.17E+07	164.554
	5	33	5.81E+02	6.88E+07	164.554
50	0	51.25	1.04E+03	8.26E+07	93.179
	1	48.5	9.83E+02	7.81E+07	93.179
	5	40.25	8.16E+02	6.48E+07	93.179
60	0	55.75	1.81E+03	9.38E+07	49.243
	1	52.75	1.71E+03	8.87E+07	49.243
	5	46.5	1.51E+03	7.82E+07	49.243

4.4.1 Effect of Temperature on Limiting Current

It can be seen from Tables 4-16 to 4-19, that the specific current is 29 mA/cm^2 at a temperature of 20 °C, and when the temperature increases, it gradually increases until it reaches 55 mA/cm^2 at 60 °C, as well as for the mass transfer coefficient and Sherwood number that as the temperature increased, the mass transfer coefficient and Sherwood number increased.

When the temperatures increased, the corrosion was enhanced by the increase in O2 diffusivity and decreased O_2 solubility, the factor that led to the decrease in the corrosion rate [Basim et al. 2011]. The temperature rise may decrease the equilibrium potential of Zn and H_2 but increase the equilibrium potential of O_2. A rise in temperature increases the diffusion-controlled current density, due to an increase in the diffusion coefficient of the electroactive substance.

The effect of temperature on the corrosion rate for mass transfer control systems is represented by changing two parameters affecting the corrosion rate in conflicting

ways that are O_2 solubility and diffusivity. Increasing the temperature will increase the rate of oxygen diffusion to the metal surface by decreasing the viscosity of water and enhancing the corrosion rate. On the other hand, increasing temperature decreases oxygen solubility [Sadek, 2012].

4.4.2 Effect of Inhibitor Concentration on Limiting Current

From Tables (4-16 to 4-19), when adding 1 gm/l from rosemary We notice the salt solution that the specific current is 28.25 mA/cm^2 at a temperature of 20 °C, and when the concentration increases to 5 gm/l, it reaches 25 mA/cm^2, as well as for the mass transfer coefficient and Sherwood number.

it can be seen that limiting current decreased with increasing inhibitor concentration due to the reduction of surface area in contact with the electrolyte by the adsorbed inhibitor [Rivera-Grau, L 2012].

The oxide layer build-up increased the resistance to oxygen diffusion. This led to a decrease in the cathodic current and it corresponded to the decrease in the limiting current density for oxygen reduction on the metal surface [Rivera-Grau, L 2012].

Chapter Five

Conclusions and Recommendations for Future Work

5.1 Conclusions

From the study's results, the following conclusions can be listed:

- As obtained results have shown, rosemary, reed leaves, reed stems, and orange peels as green inhibitors can be applied to reduce the corrosion rate of zinc in 0.1M HCl solution and 3.5% NaCl solution at 20 ^{o}C, 30 ^{o}C, 40 ^{o}C, 50 ^{o}C, 60 ^{o}C.
- The inhibition efficiency was found to increase by increasing inhibitor concentrations and decrease with increasing temperature. The highest inhibition efficiencies of 49 % were obtained using rosemary and 75% using reed stems at a concentration of 5 gm/l at 20 °C for the acid and salt solution, respectively.
- the corrosion potential became less negative with increasing green inhibitor concentration and became more negative with increasing temperature in acid or salt solution. The best results are when adding 5 gm/l of the reed stems in the salt medium, where it recorded -639 mv at 20 ^{o}C .
- in polarization experiments, the reed stems had the best performance At a concentration of 5 gm/l Where the lowest corrosion potential was recorded - 670 mv, and the corrosion current was 0.9 mA/cm^2 in a salt solution at 20 ^{o}C.
- The type of inhibitor used was a mixed inhibitor for acid or salt solution.

- it can be seen that limiting current decreased with increasing inhibitor concentration due to the reduction of surface area in contact with the electrolyte by the adsorbed inhibitor

5.2 Recommendations for Future Works:

- Using another type of green inhibitor such as rosemary oil, Opuntia ficus-indica.
- Using different concentrations of green inhibitors.
- Using of compounds to increase the efficiency of the green inhibitor
- Using different concentrations of acid or salt solution as a corrosive solution and comparing the results.
- Using zinc alloys or other metals such as copper or their alloys, as the working electrode.

References

[1] A.Y. El-Etre. (2006). Natural onion juice as inhibitor for zinc corrosion. *Bulletin of Electrochemistry*,*22*(2),7578.http://www.academia.edu/10304833/Natural_onion_juice_as_inhibitor_for_zinc_corrosion

[2] Abdallah, M., & Al Karanee, S. O. (2009). Corrosion behavior of nickel and its alloys in HCl and its inhibition by natural rosemary oil. *Zaštita Materijala*, *50*(4), 205–212.

[3] Abdul Jalell, H. A (2019) Corrosion Inhibition of Mild Steel in Concrete Using Drug Inhibitors,M. Sc. Thesis Dept. of Chem. Eng., University of Babylon.

[4] Abiola, O. K., & James, A. O. (2010). The effects of Aloe vera extract on corrosion and kinetics of corrosion process of zinc in HCl solution. *Corrosion Science*, *52*(2), 661–664.

[5] Ahmad, Z. (2006). *Principles of corrosion engineering and corrosion control*. Elsevier.

[6] Al-Anbaky, H. A. M. (2006). *CORROSION UNDER TWO – PHASE FLOW KEROSENE / WATER SIMULATED BY TURBLENTLY AGITATED SYSTEMS*. M.Sc. thesis, Chemical Engineering Department, College of Engineeing, Al-Nahrain University, Iraq.

[7] Al-Areqi, N. A., & Al-Maleeh, G. (2021) Two Environmental Friendly Compounds As Zinc Corrosion Inhibitors in HCl Media.

[8] Ali, A. I., Megahed, H. E., El-Etre, M. A., & Ismail, M. N. (2014). Zinc corrosion in HCl in the presence of aqueous extract of Achillea fragrantissima. *Journal of Materials and Environmental Science*, *5*(3), 923–930.

[9] ALI, S. M., & Al LEHAIBI, H. A. (2016). Control of zinc corrosion in acidic media: Green fenugreek inhibitor. *Transactions of Nonferrous Metals Society of China*, *26*(11), 3034–3045.

[10] Aliofkhazraei, M. (2014). Developments in Corrosion Protection. In M. Aliofkhazraei (Ed.), *Developments in Corrosion Protection*. InTech.

[11] Al-Kelaby, S. S. B. (2007). *Inhabitation of Galvanic Corrosion by Phenylethiourea Under Flowing Conditions in Hydrochloric Acid Solution*. Ph.D thesis, Chemical Engineering Department, College of Engineering, Al-Nahrain University, Iraq.

[12] AL-Rawi, E. M. J. (2009). Simulation Of Iron Corrosion In Aerated Acid Solutions. M.Sc. thesis, Chemical Engineering Department, College of Engineeing, Al-Nahrain University, Iraq.

[13] Banerjee, S. N. (1985). An introduction to science of corrosion and its inhibition. Oxonian Press.

[14] Bard, A. J., & Faulkner, L. R., (2001). *ELECTROCHEMICAL METHODS Fundamentals and Applications* (Second Edi). John Wiley & Sons.

[15] Bardal, E. (2004). Engineering Materials and Processes. Corrosion and Protection, Springer-Verlag, London Berlin Heidelberg, 5-10.

[16] Benjamin, D. Craig., Richard, A. Lane., & David, H. Rose. (2006). Corrosion Prevention and Control: A Program Management Guide for Selecting Materials, AMMTIAC, September,

[17] Bozin, B., Mimica-Dukic, N., Samojlik, I., & Jovin, E. (2007). Antimicrobial and Antioxidant Properties of Rosemary and Sage (Rosmarinus officinalis L. and Salvia officinalis L., Lamiaceae) Essential Oils. *Journal of Agricultural and Food Chemistry*, *55*(19), 7879–7885.

[18] Cang, H., Fei, Z., Xiao, H., Huang, J., & Xu, Q. (2012). Inhibition effect of reed leaves extract on steel in hydrochloric acid and sulphuric acid solutions. *International Journal of Electrochemical Science*, *7*(9), 8869–8882.

References

[19] Ćatić, S., Obralić, E., & Bratovčić, A. (2016). Rosemary as ecologically acceptable corosion inhibitor of steel. *Glas. Hem. Tehnol. Bosne Herceg*, *40*, 47–50.

[20] Charng, T., & Lansing, F. (1982). Review of corrosion causes and corrosion control in a technical facility. In *DSN Engineerign Section* (p. TDA Progress Report, 42-69).

[21] Da Rocha, J. C., da Cunha Ponciano Gomes, J. A., & D'Elia, E. (2010). Corrosion inhibition of carbon steel in hydrochloric acid solution by fruit peel aqueous extracts. *Corrosion Science*, *52*(7), 2341–2348.

[22] Dariva, C. G., & Galio, A. F. (2014). Corrosion inhibitors–principles, mechanisms and applications. Developments in corrosion protection, 16, 365-378.

[23] Deyab, M. A. (2016). Corrosion inhibition of aluminum in biodiesel by ethanol extracts of Rosemary leaves. *Journal of the Taiwan Institute of Chemical Engineers*, *58*, 536–541.

[24] Dhawan, S. K., Bhandari, H., Ruhi, G., Bisht, B. M. S., & Sambyal, P. (2020). Corrosion Preventive Materials and Corrosion Testing. In *Corrosion Preventive Materials and Corrosion Testing*. CRC Press.

[25] Farhan, Z. A., (2016) Zinc Corrosion Inhibition under Variable Conditions, ,M. Sc. Thesis Dept. of Chem. Eng., University of Babylon .

[26] Fontana, M. G. (1987). *Corrosion Engineering* (Thid Editi). McGraw-Hill, New York.

[27] Forest, I., & Suffern, P. O. B. (1983). The Corrosion Resistance of Nickel-Containing Alloys in Sulfuric Acid and Related Compounds. *The International Nickel Company, Inc.*, 1–88.

References

[28] Fouda, A. S., Aggour, Y., Bekheit, G., & Ismail, M. A. (2014). Moringa oleifera extract as green corrosion inhibitor for zinc in polluted sodium chloride solutions. *International Journal of Advanced Research*, *2*(7), 1158–1170.

[29] Hadi, A. A. A. (2015). Use Reed Leaves as a Natural Inhibitor to Reduce the Corrosion of Low Carbon Steel. *International Journal of Engineering Research and General Science*, *3*(3), 514–521.

[30] Hadi, Z. A., (2019). ECO-FRIENDLY CORROSION INHIBITOR FOR REINFORCING STEEL IN CONCRETE CASTING. M.Sc. thesis, Chemical Engineering Department, College of Engineeing, Babylon University, Iraq.

[31] Hadi, Z. A., Mahdi, A. S., & Bahar, S. S. (2020). Reed Leaves Extract as Corrosion Inhibitor for Reinforcing Steel in Concrete. *The First International Conference of Pure and Engineering Sciences*, *871*(1).

[32] Hart, E. (Ed.). (2017). *Corrosion Inhibitors Principle, Mechanisims and Applications*. Nova Science Publishers.

[33] Hasan, B. O. (2010). Effect of Salt Content on The Corrosion Rate of Steel Pipe in Turbulently Flowing Solutions. *Nahrain University,College of Engineering Journal*, *13*(1), 66–73.

[34] Hassan, B. (2020). *Study the Mass and Heat Transport on Corrosion of Carbon Steel Immersed in Crude Oil Under Variable Condition*. M.Sc. Thesis, Electrochemical Engineering ,College of Engineering University of Babylon, Iraq.

[35] Hayashi, K., & Miyoshi, Y. (1994). Corrosion mechanisms of zinc alloy coated steel sheets for automobile body use. *K. Hayashi, Y. Miyoshi, and Y. Ito (Technical Development Bureau), Nippon Steel Technical Report*, *63*, 8–15.

[36] Ibrahim, T. H., & Zour, M. A. (2011). Corrosion inhibition of mild steel using fig leaves extract in hydrochloric acid solution. *International Journal of Electrochemical Science*, *6*(12), 6442–6455.

References

[37] K. M. O. Goni, L., & A. J. Mazumder, M. (2019). Green Corrosion Inhibitors. In *Corrosion Inhibitors*. IntechOpen.

[38] Kader, H. D. A. (2013). Study the Effect of Different Parameters on the Corrosion and Inhibition Rate for Copper in Saline Solutions. Al-Nahrain Journal for Engineering Sciences, 16(2), 269-285.

[39] Kliškić, M., Radošević, J., Gudić, S., & Katalinić, V. (2000). Aqueous extract of Rosmarinus officinalis L. as inhibitor of Al-Mg alloy corrosion in chloride solution. *Journal of Applied Electrochemistry*, *30*(7), 823–830.

[40] Koch, G. (2017). Cost of corrosion. In *Trends in Oil and Gas Corrosion Research and Technologies: Production and Transmission*. Elsevier Ltd.

[41] Lebrini, M., Suedile, F., Salvin, P., Roos, C., Zarrouk, A., Jama, C., & Bentiss, F. (2020). Bagassa guianensis ethanol extract used as sustainable eco-friendly inhibitor for zinc corrosion in 3% NaCl: Electrochemical and XPS studies. *Surfaces and Interfaces*, *20*(May), 100588.

[42] Loto, R. T. (2018). Surface coverage and corrosion inhibition effect of Rosmarinus officinalis and zinc oxide on the electrochemical performance of low carbon steel in dilute acid solutions. *Results in Physics*, *8*, 172–179.

[43] M'hiri, N., Veys-Renaux, D., Rocca, E., Ioannou, I., Boudhrioua, N. M., & Ghoul, M. (2016). Corrosion inhibition of carbon steel in acidic medium by orange peel extract and its main antioxidant compounds. *Corrosion Science*, *102*, 55–62.

[44] Marcus, P. (2002). Corrosion Mechanisms in Theory and Practice. In P. Marcus (Ed.), *Corrosion Mechanisms in Theory and Practice* (Second Edi). CRC Press.

[45] Marcus, P. (2012). Corrosion mechanisms in theory and practice. In P. Marcus (Ed.), *Corrosion Technology* (Third Edit). CRC Press.

References

[46] Marzorati, S., Verotta, L., & Trasatti, S. P. (2019). Green corrosion inhibitors from natural sources and biomass wastes. *Molecules*, *24*(1).

[47] McCafferty, E. (2010). Introduction to Corrosion Science. In *Angewandte Chemie International Edition, 6(11), 951–952.* (Vol. 4, Issue 1). Springer New York.

[48] Murata, K., Noguchi, K., Kondo, M., Onishi, M., Watanabe, N., Okamura, K., & Matsuda, H. (2013). Promotion of Hair Growth by Rosmarinus officinalis Leaf Extract. *Phytotherapy Research*, *27*(2), 212–217.

[49] Perez, N. (2004). *Electrochemistry and corrosion science*. Springer.

[50] Petchiammal, A., Deepa Rani P, Selvaraj, S., & Kalirajan, K. (2012). Corrosion protection of zinc in natural sea water using citrullus vulgaris peel as an inhibitor. *Research Journal of Chemical Science*, *2*(4), 24–34.

[51] Piere, R. R. (2008). Corrosion Engineering-Principles and Practice.

[52] Porter, F. C. (1994). *Resistance Zinc and Zinc Alloys*. Marcel Dekker.

[53] Pourriahi, M., Nasr-Esfahani, M., & Motalebi, A. (2014). Effect of henna and rosemary extracts on the corrosion of 304L stainless steel in 3.5% NaCl solution. *Surface Engineering and Applied Electrochemistry*, *50*(6), 525–533.

[54] Rajendran, S., & Singh, G. (2019). *Titanic corrosion*. CRC Press.

[55] Rani, B. E. A., & Basu, B. B. J. (2012). Green Inhibitors for Corrosion Protection of Metals and Alloys: An Overview. *International Journal of Corrosion*, *2012*(i), 1–15.

[56] Revie, R. W. (2008). Corrosion and corrosion control: an introduction to corrosion science and engineering. John Wiley & Sons .

[57] Rezanejad, R., Ojagh, S. M., Heidarieh, M., Raeisi, M., Rafiee, G., & Alishahi, A. (2019). Characterization of gamma-irradiated rosmarinus officinalis l. (rosemary). *Turkish Journal of Pharmaceutical Sciences*, *16*(1), 43–47.

References

[58] Rezzadori, K., Benedetti, S., & Amante, E. R. (2012). Proposals for the residues recovery: Orange waste as raw material for new products. *Food and Bioproducts Processing*, *90*(4), 606–614.

[59] Rivera-Grau, L. M., Casales, M., Regla, I., Ortega-Toledo, D. M., Ascencio-Gutierrez, J. A., Porcayo-Calderon, J., & Martinez-Gomez, L. (2013). Effect of organic corrosion inhibitors on the corrosion performance of 1018 carbon steel in 3% NaCl solution. International Journal of Electrochemical Science, 8(2), 2491-2503.

[60] Roberge, P. R. (n.d.). *Corrosion Engineering: Principles and Practice, 2008*. McGraw-Hill, New York.

[61] Sadek, S. A. (2012). *Corrosion of Carbon Steel in Acidic Salt Solutions Under Flow Conditions*. M.Sc. thesis, Chemical Engineering Department, College of Engineering, Al-Nahrain University, Iraq.

[62] Saleh, R. M., Ismail, A. A., & Hosary, A. H. E. (1982). Corrosion Inhibition by Naturally Occurring Substances. *British Corrosion Journal*, *17*(3), 3–7.

[63] Sastri, V. S. (2012). *Green corrosion inhibitors: theory and practice* (Vol. 10). John Wiley & Sons.

[64] Sastri, V. S., Ghali, E., & Elboujdaini, M. (2007). Corrosion Prevention and Protection. In *Corrosion Prevention and Protection: Practical Solutions*. John Wiley & Sons, Ltd.

[65] Schweitzer, P. A. (2003). *Metallic materials: physical, mechanical, and corrosion properties* (Vol. 19). CRC press.

[66] Schweitzer, P. A. (2010). *Fundamentals of corrosion*. CRC press.

[67] Shimaa, M. A., and Hamedh, A. A. (2016) Control of zinc corrosion in acidic media: green fenugreek inhibitor Trans. Nonferrous Met. Soc. China 26(3034) 3045.

References

[68] Shreir, L. L. (Ed.). (1976). Corrosion Control. In *Corrosion* (Second, Vol. 2). Butterworth & Co. Ltd.

[69] Shreir, L. L., Jarman, R. A., & Burstein, G. T. (1994). Corrosion Control,vol. 2.

[70] Slaiman, Q. J. M., & Al-khasab, A. A. (2015). Performance of Corrosion Inhibitors Blend for Simulated Industrial Cooling Waters under Dynamic Conditions. *Iraqi Journal of Chemical and Petroleum Engineering*, *16*(1), 1–12.

[71] Stanojevic, D., Toskovic, D., & Rajkovic, M. B. (2005). Intensification of zinc dissolution process in sulphuric acid. *Journal of Mining and Metallurgy, Section B: Metallurgy*, *41*(1), 47–66.

[72] Stansbury, E. E., & Buchanan, R. A. (2000). Fundamentals of electrochemical corrosion. ASM international.

[73] Stern, M., A. L. G. (1957). Electrochemical Polarization: I . A Theoretical Analysis of the Shape of Polarization Curves. *Journal of The Electrochemical Society*, *104*(1), 56.

[74] Suedile, F., Robert, F., Roos, C., & Lebrini, M. (2014). Corrosion inhibition of zinc by Mansoa alliacea plant extract in sodium chloride media: Extraction, Characterization and Electrochemical Studies. *Electrochimica Acta*, *133*, 631–638.

[75] Sun, C. X., Chen, Y. M., Xu, H. W., Huang, C. S., Zhang, M., Wu, J. Y., Chen, M., & Xue, M. (2017). Research on the corrosion inhibitors of zinc in hydrochloric acid. *IOP Conference Series: Materials Science and Engineering*, *213*(1), 12043.

[76] Tansuğ, G., & Tüken, T. (2016). Organic corrosion inhibitors and industrial applications.

References

[77] Taucher, W., Binder, L., & Kordesch, K. (1992). Conductive fillers for immobilized alkaline zinc anodes. *Journal of Applied Electrochemistry*, *22*(2), 95–98.

[78] Thomas, S., Birbilis, N., Venkatraman, M. S., & Cole, I. S. (2012). Corrosion of Zinc as a Function of pH. *CORROSION*, *68*(1), 015009-1-015009–9.

[79] Thompson, N. G., Yunovich, M., & Dunmire, D. (2007). Cost of corrosion and corrosion maintenance strategies. *Corrosion Reviews*, *25*(3–4), 247–261.

[80] Umoren, S. A., & Ebenso, E. E. (2007). The synergistic effect of polyacrylamide and iodide ions on the corrosion inhibition of mild steel in H2SO4. Materials Chemistry and Physics, 106(2-3), 387-393.

[81] Umoren, S. A., & Solomon, M. M. (2017). Application of polymer composites and nanocomposites as corrosion inhibitors. Corrosion inhibitors, principles, mechanisms, and applications, 27-58.

[82] ur Rahman, M., Gul, S., Umair, M., Anwar, A., & Achakzai, A. K. K. (2016). Anticorrosive activity of Rosemarinus officinalis L. leaves extract against mild steel in dilute hydrochloric acid. Int J Innov Res Adv Eng, 3, 385-343.

[83] Velázquez-González, M. A., Gonzalez-Rodriguez, J. G., Valladares-Cisneros, M. G., & Hermoso-Diaz, I. A. (2014). Use of Rosmarinus officinalis as Green Corrosion Inhibitor for Carbon Steel in Acid Medium. *American Journal of Analytical Chemistry*, *05*(02), 55–64.

[84] Yadla, S. V., Sridevi, V., Chandana Lakshmi, M. V. V, & Kiran Kumari, S. P. (2012). a Review on Corrosion of Metals and Protection. *International Journal of Engineering Science & Advanced Technology*, *2*(3), 637–644.

[85] Zhang, X. G. (1996). *Corrosion and electrochemistry of zinc*. Springer Science & Business Media.

References

[86] Zheng, Q., Li, W., Lv, Z., & Fan, J. (2019). Study on Extraction Method of rosemary antioxidant. *IOP Conference Series: Earth and Environmental Science*, *300*(5), 052013.

Appendix A

Properties and Equations

A-1: Properties of the specimen

Length of specimen (L) = 5 cm

Width of specimen (W) = 2 cm

Thickness of specimen =0.1 cm

surface area = 2 x L x W = 2 x 10^{-3} m^2

A-2: The Equations

gmd (g/m^2.day) = $\frac{\Delta w}{A.t}$

mm/y = $\frac{gmd}{2.74}$

mpy = $\frac{mm/y}{0.0254}$

id = $\frac{\Delta W.Z.F}{MWt.A.t}$ *10^3, where;

id = dissolution current density (mA/cm^2).

Δw = weight loss (g).

Z = number of electrons.

F = Faradays number [96487 c/g. equivalents = nF(c/g.mol).

M.Wt = Molecular weight of metal = 65.41 g/gmol

t= exposure time (s) = 2 hour = 7200 second = 0.0833 day

A = surface area of metal specimen (cm^2)

$i_L = zFkC_b$

$Sh = k\,L/D$

$Sc = \nu/D$

Where:

μ = Fluid viscosity (kg/m.s).

k = mass transfer coefficient (m/s).

To find the volume of the acid must be added to distilled water to give 0.1N of solution:

The Normality of HCL solution = 0.1 N

Molecular weight of HCl= 36.458 gm/mole

Specific gravity of HCl= 1.18

Purity = 35% - 38%

Equivalent weight = 36.458

N_2=11.8N

N_2=M_2=11.8 M

$C_1 \times V_1 = C_2 \times V_2$

V_2 = 4.24 ml of HCl

A-3: Water Properties

➢ Fresh water Properties

Temp. (^{O}C)	Density (g/cm³)	Kinematic Viscosity (cm²/s)	Dynamic Viscosity (mpa.s)	Solubility, Salinity 0% (mol/cm^3)	Diffusivity (cm^2/s)
20	0.9982	1.0034E-02	1.0020E-02	5.06E-07	1.49E-05
30	0.9956	8.0071E-03	7.9700E-03	4.222E-07	2.81E-05
40	0.9922	6.5785E-03	6.5300E-03	3.61E-07	4.58E-05
50	0.9880	5.5313E-03	5.4700E-03	3.11E-07	6.84E-05
60	0.9832	4.7400E-03	4.6604E-03	2.22E-07	9.63E-05

➢ Standard Saltwater Properties

Temp. (^{O}C)	Density (g/cm³)	Kinematic Viscosity (cm²/s)	Dynamic Viscosity (mpa.s)	Solubility, Salinity 3.5% (mol/cm3)	Diffusivity (cm^2/s)
20	1.02481	1.05E-02	1.0770E-02	4.00E-07	1.39E-05
30	1.02177	8.43E-03	8.6100E-03	3.39E-07	2.60E-05
40	1.01801	6.95E-03	7.0800E-03	2.94E-07	4.22E-05
50	1.01368	5.86E-03	5.9400E-03	2.56E-07	6.29E-05
60	0.9832	4.74E-03	4.6604E-03	1.60E-07	9.63E-05

Appendix B Free corrosion potential Results

Table B-1: Behavior of Zinc Corrosion Potential vs. SCE with Time in air-saturated 0.1N HCl without Inhibitor.

Temperature(°C)	***20***	***30***	***40***	***50***	***60***
Time(min)	Potential(mv)				
0	-630	-640	-657	-662	-667
10	-637	-650	-662	-666	-673
20	-640	-657	-667	-668	-678
30	-645	-660	-670	-670	-679
40	-650	-663	-673	-672	-682
50	-651	-665	-674	-674	-685
60	-652	-666	-674	-675	-686
70	-653	-669	-675	-675	-686
80	-654	-671	-676	-677	-687
90	-654	-671	-676	-677	-688
100	-655	-672	-676	-678	-689
110	-656	-672	-677	-679	-689
120	-656	-672	-677	-679	-689

Table B-2: Behavior of Zinc Corrosion Potential vs. SCE with Time in air-saturated 0.1N HCl with 1 g/l of rosemary Inhibitor.

Temperature(°C)	***20***	***30***	***40***	***50***	***60***
Time(min)	Potential(mv)				
0	-627	-638	-654	-660	-665
10	-629	-641	-659	-665	-670
20	-630	-642	-660	-665	-671
30	-630	-643	-660	-666	-671
40	-630	-643	-661	-667	-673
50	-631	-645	-661	-667	-674
60	-631	-646	-663	-668	-677
70	-632	-646	-665	-669	-677
80	-635	-648	-665	-669	-676
90	-635	-648	-666	-669	-677
100	-636	-649	-668	-670	-678
110	-636	-649	-668	-672	-679
120	-636	-649	-668	-672	-679

Table B-3: Behavior of Zinc Corrosion Potential vs. SCE with Time in air-saturated 0.1N HCl with 5 g/l of rosemary Inhibitor.

Temperature(°C)	***20***	***30***	***40***	***50***	***60***
Time(min)	Potential(mv)				
0	-621	-632	-641	-642	-650
10	-621	-633	-642	-645	-651
20	-622	-633	-642	-646	-651
30	-622	-634	-644	-646	-653
40	-622	-636	-645	-647	-654
50	-623	-636	-645	-647	-657
60	-623	-637	-645	-647	-657
70	-624	-638	-646	-647	-659
80	-624	-639	-646	-649	-659
90	-626	-639	-648	-650	-660
100	-627	-639	-649	-651	-661
110	-627	-640	-651	-652	-661
120	-627	-640	-651	-652	-662

Table B-4: Behavior of Zinc Corrosion Potential vs. SCE with Time in air-saturated 3.5% NaCl without Inhibitor.

Temperature(°C)	***20***	***30***	***40***	***50***	***60***
Time(min)	Potential(mv)				
0	-644	-651	-658	-670	-679
10	-654	-659	-668	-679	-687
20	-658	-664	-674	-685	-693
30	-661	-667	-677	-688	-697
40	-663	-668	-679	-689	-698
50	-664	-669	-680	-690	-700
60	-666	-670	-681	-691	-701
70	-667	-673	-681	-693	-703
80	-668	-674	-682	-694	-704
90	-668	-675	-683	-695	-704
100	-669	-676	-684	-695	-705
110	-670	-676	-685	-696	-706
120	-670	-677	-685	-697	-707

Table B-5: Behavior of Zinc Corrosion Potential vs. SCE with Time in air-saturated 3.5%NaCl with 1 g/l rosemary Inhibitor.

Temperature(°C)	***20***	***30***	***40***	***50***	***60***
Time(min)	Potential(mv)				
0	-640	-646	-653	-664	-671
10	-646	-651	-657	-669	-677
20	-649	-654	-660	-673	-680
30	-651	-656	-662	-675	-682
40	-653	-657	-664	-677	-683
50	-654	-658	-665	-678	-684
60	-655	-660	-666	-680	-685
70	-656	-662	-667	-681	-686
80	-657	-663	-668	-682	-688
90	-658	-664	-670	-683	-689
100	-659	-664	-671	-684	-690
110	-660	-665	-672	-684	-691
120	-660	-665	-672	-685	-691

Table B-6: Behavior of Zinc Corrosion Potential vs. SCE with Time in air-saturated 3.5%NaCl with 5 g/l rosemary Inhibitor.

Temperature(°C)	***20***	***30***	***40***	***50***	***60***
Time(min)	Potential(mv)				
0	-636	-639	-649	-658	-665
10	-639	-642	-651	-662	-669
20	-641	-643	-653	-664	-671
30	-642	-645	-654	-666	-673
40	-643	-646	-654	-666	-674
50	-644	-647	-655	-667	-675
60	-645	-648	-656	-668	-675
70	-646	-649	-657	-669	-676
80	-647	-650	-657	-669	-677
90	-647	-651	-658	-670	-678
100	-648	-651	-659	-670	-678
110	-648	-652	-659	-671	-679
120	-648	-652	-660	-671	-679

Table B-7: Behavior of Zinc Corrosion Potential vs. SCE with Time in air-saturated 3.5%NaCl with 1 g/l reed leaves Inhibitor.

Temperature(°C)	***20***	***30***	***40***	***50***	***60***
Time(min)	Potential(mv)				
0	-639	-644	-654	-662	-670
10	-644	-648	-657	-665	-674
20	-647	-650	-660	-669	-676
30	-648	-652	-663	-672	-678
40	-649	-654	-664	-673	-680
50	-651	-655	-667	-675	-681
60	-652	-657	-667	-676	-683
70	-653	-658	-668	-676	-684
80	-654	-659	-669	-677	-685
90	-655	-660	-670	-678	-686
100	-655	-661	-670	-679	-687
110	-656	-661	-671	-680	-687
120	-656	-662	-671	-680	-688

Table B-8: Behavior of Zinc Corrosion Potential vs. SCE with Time in air-saturated 3.5%NaCl with 5 g/l reed leaves Inhibitor.

Temperature(°C)	***20***	***30***	***40***	***50***	***60***
Time(min)	Potential(mv)				
0	-633	-639	-650	-658	-667
10	-635	-641	-652	-661	-670
20	-637	-642	-654	-663	-672
30	-638	-644	-655	-664	-674
40	-639	-645	-656	-665	-675
50	-639	-646	-657	-665	-676
60	-640	-646	-657	-666	-676
70	-640	-647	-658	-667	-677
80	-641	-648	-658	-668	-678
90	-641	-649	-659	-669	-678
100	-642	-649	-660	-669	-679
110	-642	-650	-660	-670	-679
120	-643	-650	-660	-670	-679

Table B-9: Behavior of Zinc corrosion Potential vs. SCE with Time in air-saturated 3.5%NaCl with 1 g/l reed stems Inhibitor .

Temperature(°C)	***20***	***30***	***40***	***50***	***60***
Time(min)	Potential(mv)				
0	-637	-643	-652	-661	-668
10	-641	-648	-656	-665	-671
20	-643	-651	-659	-667	-673
30	-645	-653	-660	-669	-675
40	-646	-654	-661	-670	-677
50	-647	-655	-662	-672	-678
60	-648	-656	-663	-673	-679
70	-650	-657	-664	-674	-680
80	-651	-658	-665	-675	-681
90	-652	-659	-666	-676	-682
100	-652	-659	-666	-677	-683
110	-653	-660	-667	-678	-683
120	-653	-660	-667	-678	-684

Table B-10: Behavior of Zinc corrosion Potential vs. SCE with Time in air-saturated 3.5%NaCl with 5 g/l reed stems Inhibitor .

Temperature(°C)	***20***	***30***	***40***	***50***	***60***
Time(min)	Potential(mv)				
0	-630	-636	-648	-656	-663
10	-632	-639	-650	-658	-666
20	-633	-640	-652	-660	-668
30	-635	-641	-653	-661	-669
40	-635	-642	-653	-662	-670
50	-636	-643	-654	-663	-671
60	-637	-643	-655	-664	-672
70	-638	-644	-656	-664	-672
80	-638	-645	-657	-665	-673
90	-639	-645	-657	-665	-673
100	-639	-646	-658	-666	-673
110	-639	-646	-658	-666	-674
120	-639	-646	-658	-666	-674

Table B-11: Behavior of Zinc Corrosion Potential vs. SCE with Time in air-saturated 3.5%NaCl with 1 g/l of orange peels Inhibitor.

Temperature(°C)	***20***	***30***	***40***	***50***	***60***
Time(min)	Potential(mv)				
0	-641	-645	-654	-665	-673
10	-647	-649	-658	-667	-677
20	-650	-652	-662	-670	-678
30	-653	-655	-664	-672	-679
40	-655	-657	-665	-673	-681
50	-657	-658	-666	-675	-684
60	-658	-659	-667	-677	-686
70	-659	-660	-668	-678	-687
80	-659	-661	-669	-681	-688
90	-660	-662	-670	-682	-689
100	-661	-663	-671	-684	-690
110	-662	-663	-672	-684	-691
120	-662	-664	-672	-685	-691

Table B-12: Behavior of Zinc Corrosion Potential vs. SCE with Time in air-saturated 3.5%NaCl with 5 g/l of orange peels Inhibitor.

Temperature(°C)	***20***	***30***	***40***	***50***	***60***
Time(min)	Potential(mv)				
0	-637	-639	-648	-657	-666
10	-640	-643	-651	-660	-669
20	-642	-645	-653	-662	-671
30	-644	-646	-655	-663	-672
40	-646	-648	-656	-664	-673
50	-647	-649	-657	-664	-674
60	-648	-649	-658	-665	-675
70	-649	-650	-659	-666	-675
80	-650	-651	-660	-667	-676
90	-651	-652	-661	-668	-677
100	-652	-652	-661	-668	-677
110	-652	-653	-662	-669	-678
120	-652	-653	-662	-669	-678

Appendix C Polarization Results

Table C-1: The Values of Current and Potential of Zinc Specimen in 3.5% NaCl without Inhibitor .

T=20 ^{O}C		T=30 ^{O}C		T=40 ^{O}C		T=50 ^{O}C		T=60 ^{O}C	
I(mA)	E(mV)	I(mA)	E(mV)	I(mA)	E(mV)	I(mA)	E(mV)	I(mA)	E(mV)
1110	-3320	1680	-3660	1800	-3930	2000	-4200	2180	-4430
960	-3200	1450	-3560	1760	-3870	1850	-4010	2060	-4370
790	-3120	1290	-3440	1650	-3660	1680	-3930	1800	-4220
560	-2850	1120	-3250	1490	-3490	1520	-3800	1710	-3980
450	-2620	670	-2870	1090	-3010	840	-2650	1500	-3410
340	-2430	460	-2550	610	-2550	540	-2280	880	-2580
210	-2000	280	-2110	370	-2080	420	-1970	550	-2110
130	-1610	140	-1506	180	-1538	130	-1400	240	-1594
80	-1390	80	-1235	70	-1150	80	-1180	80	-1081
50	-1210	60	-1153	40	-988	50	-990	50	-947
10	-820	10	-841	10	-768	10	-842	10	-724
1	-790	1	-749	1	-739	1	-724	1	-723
1	-684	1	-746	1	-737	1	-722	1	-722
1	-685	1	-737	1	-726	1	-716	1	-718
1	-681	1	-738	1	-725	1	-715	1	-712
1	-674	1	-734	1	-724	1	-713	1	-708
1	-660	1	-721	1	-723	1	-710	1	-690
1	-654	1	-720	1	-720	1	-695	1	-688
1	-644	1	-718	1	-718	1	-686	1	-684
1	-643	1	-715	1	-714	1	-662	1	-633
10	-630	1	-713	1	-709	1	-654	1	-601
80	-590	1	-710	10	-705	1	-651	10	-691
120	-579	10	-633	20	-678	10	-612	70	-628
180	-573	90	-549	80	-565	20	-530	100	-606
580	-439	110	-517	110	-540	80	-469	180	-539
610	-362	190	-464	190	-420	110	-402	580	-262
750	-245	650	-217	640	-95	650	-230	750	-145
1030	-66	940	-37	930	-37	930	-37	1030	-66

Table C-2: The Values of Current and Potential of Zinc Specimen in 3.5% NaCl with 1 g/l of rosemary Inhibitor .

T=20 ^{O}C		T=30 ^{O}C		T=40 ^{O}C		T=50 ^{O}C		T=60 ^{O}C	
I(mA)	E(mV)	I(mA)	E(mV)	I(mA)	E(mV)	I(mA)	E(mV)	I(mA)	E(mV)
1060	-2900	1500	-3100	1710	-3380	1980	-3770	2000	-3900
1010	-2840	1280	-3040	1590	-3260	1840	-3630	1970	-3760
970	-2690	1140	-2900	1440	-3100	1610	-3480	1800	-3680
930	-2620	1020	-2730	1300	-2950	1470	-3350	1650	-3540
650	-2060	830	-2340	960	-2290	1100	-2780	1260	-2920
500	-1850	690	-2010	690	-1904	760	-2050	960	-2360
400	-1628	540	-1821	390	-1490	390	-1443	550	-1660
140	-1291	360	-1547	130	-1137	130	-1000	250	-1228
80	-1157	120	-1195	80	-1005	80	-918	110	-1036
60	-1090	70	-1024	50	-930	50	-857	60	-976
10	-929	50	-968	10	-816	10	-781	10	-781
1	-714	10	-887	1	-784	1	-758	1	-666
1	-671	1	-724	1	-737	1	-680	1	-651
1	-666	1	-643	1	-694	1	-657	1	-644
1	-649	1	-649	1	-670	1	-657	1	-643
1	-643	1	-651	1	-668	1	-645	1	-640
1	-636	1	-651	1	-643	1	-646	1	-637
1	-633	1	-637	1	-635	1	-644	1	-634
1	-627	1	-634	1	-623	1	-639	1	-629
1	-616	1	-631	1	-620	1	-632	1	-626
1	-613	1	-629	1	-615	10	-625	10	-623
1	-607	1	-627	10	-604	20	-619	20	-613
10	-607	10	-617	20	-604	80	-475	90	-506
20	-590	60	-489	80	-414	120	-410	120	-439
90	-496	90	-411	100	-331	190	-270	210	-300
120	-477	170	-357	170	-263	540	-90	620	-108
200	-394	430	-112	510	-131			790	-92
560	-30	790	-66	850	-30				

Table C-3: The Values of Current and Potential of Zinc Specimen in 3.5% NaCl with 5 g/l of rosemary Inhibitor .

T=20 ^{O}C		T=30 ^{O}C		T=40 ^{O}C		T=50 ^{O}C		T=60 ^{O}C	
I(mA)	E(mV)	I(mA)	E(mV)	I(mA)	E(mV)	I(mA)	E(mV)	I(mA)	E(mV)
900	-2600	1230	-2750	1380	-2820	1580	-2970	1820	-3100
850	-2550	1160	-2650	1280	-2700	1520	-2700	1740	-2940
730	-2460	1090	-2570	1110	-2630	1380	-2610	1570	-2840
680	-2380	980	-2470	990	-2500	1210	-2450	1300	-2580
510	-2040	710	-2140	780	-2140	820	-2000	950	-2070
420	-1780	560	-1820	620	-1849	620	-1676	750	-1793
310	-1550	390	-1509	400	-1455	520	-1499	530	-1470
130	-1241	150	-1064	180	-1039	240	-1033	150	-1013
50	-977	90	-988	70	-912	110	-928	80	-906
10	-835	50	-907	50	-873	60	-864	60	-847
1	-751	10	-795	10	-784	10	-790	10	-765
1	-718	1	-751	1	-754	1	-720	1	-712
1	-660	1	-711	1	-700	1	-685	1	-679
1	-645	1	-695	1	-670	1	-676	1	-644
1	-623	1	-671	1	-659	1	-650	1	-633
1	-620	1	-660	1	-644	1	-642	1	-630
1	-618	1	-625	1	-643	1	-632	1	-625
1	-615	1	-618	1	-635	1	-627	1	-623
1	-609	1	-606	1	-627	1	-621	1	-619
10	-599	10	-605	10	-622	10	-617	10	-616
20	-553	20	-570	20	-595	20	-592	20	-615
80	-512	70	-496	80	-560	80	-471	80	-548
120	-475	100	-449	110	-532	100	-467	100	-527
190	-303	170	-339	180	-482	170	-363	180	-464
560	-156	520	-10	550	-195	530	-223	520	-180
720	-48			700	-116	660	-131	660	-82
				940	-102	950	-80		

Table C-4: The Values of Current and Potential of Zinc Specimen in 3.5% NaCl with 1 g/l of reed leaves Inhibitor .

T=20 ^{O}C		T=30 ^{O}C		T=40 ^{O}C		T=50 ^{O}C		T=60 ^{O}C	
I(mA)	E(mV)	I(mA)	E(mV)	I(mA)	E(mV)	I(mA)	E(mV)	I(mA)	E(mV)
1020	-2800	1400	-3030	1740	-3270	1900	-3300	2030	-3580
860	-2710	1280	-2940	1620	-3160	1740	-3230	1930	-3410
790	-2590	1160	-2800	1400	-3090	1410	-2880	1820	-3270
660	-2450	990	-2630	1270	-2930	1170	-2150	1690	-2820
440	-1950	730	-2240	890	-2240	900	-1697	1460	-2410
360	-1750	590	-2010	690	-1938	760	-1544	1240	-2030
200	-1340	440	-1721	420	-1564	490	-1320	660	-1424
120	-1030	260	-1347	320	-1305	330	-1200	420	-1238
70	-900	120	-995	150	-1014	120	-915	170	-1026
50	-824	80	-860	70	-866	80	-851	80	-851
10	-709	50	-768	50	-780	50	-788	40	-782
1	-672	10	-687	10	-745	10	-750	10	-727
1	-666	1	-654	1	-711	1	-687	1	-737
1	-654	1	-651	1	-708	1	-657	1	-642
1	-641	1	-649	1	-701	1	-650	1	-650
1	-631	1	-643	1	-699	1	-645	1	-653
1	-623	1	-640	1	-663	1	-642	1	-649
1	-621	1	-637	1	-643	1	-640	1	-627
1	-616	1	-634	1	-636	1	-636	1	-620
1	-591	1	-631	10	-624	10	-620	10	-618
10	-582	10	-629	20	-617	20	-609	20	-605
20	-565	10	-627	70	-468	80	-476	80	-525
70	-464	60	-529	100	-352	120	-420	100	-510
90	-406	90	-468	160	-313	290	-140	170	-433
150	-281	170	-333	420	-159	540	-70	520	-68
400	-120	430	-212	550	-88				
		790	-166	720	-62				

Table C-5: The Values of Current and Potential of Zinc Specimen in 3.5%NaCl with 5 g/l of reed leaves Inhibitor .

T=20 ^{O}C		T=30 ^{O}C		T=40 ^{O}C		T=50 ^{O}C		T=60 ^{O}C	
I(mA)	E(mV)	I(mA)	E(mV)	I(mA)	E(mV)	I(mA)	E(mV)	I(mA)	E(mV)
880	-2450	1210	-2650	1350	-2700	1560	-2810	1800	-2930
810	-2340	1130	-2560	1240	-2580	1480	-2640	1670	-2750
750	-2230	1010	-2370	1190	-2410	1310	-2500	1520	-2620
710	-1960	950	-2140	1050	-2270	1220	-2310	1380	-2500
590	-1510	690	-1620	860	-1820	1020	-1910	1130	-2010
450	-1290	510	-1402	690	-1470	960	-1870	960	-1640
360	-1200	390	-1219	430	-1150	650	-1396	780	-1410
220	-1060	240	-1054	370	-1085	340	-1039	520	-1143
70	-895	80	-915	170	-991	180	-923	370	-1014
50	-844	60	-898	80	-910	90	-877	250	-878
10	-702	10	-702	10	-746	60	-824	90	-805
1	-649	1	-686	1	-687	10	-766	10	-784
1	-642	1	-675	1	-676	1	-713	1	-710
1	-635	1	-668	1	-638	1	-696	1	-688
1	-633	1	-648	1	-636	1	-682	1	-675
1	-628	1	-645	1	-635	1	-675	1	-645
1	-625	1	-641	1	-622	1	-636	1	-631
1	-621	1	-636	1	-608	1	-612	1	-631
1	-620	1	-630	1	-590	10	-602	1	-622
1	-596	10	-625	10	-585	20	-597	10	-606
10	-593	20	-612	20	-568	80	-472	20	-558
20	-571	70	-496	70	-429	100	-461	80	-340
70	-456	100	-347	100	-309	170	-366	100	-269
100	-410	170	-230	170	-164	560	-243	170	-219
170	-264	430	-20	510	-45	650	-133	520	-100
560	-45					940	-70	650	-30

Table C-6: The Values of Current and Potential of Zinc Specimen in 3.5% NaCl with 1 g/l of reed stems Inhibitor .

T=20 ^{O}C		T=30 ^{O}C		T=40 ^{O}C		T=50 ^{O}C		T=60 ^{O}C	
I(mA)	E(mV)	I(mA)	E(mV)	I(mA)	E(mV)	I(mA)	E(mV)	I(mA)	E(mV)
830	-2780	1200	-2900	1690	-3100	1880	-3270	1900	-3500
780	-2660	1080	-2740	1540	-2980	1740	-3080	1850	-3330
660	-2570	990	-2600	1300	-2860	1510	-2980	1790	-3130
580	-2420	920	-2430	970	-2550	1370	-2850	1560	-2970
400	-2010	730	-2040	740	-2230	900	-2380	1250	-2680
310	-1813	590	-1916	520	-1950	660	-2050	900	-2220
250	-1630	440	-1721	340	-1659	490	-1743	740	-1950
170	-1376	360	-1647	120	-1126	230	-1300	420	-1445
60	-983	120	-1195	90	-993	180	-1218	270	-1184
10	-805	50	-968	50	-845	70	-1057	110	-993
1	-722	10	-787	10	-756	10	-781	10	-813
1	-662	1	-652	1	-720	1	-758	1	-708
1	-647	1	-651	1	-683	1	-680	1	-690
1	-640	1	-649	1	-664	1	-659	1	-656
1	-636	1	-645	1	-646	1	-657	1	-660
1	-632	1	-637	1	-652	1	-645	1	-655
1	-628	1	-634	1	-630	1	-646	1	-645
1	-627	1	-627	1	-628	1	-642	1	-638
1	-623	1	-619	10	-621	1	-638	10	-594
10	-620	10	-614	20	-617	10	-632	20	-549
20	-607	60	-589	80	-580	20	-539	80	-268
70	-541	90	-568	100	-546	80	-375	180	-125
110	-512	170	-433	160	-396	120	-310	480	377
180	-481	430	-212	480	-80	190	-270	570	462
540	-168	690	-66	580	96	540	-60	780	730
680	-39			750	369				

Table C-7: The Values of Current and Potential of Zinc Specimen in 3.5% NaCl with 5 g/l of reed stems Inhibitor .

T=20 ^{O}C		T=30 ^{O}C		T=40 ^{O}C		T=50 ^{O}C		T=60 ^{O}C	
I(mA)	E(mV)	I(mA)	E(mV)	I(mA)	E(mV)	I(mA)	E(mV)	I(mA)	E(mV)
680	-2470	950	-2670	1190	-2510	1350	-2760	1740	-2830
650	-2370	870	-2500	1150	-2480	1260	-2600	1680	-2750
630	-2330	790	-2330	1020	-2370	1180	-2430	1570	-2630
620	-2290	690	-2250	980	-2330	1010	-2280	1340	-2400
470	-2030	570	-2040	760	-2030	820	-2010	970	-2040
380	-1871	490	-1920	430	-1654	520	-1506	680	-1720
220	-1457	360	-1655	350	-1449	420	-1399	520	-1470
120	-1168	230	-1305	170	-1148	240	-1133	320	-1126
70	-1018	120	-1107	90	-922	180	-988	170	-917
50	-925	70	-988	50	-830	80	-824	50	-730
10	-756	10	-724	10	-741	60	-798	10	-700
1	-704	1	-706	1	-725	10	-750	1	-692
1	-666	1	-692	1	-674	1	-707	1	-675
1	-641	1	-669	1	-641	1	-689	1	-647
1	-628	1	-660	1	-636	1	-685	1	-644
1	-610	1	-650	1	-634	1	-676	1	-635
1	-603	1	-634	1	-611	1	-632	1	-612
1	-599	1	-624	1	-607	10	-617	10	-609
1	-581	1	-616	10	-595	20	-592	20	-559
10	-593	10	-605	20	-594	80	-482	60	-404
20	-578	20	-506	80	-508	100	-460	90	-365
80	-473	70	-476	100	-488	170	-363	150	-282
100	-448	100	-420	170	-404	540	-150	400	-159
160	-353	170	-330	490	-179	610	-120	640	-30
510	-100	520	-10			950	-50		

Table C-8: The Values of Current and Potential of Zinc Specimen in 3.5% NaCl with 1 g/l of orange peels Inhibitor .

T=20 ^{O}C		T=30 ^{O}C		T=40 ^{O}C		T=50 ^{O}C		T=60 ^{O}C	
I(mA)	E(mV)	I(mA)	E(mV)	I(mA)	E(mV)	I(mA)	E(mV)	I(mA)	E(mV)
950	-2860	1300	-3100	1690	-3280	1890	-3320	2020	-3600
830	-2760	1180	-3020	1550	-3140	1690	-3230	1970	-3440
740	-2690	1040	-2900	1330	-2910	1510	-3140	1790	-3200
690	-2590	920	-2830	1190	-2830	1280	-2970	1560	-3050
540	-2020	830	-2440	800	-2350	990	-2490	1210	-2570
460	-1840	590	-2010	600	-1950	660	-1860	820	-2070
310	-1530	440	-1621	530	-1780	570	-1640	510	-1530
110	-1189	260	-1347	220	-1155	330	-1225	350	-1191
70	-1080	120	-1095	120	-1019	180	-981	280	-1081
50	-998	70	-1024	70	-934	50	-826	90	-886
10	-891	50	-987	10	-766	10	-730	10	-765
1	-838	10	-824	1	-684	1	-695	1	-692
1	-786	1	-743	1	-677	1	-682	1	-671
1	-690	1	-686	1	-664	1	-671	1	-659
1	-640	1	-649	1	-659	1	-650	1	-634
1	-633	1	-651	1	-655	1	-645	1	-626
1	-628	1	-651	1	-653	1	-644	1	-610
1	-622	1	-637	1	-647	1	-641	10	-598
1	-615	1	-634	1	-582	1	-639	20	-593
1	-611	10	-627	10	-558	10	-630	80	-553
10	-608	60	-589	20	-485	20	-533	110	-591
20	-593	90	-568	70	-250	80	-365	180	-555
70	-482	170	-433	100	-142	100	-310	580	-368
90	-452	430	-212			160	-250	980	-169
150	-354	890	-66			580	-40		
420	-133								

Table C-9: The Values of Current and Potential of Zinc Specimen in 3.5% NaCl with 5 g/l of orange peels Inhibitor .

T=20 ^{O}C		T=30 ^{O}C		T=40 ^{O}C		T=50 ^{O}C		T=60 ^{O}C	
I(mA)	E(mV)	I(mA)	E(mV)	I(mA)	E(mV)	I(mA)	E(mV)	I(mA)	E(mV)
860	-2560	1240	-2750	1270	-2920	1550	-2770	1810	-2920
810	-2430	1120	-2650	1140	-2820	1380	-2650	1680	-2840
780	-2340	1080	-2570	1020	-2750	1230	-2400	1230	-2630
750	-2290	870	-2340	890	-2590	1160	-2320	1090	-2480
540	-2010	690	-2040	720	-2220	890	-2020	820	-2040
420	-1852	450	-1800	610	-2010	560	-1666	570	-1591
240	-1566	330	-1609	440	-1617	340	-1384	380	-1296
120	-1290	120	-1212	220	-1300	170	-1021	230	-1086
70	-1096	70	-1020	170	-1169	80	-839	120	-873
40	-957	50	-954	50	-853	60	-800	50	-805
10	-853	10	-770	10	-792	10	-750	10	-773
1	-704	1	-713	1	-704	1	-712	1	-690
1	-668	1	-689	1	-647	1	-698	1	-678
1	-662	1	-673	1	-640	1	-685	1	-665
1	-656	1	-661	1	-636	1	-680	1	-656
1	-648	1	-655	1	-636	1	-671	1	-651
1	-633	1	-626	1	-619	1	-635	1	-638
1	-620	10	-625	1	-615	1	-624	1	-632
1	-601	20	-609	1	-609	10	-611	1	-624
10	-554	70	-470	10	-606	20	-594	10	-585
80	-340	100	-445	20	-570	80	-478	20	-515
100	-278	170	-332	80	-439	100	-436	80	-392
160	-87	460	-30	100	-366	170	-378	110	-322
				170	-214	520	-232	190	-195
						650	-120	470	-10
						850	-10		

الخلاصة

في هذه الرسالة تم استخدام إكليل الجبل وأوراق القصب وسيقان القصب وقشور البرتقال كمثبطات خضراء للزنك. تمت دراسة عينة من الزنك بطول 2 سم وعرض 2 سم مغمورة في حامض الهيدروكلوريك ومحلول ملح كلوريد الصوديوم بدون مثبط ومع إكليل الجبل وأوراق القصب وسيقان القصب وقشور البرتقال بتركيزات 1 و5 غم / لتر باستخدام تقنيات كهروكيميائية مختلفة مثل فقدان الوزن، وجهد التآكل الحر، واستقطاب التافل.

كان وسط التجارب عبارة عن محلول ملح كلوريد الصوديوم 3.5٪ ومحلول حامض الهيدروكلوريك 0.1N تم اختبار أداء عملية التآكل عند درجات حرارة(20 ، 30 ، 40، 50 ، و 60) درجة مئوية لمدة ساعتين.

أظهرت النتائج في تجربة فقدان الوزن أن معدل التآكل ينخفض مع زيادة تركيز المثبط في المحاليل الحامضية أو الملحية نتيجة تكوين طبقة رقيقة على سطح الزنك ولكنها تزداد مع زيادة درجة الحرارة. تؤثر درجة الحرارة على معدل التآكل عن طريق تغيير عاملين رئيسيين: قابلية ذوبان الأكسجين وانتشاره. لقد ثبت أن أفضل كفاءة في محلول الملح ، ساق القصب بتركيز 5 غم / لتر هو المانع الأخضر الأكثر فاعلية ، بكفاءة 75٪ ، بينما وجد أن إكليل الجبل هو المانع الاخضر الأكثر فاعلية في الحامض بكفاءة 49٪.

وفقًا لنتائج تجارب جهد التآكل الحر ، عندما زادت درجة الحرارة ، أصبحت جهود التآكل أكثر سلبية ، ومع زيادة تركيز المثبط ، أصبحت أكثر نبلاً (أقل سلبية). أفضل النتائج عند إضافة 5 غم / لتر من سيقان القصب في وسط الملح ، حيث سجلت -639 ملي فولت عند 20 درجة مئوية.

في تجارب الاستقطاب ، تتحول منحنيات الاستقطاب الأنودي والكاثودي إلى شدة تيار منخفضة وجهود تآكل أقل سلبية عند إضافة المثبط مما يعني أن معدل التآكل يتناقص مع المثبطات. كان لسيقان القصب أفضل أداء بتركيز 5 غم / لتر حيث تم تسجيل أدنى جهد تآكل - 670 ملي فولت

وكان تيار التآكل 0.9 ملي امبير/سم^2 في محلول ملحي عند 20 درجة مئوية. تم استنتاج أن نوع المثبطات الاربعة هي مثبطات مختلطة.

يمكن استنتاج شدة التيار المحدد من منحنيات الاستقطاب ومنه تم استنتاج معامل انتقال الكتلة ومعامل شيروود. يمكن ملاحظة أن التيار المحدد انخفض مع زيادة تركيز المثبط بسبب تقليل مساحة السطح الملامسة للإلكتروليت بواسطة المثبط الممتز، أيضًا زادت كثافة التيار المحدود مع زيادة درجة الحرارة.

جمهورية العراق

وازرة التعليم العالي والبحث العلمي

جامعة بابل/ كلية الهندسة

قسم الهندسة الكيمياوية

تحقيق الحماية من التآكل لمعدن الزنك باستخدام المثبطات الخضراء

الرسالة

مقدمة إلى كلية الهندسة ـ جامعة بابل كجزء من متطلبات نيل

الماجستير في الهندسة/الهندسة الكيمياوية

من قبل

حنين فالح والي سعد

إشراف

أ. م. د. شاكر صالح بحر

2022